EXPERIMENTAL AND COMPUTATIONAL STUDIES ON THE TEMPERATURE DEPENDENCE OF THERMAL CONDUCTIVITIES FOR WATER, ETHYLENE GLYCOL, GLYCEROL, AND PROPYLENE GLYCOL, USING THE TRANSIENT HOT-WIRE METHOD

A Thesis

Presented in Partial Fulfillment of the Requirements for the

Degree of Master of Science

with a

Major in Mechanical Engineering

in the

College of Graduate Studies

University of Idaho

by

Salman M. Alharbi

Major Professor: Kamal Kumar, Ph.D.

Committee Members: John C. Crepeau, Ph.D., Behnaz Rezaie, Ph.D.

Department Administrator: Steven Beyerlein, Ph.D.

August 2018

Authorization to Submit Thesis

This thesis of Salman M. Alharbi, submitted for the degree of Master of Science with a Major in Mechanical Engineering and titled "Experimental and Computational Studies on the Temperature Dependence of Thermal Conductivities for Water, Ethylene Glycol, Glycerol, and Propylene Glycol, Using the Transient Hot-Wire Method," has been reviewed in final form. Permission, as indicated by the signatures and dates below, is now granted to submit final copies to the College of Graduate Studies for approval.

Major Professor: ________________________________ Date: ________________

Kamal Kumar, Ph.D.

Committee Members: ________________________________ Date: ________________

John C. Crepeau, Ph.D.

________________________________ Date: ________________

Behnaz Rezaie, Ph.D.

Department

Administrator: ________________________________ Date: ________________

Steven Beyerlein, Ph.D.

Abstract

The goal of this work is to provide experimental measurements of thermal conductivity of water, ethylene glycol, glycerol, and propylene glycol as a function of temperature. The transient hot wire method was used to measure the thermal conductivity over temperatures ranging from $235-340\ K$. This work also involved in-house apparatus fabrication along with integration of data acquisition and processing software. The experiments are carried out for a fixed current of 250 mA and the resulting temperature rise of a 95.33 mm long, 25-micron radius platinum wire is used to infer the thermal conductivity using the known solution to the heat conduction equation for a continuous line source in an infinite medium. It is important to account for the variable temperature coefficient of resistance of the platinum wire as a function of temperature when seeking to obtain the correct temperature dependence of the thermal conductivity. A data reduction procedure that improves the accuracy of the reported values by identifying the onset of convection in the fluid is proposed. We use the peak value of the slope (S) obtained using a third order polynomial fit to the apparent linear region to estimate the thermal conductivity. The high-resolution data acquired at closely spaced temperature intervals is used to derive a correlation between thermal conductivity values and the fluid temperature. Additionally, numerical results for temperature and velocity field near the heated wire are also presented to help understand the non-idealities present in the experiments. The experimental temperature rise obtained from the transient hot-wire experiments is compared to computed values for water at room temperature, and a good agreement is found. There is a fair agreement between the current data sets and the very limited data for the four liquids reported in the literature. This work provides robust and comprehensive experimental data for thermal conductivities of the four common heat transfer fluids over the typical range of temperatures they are frequently used.

Acknowledgements

I gratefully acknowledge the financial support for my graduate studies from the ministry of interior and the ministry of education, Kingdom of Saudi Arabia.

I am thankful for the support from the department faculty and staff during my stay here, especially Prof. John Crepeau and Prof. Steve Beyerlein for initially helping me with the admissions process, and the initial advising related to coursework selection. I would like to thank Prof. John Crepeau and Prof. Behnaz Rezaie for periodically reviewing my research progress and serving on my thesis defense committee.

The assistance from my lab-members Rick Leathers and Samuel Stuhlman during the experiments is also acknowledged. Special thanks to Elyasa for sharing his knowledge and the insightful conversations.

Finally, I would like to thank Prof. Kamal Kumar for providing constant guidance during the course of this research. He kept me focused on my goals and pushed me to succeed in my professional efforts.

Dedication

Dedicated to the memory of my mother.

I would also like to thank my father Mohammed Salman Alharbi for his encouragement and guidance throughout my life. My sincere gratitude to my brother Maher for his support. This work would not have been possible without the help from my wife Abrar, who was very patient and caring during my graduate studies. To my children Mira, Mohammed, and Abdullah for providing joy in my life.

Table of Contents

List of Tables

List of Figures

Chapter 1. Introduction

1.1 Heat Transfer—A Historical Perspective

The flow of energy because of temperature differences forms the basis for the discipline of heat transfer. The distinction between heat and temperature was not clear during the 18th century. An anonymously published work titled “Scala Graduum Caloris” [1] was an initial attempt to establish a temperature scale. According to Sayre [2], the title of this article first published in 1701 had been translated as “Scales of the degree of heat”, and uses the present concepts of ‘heat’ and ‘temperature’ interchangeably. There is some evidence to claim that the author of this work was probably Sir Isaac Newton. The scale for the degree of calor in the low range was determined using the principles of thermal expansion of liquid, with the melting calor of lead being the upper limit. The process for determining the higher degrees of calor involved the measurement of time required cooling of various combinations of different metal pieces placed on an initially glowing iron bar. The mention of the second method in this work, in the opinion of Sayre [2], is the only link between ‘the law of cooling’ and Newton. A key postulate of this work was that the uniform flow of air removed calor from the hot body in proportion to the calor difference.

In the later part of the eighteenth century, two rival theories of heat emerged. The first was the caloric theory of heat proposed by Antoine Lavoisier [3]. The concept of the caloric theory was that the heat was an invisible subtle fluid whose particles were in motion [4]. The fluid was tasteless, odorless, massless, and colorless. This fluid was transferred from a hot to a cold body during the heating process. This idea was popular among the chemists and presupposed the existence of atoms surrounded by the fluid. The caloric theory was successfully used to explain all known heat related phenomena and was accepted by scientists such as

Laplace, Lavoisier, Priestley, Petit and Dulong [5]. Based on this (incorrect) theory the French engineer Sadi Carnot (correctly) deduced the fundamental limitations of conversion of heat to work [6]. The second theory, accepted among physicists and mathematicians, stated that there was no such fluid and that the motion of 'atoms' could account for heat. Interestingly, the first law of thermodynamics and the atomic theory of matter were still unknown at the time. The cannon boring experiments of Count Rumford provided conclusive evidence against the caloric theory. A blunt cannon borer was seemingly able to provide a limitless amount of the caloric fluid. He stated the problem as [5]:

"Whence then came this heat? And what is heat actually? I must confess that it has always been impossible for me to explain the results of such experiments except by taking refuge in the very old doctrine which rests upon the supposition that heat is nothing but a vibratory motion taking place among the particles of the body".

This idea helped to develop the law of conservation of energy, and J.P Joule established the equivalence between mechanical work and heat in 1842 [7]. This equivalence is what is now referred to as the First Law of Thermodynamics. Two decades prior, Fourier's work on the Analytic Theory of Heat outlined the basic principles of heat transfer [8]. His work showed that the flow of heat was a result of differences in temperature between adjacent particles, or simply put due to spatial temperature gradients. The principles of conduction heat transfer had now been firmly established.

1.2 Conduction Heat Transfer

Heat transfer is thermal energy in motion. It involves exchange in thermal energy from one object to another object because of temperature differences. Thermal energy is always transferred from a high temperature to the low temperature object until both reach the same temperature. The origin of conduction heat transfer can be traced to molecular vibrations in a medium where there is no bulk motion. This mode can exist in either solids, liquids, or gases. For the case of solids the transfer of heat is attributed to lattice vibrations and electronic contributions, whereas for liquids and gases the random molecular motions are important [9].

For simplicity, let us consider the simple example of heat flow due to conduction in a solid one-dimensional rod. Following the analysis in the text of Haberman [10] let us consider a rod of length L aligned with the x-axis. Let the thermal energy density be given by:

$$e(x,t) \equiv \text{thermal energy density} \tag{1.1}$$

Let the flow of thermal energy, i.e., the quantity of thermal energy flowing per unit time per unit area equal to

$$\phi(x,t) = \text{Heat Flux} \tag{1.2}$$

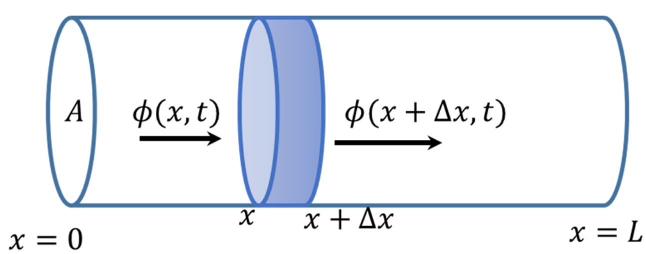

Figure 1.1: Heat Flow in a one-dimensional rod.

For generality, let us assume that the rod possesses some source of internal energy generation whose strength (heat generated per unit volume per unit time) is given by

$$Q(x,t) = \text{Heat generated per unit volume per unit time} \tag{1.3}$$

The conservation of energy principle applied to the slice of length Δx can be stated as:

$$\begin{pmatrix}\text{Rate of change}\\ \text{of heat energy}\\ \text{in time}\end{pmatrix} = \begin{pmatrix}\text{heat energy flowing}\\ \text{across boundaries}\\ \text{per unit time}\end{pmatrix} + \begin{pmatrix}\text{Internal generation of}\\ \text{heat energy}\\ \text{per unit time}\end{pmatrix} \tag{1.4}$$

For a thin slice of width Δx the total thermal energy generated is given by $Q(x,t)A\Delta x$ while the heat energy contained within it is $e(x,t)A\Delta x$. Here we are assuming negligible variation in $e(x,t)$ and $Q(x,t)$ over the thin slice. The conservation principle stated in equation 1.4 can be more precisely stated as

$$\frac{\partial(e(x,t)A\Delta x)}{\partial t} = \phi(x,t)A - \phi(x+\Delta x)A + Q(x,t)A\Delta x \tag{1.5}$$

Dividing throughout by Δx and taking the limit $\Delta x \to 0$, we obtain

$$\frac{\partial e}{\partial t} = \lim_{\Delta x \to 0} \frac{\phi(x,t) - \phi(x+\Delta x,t)}{\Delta x} + Q(x,t) \tag{1.6}$$

While taking the limit $\Delta x \to 0$ the time is held constant. Therefore, by the definition of the partial derivative one can simplify the above equation to

$$\frac{\partial e}{\partial t} = -\frac{\partial \phi}{\partial x} + Q \tag{1.7}$$

Equation 1.7 contains two variables e (thermal energy density) and ϕ (heat flux) which must be represented or modeled in terms of some common variable. Physically, this variable is called the temperature T. We must therefore provide a relationship between the temperature and the thermal energy. This relationship can be shown to be of the form

$$e(x,t) = \rho(x)c(x)T(x,t)$$

Where ρ and c represent the density and specific heat. This relationship between thermal energy and temperature had confounded the early practitioners of the science of heat, and the notions of heat and temperature were often used interchangeably [2]

Next, we need to model the heat flux ϕ in terms of the temperature field. This will reduce equation 1.7 to one unknown, namely T. Fourier established the relationship between the temperature field and the heat flux. He initially formulated heat conduction as an n-body problem similar to Biot who had worked on the problem it before him. Biot, who belonged to the Laplace's school of thought, adhered to the principle of action at a distance between bodies. His concept involved only the temperature difference between points, and that the temperature at a given point was influenced by all neighboring points. Critically, it did not involve distances and hence the temperature gradients. Fourier, subsequently abandoned the discontinuous n-body approach and adopted a continuous approach. He assumed that the temperature within an infinitesimal element was affected only by elements in its immediate vicinity, and consequently formulated the heat diffusion equation for a continuum. His empirical approach involved spatial transport of heat, storage of heat, and the interaction of the domain with the boundary conditions [11]. This approach also led to what is known as Fourier's law of heat conduction which relates the heat flux ϕ to the spatial temperature gradient as

$$\vec{\phi} = -k\vec{\nabla}T \qquad 1.8$$

The quantity k is proportionality constant called the thermal conductivity and is a material dependent property. Fourier's 1807 work on the heat diffusion equation faced delays in publication and he would finally publish it himself as Théorie Analytique de la Chaleur in 1822. The delay resulted from his use of infinite trigonometric series in the solution of the problem which was not viewed favorably by Lagrange, one of the reviewers of his 1807 manuscript submitted to the French Academy [11]. The transient heat conduction equation of Fourier in the absence of heat sources is given by:

$$\rho c \frac{\partial T}{\partial t} = \vec{\nabla} \cdot k \vec{\nabla} T \qquad 1.9$$

	Year	Contribution
Fahrenheit	1724	Mercury thermometer and standardized temperature scale
Abbé Nollet	1752	Observation of osmosis across an animal membrane
Bernoulli	1752	Use of trigonometric series for solving differential equations
Black	1760	Recognition of latent heat and specific heat
Crawford	1779	Correlation between respiration of animals and their body heat
Lavoisier and Laplace	1783	First calorimeter; measurement of heat capacity, latent heat
Laplace	1789	Formulation of Laplace operator
Biot	1804	Heat conduction among discontinuous bodies
Fourier	1807	Partial differential equation for heat conduction in solids
Fourier	1882	Théorie Analytique de la Chaleur

Table 1-1 Contributions leading to the heat diffusion equation [11].

As noted earlier the heat diffusion equation includes the thermal conductivity term, which appears as a consequence of modeling the heat flux term as a function of the temperature field (gradient). Formally, the definition of thermal conductivity is based on Fourier's law of conduction and for a one-dimensional case can be written as:

$$k \equiv -\frac{\phi_x}{\partial T/\partial x} \qquad 1.10$$

Where ϕ_x is the heat flux and $\partial T/\partial x$ is the temperature gradient. In order to utilize Fourier's law of conduction, we need to have knowledge of the thermal conductivity of the material. This material property may vary as a function of position for anisotropic solids, and is often a function of temperature. It fundamentally relates to the idea of transport of heat and is a measure of the rate at which heat is transferred by diffusion [9].

1.3 Thermal Conductivity

The transport of heat in the solid-state occurs due to contributions arising from two distinct processes. First the movement of free electrons and the other due to lattice vibration waves. These two effects are additive in that the observed thermal conductivity is the sum of these two components. Thermal conductivity for metallic solids generally tends to be much higher than nonmetals where the thermal conductivity arises primarily due to the lattice vibrations. In the case of liquids and gases theory states that the thermal conductivity bears a direct proportionality to factors such as particles per unit volume (n), the mean molecular speed ($\bar{c}$), and the mean free path (λ), i.e. $k \propto n\bar{c}\lambda$ [9]. The effectiveness of thermal transport can vary over several orders of magnitude between solids, liquids, and gases as shown in Fig. 1.2.

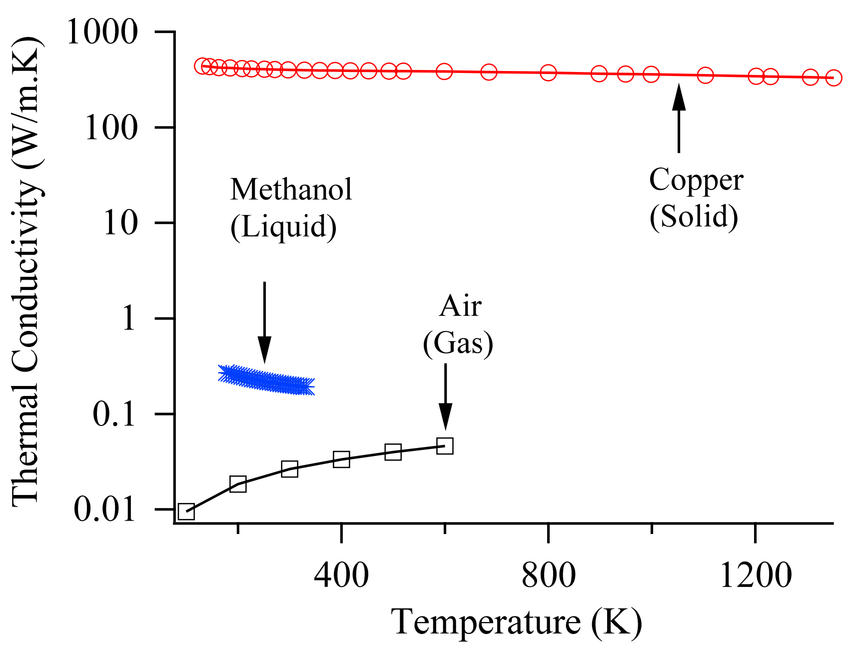

Figure 1.2: Variation of thermal conductivity with temperature for a solid [12], liquid [13], and gas [14].

Furthermore, the thermal conductivity exhibits a strong temperature dependence, which may cause it to either increase or decrease with increasing temperature depending on the material.

It is therefore of fundamental and practical interest to obtain the temperature dependence of this transport property in order to optimally design engineering systems such as heat exchangers that typically operate over a wide temperature range.

1.4 Measurement Techniques for Thermal Conductivity

There are several experimental techniques to measure thermal conductivity of materials. All of these methods can be fundamentally characterized as either steady state or transient. In this work, we use one of the transient techniques known as the transient-hot wire method to obtain the thermal conductivity as a function of temperature. A brief description of the two classes of techniques is provided in the following.

1.4.1 Steady State Methods

The steady state methods mean that the thermal conductivity of sensing device does not change with time. A commonly used steady state method is known as the concentric cylinder method. In this method the gap between the two cylinders is filled with the test material and heat is supplied to the inner cylinder and flows across the specimen in the gap. Thermocouples placed located at the inner surface of the outer cylinder r_2, and the outer surface of the inner cylinder r_1, record the temperature difference across the gap. Under steady state conditions and for a known heat supply Q_n the thermal conductivity is determined as:

$$k = \frac{ln\left(\frac{r_2}{r_1}\right) \times Q_n}{2\pi L \Delta T} \qquad 1.11$$

Here L is the length of the inner cylinder; ΔT is the different temperatures. The net power Q_n is equal to the total power supplied minus the heat loss. In general, the steady state methods requires a long test time because the temperature one must let the system to first achieve steady state.

1.4.2 Transient Methods

The most commonly used transient technique in the literature is the transient hot-wire apparatus. Other techniques such as the transient plane source and the laser flash method also are used to determine the thermal conductivity of substances. The fundamental idea in these measurements is to quickly deposit a short pulse of energy in the medium and record the transient temperature response. This temperature-time response is then compared to fundamental solutions and a curve fit procedure is often used to estimate the thermal conductivity. Oftentimes, the heat source and the sensing material are the same such as a thin platinum wire. We will discuss the transient hot-wire technique in detail in Chapter 2.

1.5 Objectives of this Work

1. Design and construct a transient hot-wire apparatus for the measurement of thermal conductivity of liquids. The design of the overall measurement system involves construction of a hot-wire cell, integration of heating and cooling baths to the system with precision temperature control, a precision power source, and a high-resolution-high-speed data acquisition device. In addition to the hardware itself, a key component of the apparatus is the software that enables high-speed data acquisition and processing in near real-time.
2. Obtain the temperature dependence of thermal conductivity of four common heat transfer fluids, namely, water, ethylene glycol, glycerol, and propylene glycol. The thermal conductivity values obtained from the system were validated using water, which is the most widely available heat transfer fluid and has extensively been studied with

respect to the variation of its thermal conductivity with temperature. Post validation, we obtain results for the other three liquids that do not have a large volume of work on their thermal conductivity values. In this work, we wish to generate sufficient number of data points for thermal conductivity over the temperature range of interest so that a robust correlation of k vs. T can be obtained.

3. Computationally examine the temperature and velocity field in the vicinity of the transient hot-wire. The simulations are required to understand the physics of the heat up process for the micron sized wire and its interaction with the surrounding fluid media as it pertains to the onset of buoyancy driven flow. The computational results provide insights into the validity of assumptions made in the process of measuring thermal conductivity of liquids using this method.

Chapter 2: The Transient Hot-Wire Technique for Measuring Thermal Conductivity

2.1 Introduction and Theory

Thermal conductivity of a heat transfer liquid is among the important properties required for proper estimation of heat transfer rates in practical engineering systems. This fundamental transport property relates the temperature gradient to heat flux. A widely used technique used for the measurement of thermal conductivity is the transient hot-wire method. This method is based on the solution to the conduction problem $(\partial T/\partial t = \kappa\nabla^2 T)$ of radial heat flow in an infinite solid medium with an instantaneous line source provided with a constant supply of heat [15]. In practice, a very thin platinum wire supplied with a constant current, and immersed in a liquid adequately approximates the ideal configuration. Assuming that the power is applied to line source at $t = 0$, and that the wire and the surrounding medium at the same temperature, the temperature at any subsequent time t and at a distance r is given by:

$$\Delta T(r,t) = \frac{q}{4\pi k} \int_{r^2/4\kappa t}^{\infty} \frac{e^{-u}}{u} du \tag{2.1}$$

Of particular interest is the temperature at the wire surface $(r = a)$. The transient hot-wire method for measuring thermal conductivity relies on the fact that at large time $(Fo = \frac{\kappa t}{a^2} \gg 1)$ the relationship between the temperature rise at the wire surface and the logarithm of time is linear. The slope of this linear fit is inversely related to the thermal conductivity for a constant heating rate. Specifically, the temperature rise of the wire $(r = a)$ and for $t \gg a^2/\kappa$ can be approximated as [16]:

$$\Delta T(a,t) = \frac{q}{4\pi k} ln\left(\frac{4\kappa t}{a^2 C}\right) \tag{2.2}$$

Here a is the radius of the wire, q the power per unit length supplied to the wire, κ and k the thermal diffusivity and conductivity of the medium surrounding the wire, and $C = e^{\gamma}$ where $\gamma = 0.577216$ is Euler's constant. The derivative of the temperature rise with respect to logarithm of time leads to:

$$\frac{d\Delta T}{dln(t)} = \frac{q}{4\pi k} \tag{2.3}$$

Referring to the quantity $d\Delta T/dln(t)$ as the slope S of the plot of ΔT versus $ln(t)$ the thermal conductivity of the surrounding medium is inferred using:

$$k = \frac{q}{4\pi S} \tag{2.4}$$

Additional details on the theory of the transient hot-wire method can be found in the studies by Blackwell [17], Healy et al.[18], and Jaeger [15]

The application of this technique in experiments for determining the thermal conductivity of fluids has been described by Roder [19] who designed a new apparatus for measuring thermal conductivity of oxygen at elevated pressures. He also performed performance checks using nitrogen, helium and argon. His work also provides a brief overview of the evolution of this technique starting from the initial experiments of Pittman [20]. A method for simultaneous measurement of thermal diffusivity and conductivity for liquids has been reported by Nagasaka and Nagashima [21] who carried out measurements on toluene under atmospheric pressure and in the temperature range of $0 - 80\ C$. Among the recent studies describing the use of the transient hot-wire apparatus for liquid thermal conductivity measurements are the studies by Bleazard et al. [22], Codreanu et al. [23], Zhang et al. [24], and Kostic and Simham [25].

The accurate experimental determination of thermal conductivity has generally been regarded as a problem of some difficulty [26]. One of the factors that tends to overwhelm experimental efforts of measurements in fluids is the onset of convection. Note that the aforementioned solution holds for heat diffusion in a solid/stationary-fluid medium, and it breaks down if natural convection sets in due to heat input to the system. This work reports the thermal conductivity of water in the $273 - 305\,K$ temperature range at a pressure of one atmosphere. Prior work on the temperature dependence of thermal conductivity of water includes the study of Woolf et al. [27] who used a concentric cylinder apparatus under steady state conditions and between 70 and 200 Fahrenheit. Lawson et al.[28] reported the thermal conductivity of water between 30 and 140 degree Celsius and for pressures between 1 to 8000 kg/cm2, also using the concentric cylinder technique. Theiss and Thodos [29] reviewed the experimental thermal conductivity and viscosity for gaseous and liquid water and developed a reduced state correlation for these transport properties. They note that while there is significant experimental work for viscosity, the thermal conductivity measurements were not as widely available. Their calculated values exhibited an average deviation of 2.31 % form the experimental data points considered in their study. A 1984 study by Sengers et al. [30] documents the available data on thermal conductivity of water since the promulgation of the first international formulation for transport properties of water substance in 1964. Their survey of experimental information summarized the thermal conductivity of water and steam from forty-three literature sources and only five sets were available for sub-ambient temperatures. About 40% of the datasets had been obtained using the transient hot-wire method. Another study by Nieto de Castro et al. [26] in 1986 examined the available thermal conductivity data for water with the purpose of establishing standard reference values along its saturation line. They noted that the thermal conductivity of fluids was one of the most difficult properties to measure and only after the technical advances during the 1970's the precision of these measurements has significantly improved. Another set of standard reference data based on new experimental data was proposed by Ramires et al [31] nearly a decade later that led to a revised and more accurate correlation. Both the aforementioned studies [26, 31] fitted experimental data from multiple sources into a quadratic function of temperature. Ramires et al.[31] described the reduced thermal conductivity of water over the normal liquid range as $k^* = -1.48445 + 4.12292T^* - 1.63866T^{*2}$ for $274 \leq T \leq 370\ K$.Where$T^* = T/298$ and $k^* = k(T)/k(298)$ with $k(298.15, 0.1\ MPa) = 0.06065 \pm 0.0036\ Wm^{-1}K^{-1}$ We will later compare the current experimental results to this correlation of Ramires et al. [31]. This study reports the thermal conductivity of water, ethylene glycol, glycerol, and propylene glycol.

2.2 Apparatus

The transient hot-wire apparatus used in the experiments consists of a stainless steel cylindrical cell 43 mm in diameter and 150 mm length. The cell is closed at the bottom and has a top lid with two electrical feedthroughs. Connected to these two electrical feeds are two copper conductors with tabs and screws to secure the platinum wire. The platinum wire is soldered to the copper conductor after securing it to the tabs to ensure a good contact. The platinum wire used in the measurement cell has a radius of 25 microns. Its purity is 99.99 % and it has is used in the hard drawn state. This wire acts as the line heat source. The length of the wire is estimated to be 95.33 mm. The length of the wire was obtained after the wire had been soldered in place by comparing its resistance to a known length of identical platinum wire. The resistance measurements were made in the 4-wire configuration using a Keithley 2440 sourcemeter. This sourcemeter was also used as a constant current source for heating the wire during the experiments. The terminal voltage at the feedthrough was measured using a 24 bit delta-sigma analog to digital converter with a nominal input voltage range of ±10 V. The measuring cell was maintained at a constant temperature by immersing it in a circulating bath such that only the top terminals were accessible for connections. A schematic of the test cell is shown in Fig. 2.1.

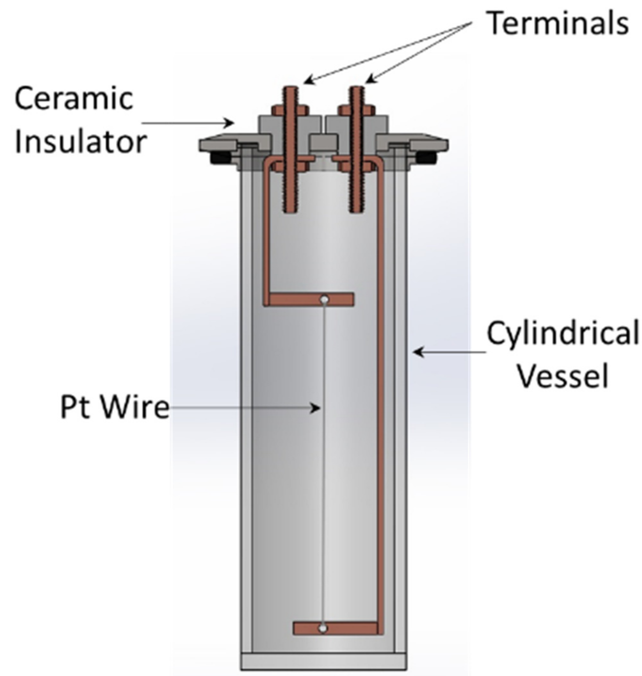

Figure 2.1: Schematic of the transient hot-wire cell.

The test cell is filled with technical grade distilled water such that it fully immerses the platinum wire. The cell is next immersed into the circulating bath and allowed to stabilize before starting measurements. The temperature of the test fluid is measured using a 1/16 inch K type thermocouple with exposed junction. This temperature was acquired by a national instruments module NI 9213, the accuracy of which is less than 0.02°C for high resolution mode, and less than 0.25°C for high speed mode. Also, the standard limits of error for the type K thermocouple in the range of 0 to 1250 °C is less than 2.2°C or 0.75%, and 2.2°C or 2 %.for -200 to 0°C .

The transient hot wire measurements consist of sending a 250 mA current pulse through the platinum wire and recording the terminal voltage using the 24 bit A/D converter. The sourcing of the current and all other measurements are initiated using a LabView program developed specifically for this experiment. The voltage data is sampled at a frequency of 4167 Hz and 25,000 samples for a duration of 6 seconds are logged.

The temperature rise of the wire, when subjected to step current change, is determined by measuring the change in resistance with time. This change in resistance due to Joule heating is related to the temperature rise, and is given by [32]:

$$R(T) = R_{ref}\left[1 + \alpha_{ref}\left(T - T_{ref}\right)\right] \tag{2.5}$$

where the reference values correspond to the values at initial time ($t = 0$) prior to the passing the current. The value of R_{ref} is taken to be that of the first data point ($t = 0$) and the reference temperature corresponds to the temperature of the test liquid.

2.3 Determination of Temperature Coefficient of Resistance

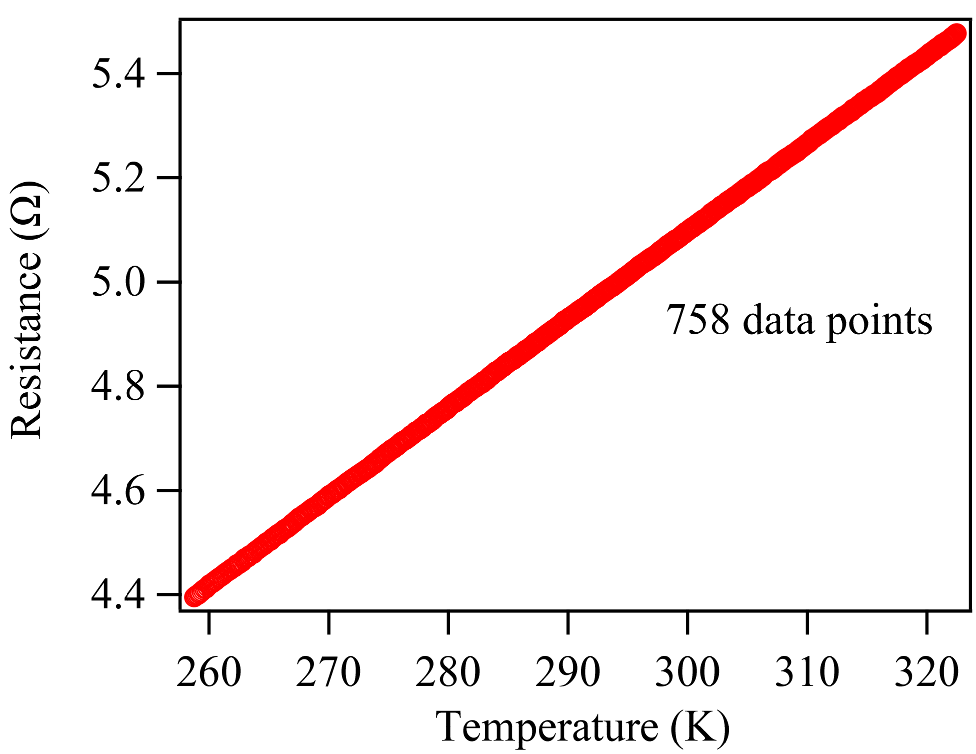

Figure 2.2: Variation of platinum wire resistance with temperature.

Recognizing that we need to vary the reference temperature, it becomes necessary to first determine the temperature coefficient of resistance (α_{ref})at each reference temperature. That is, the temperature coefficient of resistance needs to determine as a function of temperature. This is accomplished by a submerging the wire holder in a circulating bath and recording its resistance at varying bath temperatures. The resistance measurements are carried out in a 4-wire configuration with a small current (1 mA) that causes negligible heating in the wire. The variation in resistance of the wire as a function of temperature is shown in Fig. 2.2.

The local slope of the resistance versus temperature curve is next determined by selecting 75 consecutive points above and below the desired reference temperature. An example of the aforementioned procedure for obtaining the local slope in the neighborhood of T_{ref} =293.2 K is shown in Fig. 2.3.

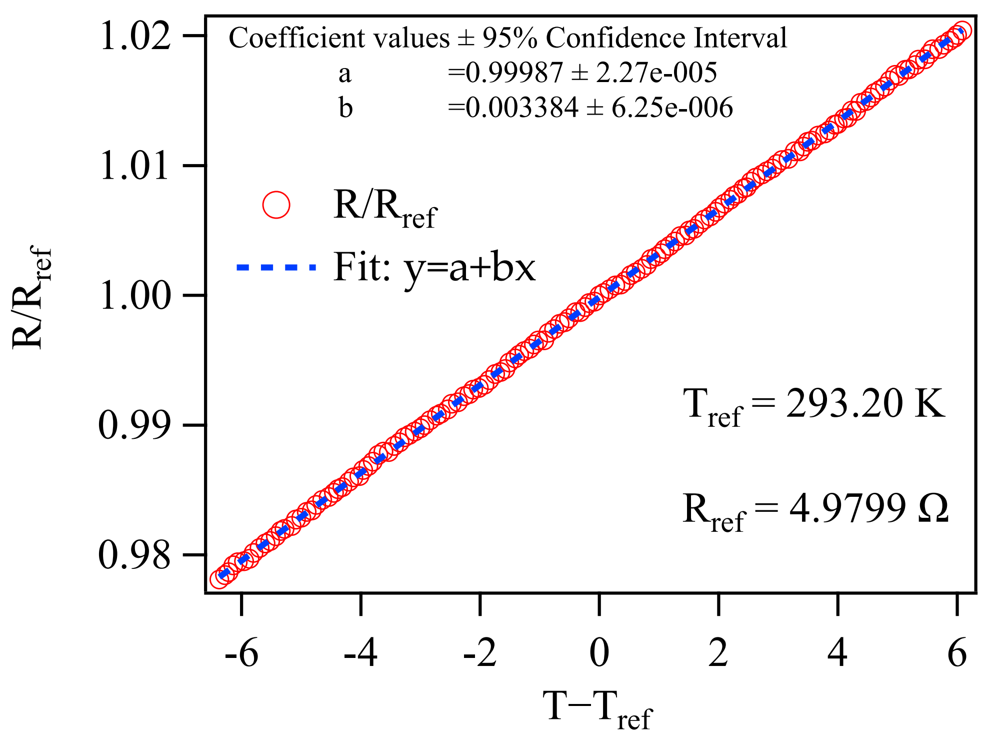

Figure 2.3: Determination of local Slope.

A similar procedure is repeated at each reference temperature to obtain the dependence of α on temperature, the results of which are shown in Fig. 2.4.

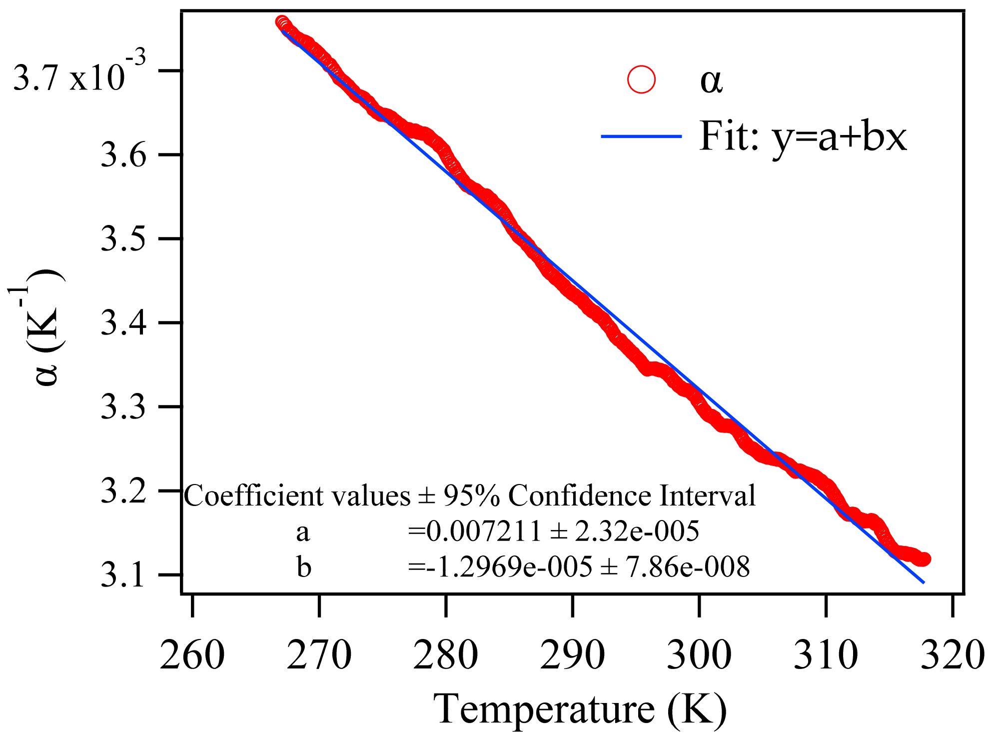

Figure 2.4: Variation of the temperature coefficient of resistance for platinum wire with temperature.

Having determined the temperature coefficient of resistance, the temperature rise of the wire due to the passage of current can be calculated using equation (4). Note that we are now recording the temperature rise during the 6-second interval that corresponds to the passage of the current. Therefore, we assume that the very first deduced temperature data point corresponds $(t = 0)$ corresponds to no heating of the wire, i.e. $\Delta T = T_{wire} - T_{liquid} = 0$. An example of the calculated temperature rise of the wire, for a 250 mA current, is shown in Fig. 2.5.

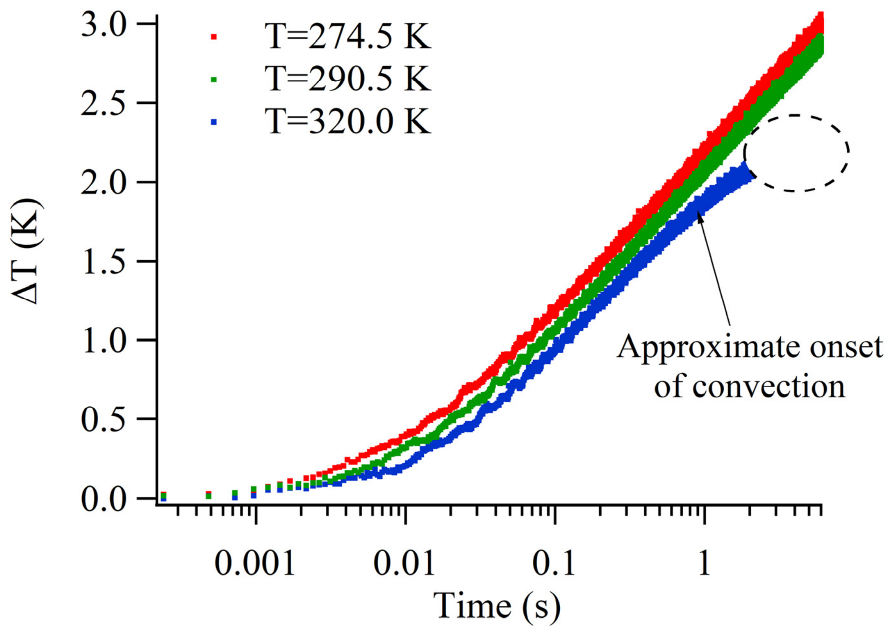

Figure 2.5: Temperature-time history for experimental runs at varying liquid temperatures.

It can be seen from Fig. 2.5 that during the initial period of approximately $0 - 0.2\ s$ the temperature rise exhibits a non-linear trend with respect to time on a logarithmic scale. This is followed by a linear rise in temperature with time on the log scale. A straight line is fit to the ΔT with $ln(t)$ trace in the region of linear temperature rise, and its slope (S) is used in equation (1), which is $k = q/4\pi S$.

2.4 Data Reduction Procedure

The choice of the range of times (t_1, t_2) to use in the linear fit in order to obtain the slope S has generally been determined based on the experience of the experimenter. This is also noted in the work by Roder at the National Bureau of Standards [19] who states that operator judgement is involved in the selection of times t_1 and t_2. We find that this is true for our experiments as well and propose a method to make the data reduction procedure more objective and free from experimenter bias. The theory suggests fitting a straight line in the region of interest ($Fo \gg 1$) assuming that the medium behaves as a solid. However, there is a practical problem with this in that the non-ideal effects are present both in the initial and terminal regions of the curve. They arise due to the finite heat capacity of the wire and the onset of convection at sufficiently large time. The existence of three distinct regions of increasing, apparently constant, and decreasing slopes due to these non-ideal effects is shown in Fig. 2.6 at a temperature of 320 K.

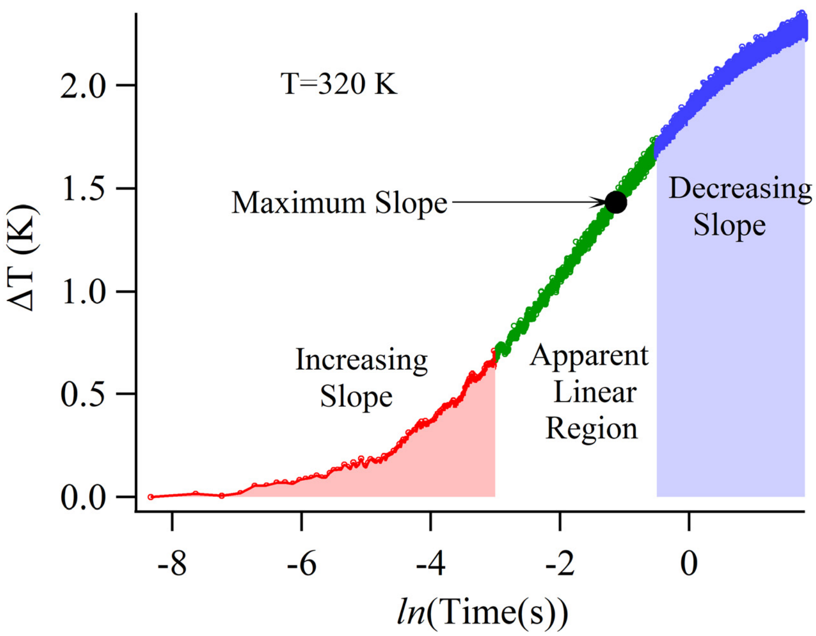

Figure 2.6: Illustration of the three distinct temperature rise regions observed in the experiments.

For the current work, as a first estimate, we choose the start time corresponding to the 1000th data point ($t_1 = 0.2398\ s$) and the end time to be the last acquired data point ($t_2 = 5.9998\ s$). This choice is based on a visual determination of the linear region observed in the experimental curve for ΔT versus time. An example of the range chosen for the fit is shown in Fig. 2.7a. The later onset of convection is however not apparent at lower temperatures of 274.5 K in the Fig. 2-7a. We find that a non-linear fit (3rd order polynomial) to region of interest helps us identify the regions of increasing and decreasing slope even in what visually appears to be straight-line segment for low temperature cases. For example, in Fig. 2-7a, the initial curvature is obvious for $-8 < ln(t) < -2$, but the effect of the onset of convection is not readily obvious in the range $-1.428 < ln(t) < 1.792$. Performing a third order fit helps us identify the point where the slope begins to decrease at longer times. This point has been identified by a filled symbol in Fig. 2-7b. Note that the value of the peak slope for the polynomial fit is within 0.7 % of the linear slope for this specific case. The maximum slope for the polynomial fit allows for a consistent choice of a value for the slope, unlike the linear fit, where the value will depend on the start and end points chosen by the experimenter. We therefore use the peak value of the slope (S) obtained using a third order polynomial fit to the apparent linear region to estimate the thermal conductivity using $k = q/(4\pi S)$. Note that the region of interest (apparent linear) must still be carefully be chosen while performing the fit.

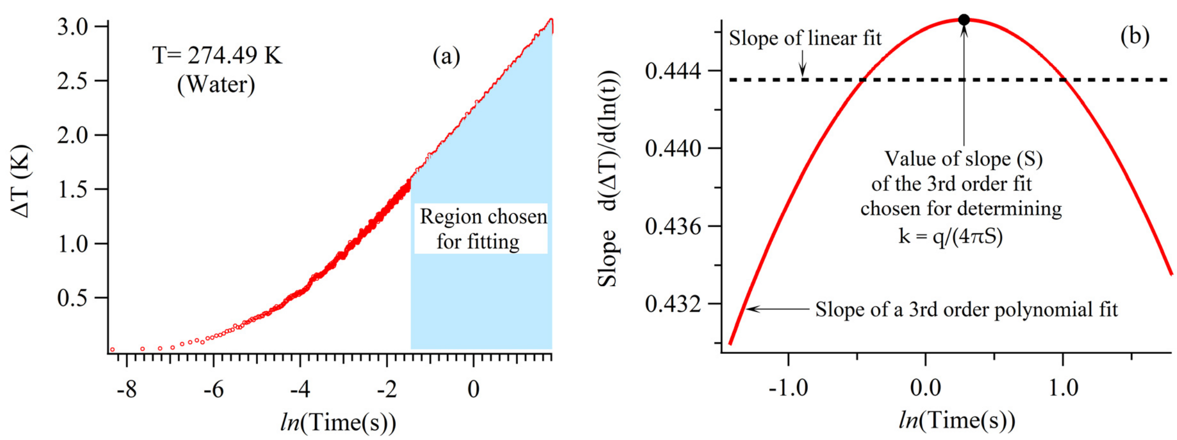

Figure 2.7: (a) Region of experiment used for fitting and extracting the slope (b) Comparison of slopes obtained using a linear and a 3rd order polynomial fit. The filled symbol represents the slope used in the experimental determination of thermal conductivity.

Chapter 3: Temperature Dependence of Thermal Conductivity for Water: Experiments and Computations

3.1 Thermal Conductivity Results for Water

Experimental thermal conductivity values for water for three different sets of experiments are shown in Figs. 3.1 (a)-(c) to illustrate the reputability and extent of scatter in the experiments. The three sets of tests were conducted with different samples of technical grade water and the temperature was slowly raised from approximately 273 K to 300 K over a 12-hour duration. The data show an increasing trend of thermal conductivity with an increase in temperature.

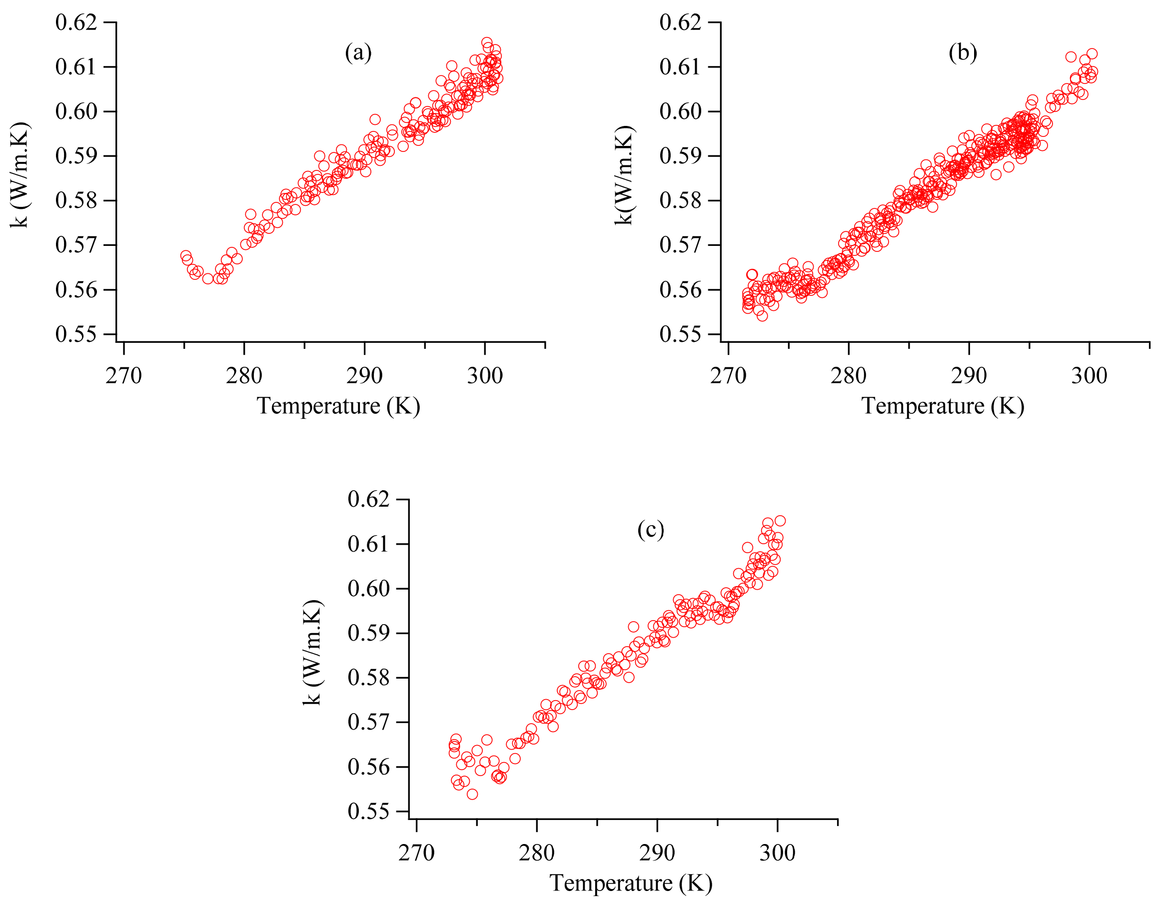

Figure 3.1: Three sets of experimental runs showing thermal conductivity variation with temperature for water.

It can be seen from Fig. 3.1 that the scatter in the experimental results tends to increase with rising temperatures. The three datasets are combined to obtain the overall results that show the temperature dependence of thermal conductivity of water. It is interesting to note that there is a local minimum in the thermal conductivity of water at around 276.89 K (3.74 °C). This slight dip appears in all the three data sets collected, as well as the consolidated data. We suspect that this is a related of the non-linear variation in density around this temperature range. Note that the maximum density for liquid water is close to 277.13 K (3.98 °C) [33].

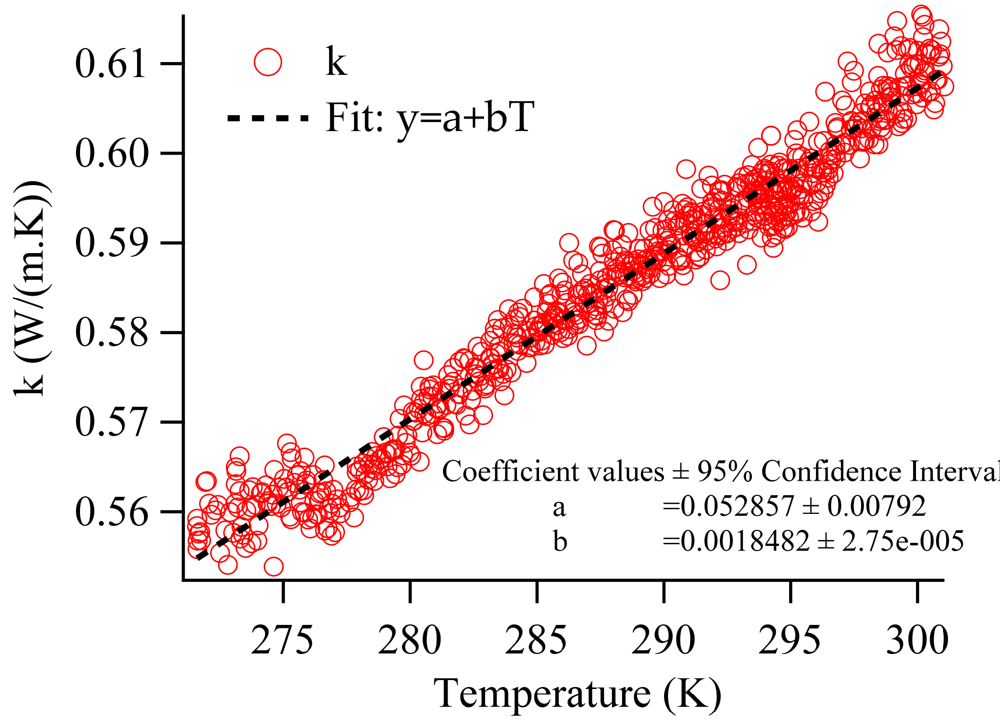

Figure 3.2: Consolidated data set for thermal conductivity as a function of temperature for current experimental sets for water.

The residuals of the fit to the experimental data are shown in Fig. 3.3. The plot in Fig. 3.3 shows that the largest one-sided residuals are observed at around 4 degree Celsius. The confidence and prediction bands for the regression analysis are shown as well.

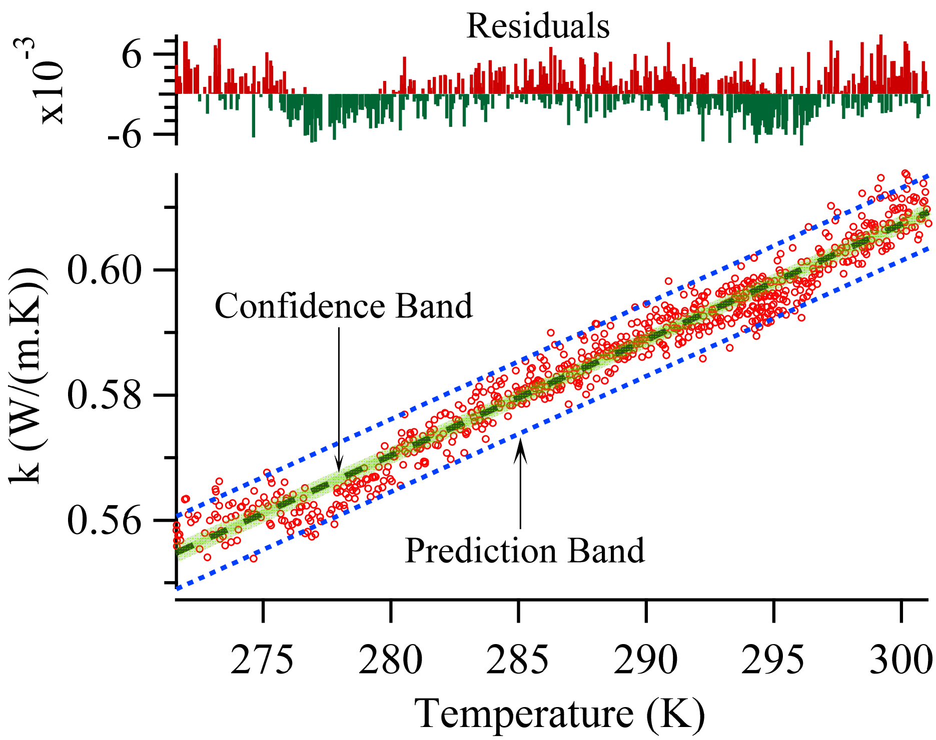

Figure 3.3: Residuals, confidence, and prediction bands (95%) for the linear fit to the current experimental data.

3.1.1 Comparison with Previously Reported Data

The current experimental results for the temperature dependence of thermal conductivity of water are compared to that reported in recent literature. The comparison also includes a dashed line showing the computed values obtained from the standard reference data from the study of Nieto de Castro et al.[26]. The work of Nieto de Castro et al. describes the reduced thermal conductivity of water as a second order polynomial over the temperature range of 274-370 K [26]. The plot in Fig. 3.4 shows that the current experiments consist of significantly larger number of data points over the temperature range of interest, exhibit the least scatter among all the experimental data sets, and are closest to the standard reference data. The current experimental observations are also nearly continuous over the entire temperature range. The plot also illustrates the utility of the current work in that it extends the experimental data to lower temperature values close to the freezing point of water.

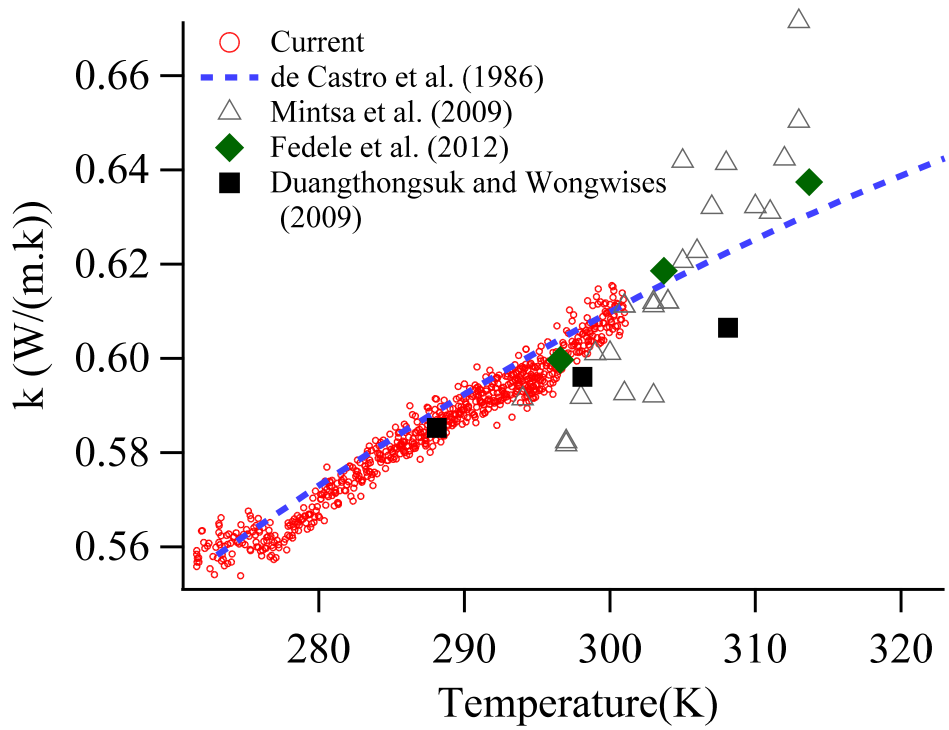

Figure 3.4: Comparison of current data with other recent studies for water.

3.2 Computed Results

3.2.1 Computational Specifications and Results

The heat transfer problem of an electrically heated platinum wire immersed in water is solved using the ANSYS Fluent CFD code. The problem is treated as axisymmetric because of the cylindrical symmetry. The governing equations for mass, momentum and energy conservation are given by [34]

$$\frac{\partial \rho}{\partial t}+\frac{\partial(\rho v_x)}{\partial x}+\frac{\partial(\rho v_r)}{\partial r}+\frac{\rho v_r}{r}=0 \qquad (3.1)$$

$$\frac{\partial(\rho\vec{v})}{\partial t}+\nabla\cdot(\rho\vec{v}\vec{v})=-\nabla p+\nabla\cdot(\bar{\bar{\tau}})+\rho\vec{g}+\vec{F} \qquad (3.2)$$

$$\frac{\partial(\rho E)}{\partial t} + \nabla \cdot \big(\vec{v}(\rho E + p)\big) = \nabla \cdot (k \nabla T) + S_h \tag{3.3}$$

Where x and r represent the axial and radial coordinates. The stress tensor $\bar{\bar{\tau}}$ in the momentum equation is given by:[34]

$$\bar{\bar{\tau}} = \mu[(\nabla \vec{v}) + (\nabla \vec{v})^T - 2/3\, \nabla \vec{v} I] \tag{3.4}$$

The quantities $\vec{F}$and S_h in the momentum and energy equation represent the external body force and volumetric heat source term, respectively. The current problem is treated as a natural convection problem, and the Boussinesq approximation is used for the density in the buoyancy term of the momentum equation.

$$\rho = \rho_o(1 - \beta(T - T_o)) \tag{3.5}$$

This approximation is valid as the temperature rise ΔT in the system is less than 3 Kelvin with $\Delta \mathrm{T} \ll 1$. Here $\beta = -\frac{1}{\rho}\left(\frac{\partial \rho}{\partial T}\right)$ is the volumetric thermal expansion coefficient, and ρ_o is the constant density of the flow at an operating temperature of T_o. The SIMPLE algorithm with a second order discretization scheme was used in the solution procedure.

Given the wide range of the length scales in the experimental apparatus ($a = 25 \times 10^{-6} m,\ L \approx 9.5\ cm$) it is prohibitively expensive to compute the solution for the entire domain while resolving the flow and thermal features near the heated wire. A section of the wire corresponding to length $150 \times a$ is considered along the axial direction, with $r = 0$ being treated as the axis. The radial extent of the problem is limited to four times the section of the wire length i.e. $600 \times a$. The grid distribution used is shown in Fig. 3.5 (a). A non-uniform grid distribution with a bias factor of 5 was used in the radial direction for the fluid domain while a constant number of equally spaced divisions was set for the solid. The electrical heating of the wire is represented by a volumetric heat source within the platinum wire. The strength of the volumetric heat source (Q) is obtained from the known experimental value of the power supplied ($317.95\ mW$) and the wire dimensions ($a = 25\ \mu m; L = 9.533\ cm$). Gravity acts along the axial direction as indicated by the arrow in Fig. 3.5 (a). The Material properties used in the simulations are summarized in Table 3-1.

Property	**Method**	**Value**
Water		
Density (kg/m3)	Boussinesq	$9.987E+02$
***Cp* (Specific Heat) (J/kg-K)**	constant	$4.186E+03$
Thermal Conductivity (W/m-K)	constant	$5.9374E-01$
Viscosity (kg/m-s)	constant	$1.0695E-03$
Thermal Expansion Coefficient (1/K)	constant	$1.7824E-04$
Platinum		
Density (kg/m3)	constant	$2.145E+04$
***Cp* (Specific Heat) (J/kg-K)**	constant	$1.330E+02$
Thermal Conductivity (W/m-K)	constant	$7.160E+01$

Table 3-1 Material Properties used in the simulations.

A pressure-inlet boundary condition was specified for the right and top boundaries with flow direction being normal to the boundary, while the left boundary was set to be of type pressure-outlet. The initial conditions correspond to a value of $T = 290.53\ K$ for both the fluid and solid domain, with a stationary fluid.

A solution corresponding to $t = 6s$ is shown in Fig. 3.5 (b). This time corresponds closely to the last acquired data point in our experiments ($Fo = 1363$) when the effects of convection are quite apparent. The streamtraces in Fig. 3.5 (b) clearly show the buoyancy induced flow along with the contours of the temperature in the fluid as well as the solid at the end of $t = 6\ s$. The maximum Rayleigh number based on the wire length, and the experimentally deduced $\Delta T = 2.87\ K$ at $t = 6s$, is calculated to be $Ra_L = \frac{g\beta\Delta T L^3}{\nu\alpha} = 2.86 \times 10^7$, and as such, a laminar free convection flow is to be expected. The transition to turbulence generally occurs over the range of $10^8 < Ra < 10^{10}$ [34].

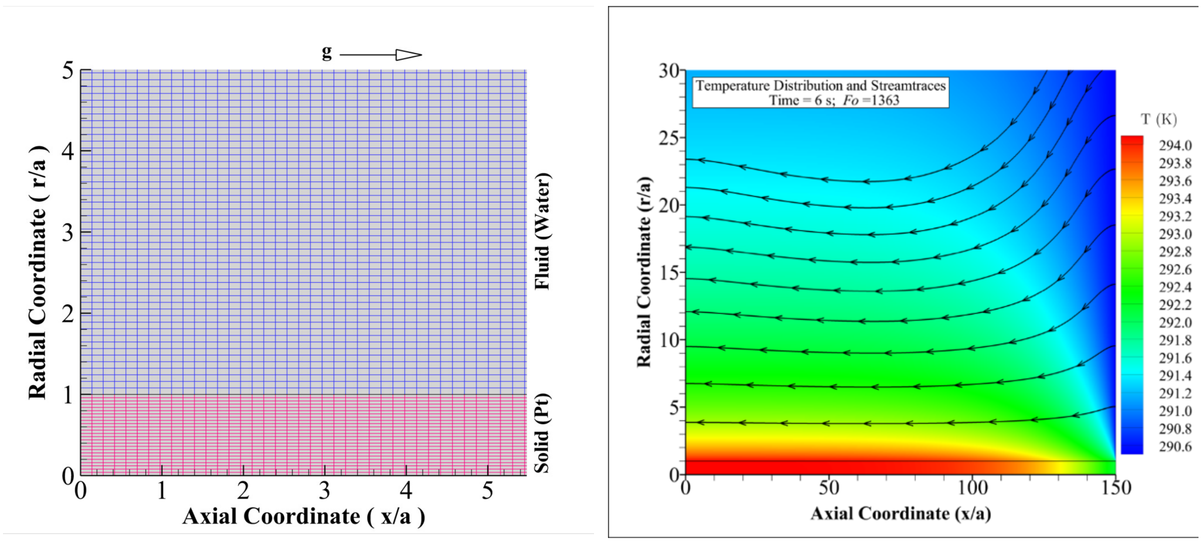

Figure 3.5: (a) A zoomed in view of the grid distribution. Note that the total simulated domain extends to 150 and 600 non-dimensional units in the axial (x/a) and radial(r/a) directions respectively. Here a *is the radius of the wire and* g *the acceleration due to gravity. (b) Streamtraces and temperature contours at t=6.0 s.*

For the given configuration, a characteristic reference velocity and can be defined as $u_0 = \sqrt{ag\beta(T_w - T_\infty)}$, where a is the wire radius. The wall temperature for evaluating this reference velocity is obtained at the axial midpoint of the wire. This velocity is can be used to non-dimensionalize the magnitude of the absolute velocities. Similarly, the temperature difference can be non-dimensionalized as $\lambda(T - T_\infty)/(Qa^2)$. Here Q is the strength of the volumetric heat source term in Watts per cubic meter.

3.2.2 Temperature Distribution and Local Heat Transfer Coefficients

The computed non-dimensional temperature and velocity magnitude contours corresponding to a time of 6-seconds is shown are Fig. 3.6 (a) and (b) respectively

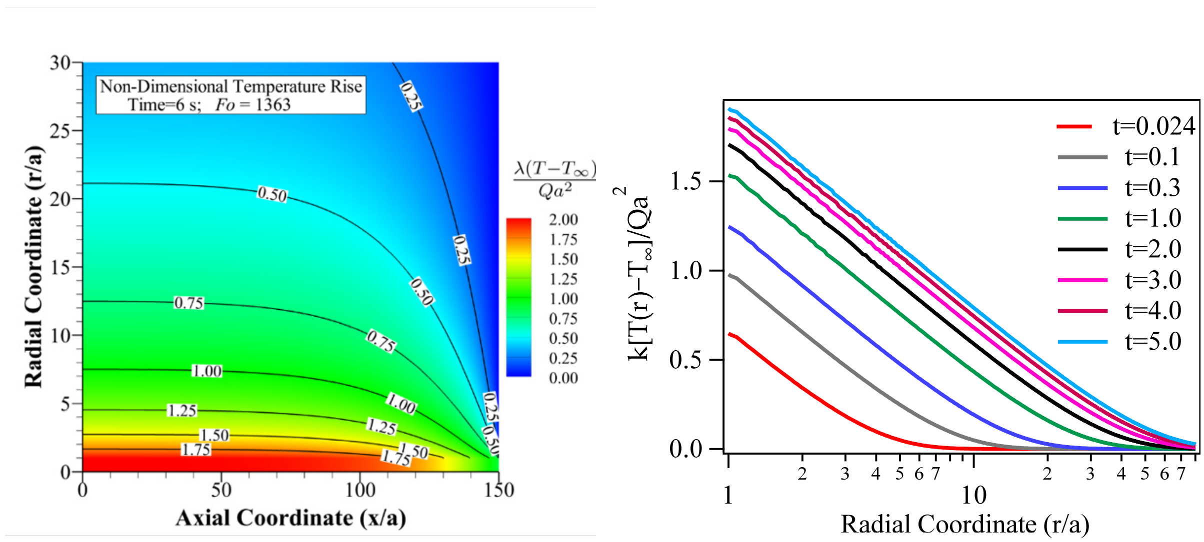

Figure 3.6: Computed contours of non-dimensional (a) Temperature rise at $t = 6s$*, and (b) the radial temperature distribution midway at* $x/a = 75$ *at various times.*

The contours of the non-dimensional temperature rise field show that the temperature along the wire surface increases as one traverses the axial direction from the right boundary inlet against the direction of gravity. This is expected since the coldest fluid is in contact with the wire surface at the inlet ($x/a = 150$). Fig. 3.6 (b) also shows the time evolution of the radial temperature distribution at the axial location corresponding to the wire midpoint. There is a relatively large change in ΔT at a given radial location during the earlier times, in that the curves are widely spaced between $t = 0.024$ and $t = 0.1$ as compared to that between $t = 4$ and $t = 5$ seconds. An interesting feature of the radial temperature distribution is that at any given time the trend is mostly logarithmic (straight line on a log scale) with respect to the radial distance except at large distances. The slopes of the straight-line segments on log-plot shown in Fig. 3.6 (b) are also very similar. This seems to suggest that the heat transfer is dominated by conduction and the fluid medium is apparently stationary. Furthermore, the radial extent diffusion of heat is limited to approximately 40 wire diameters.

Another important quantity of interest is the local heat transfer coefficient at the wire surface. The local heat transfer coefficient can be written as $h_x = \frac{q''_w(a,x)}{T_w(a,x)-T_\infty} = \frac{-k_f \frac{\partial T}{\partial r}|_{r=a}}{T_w(a,x)-T_\infty}$. Here k_f is the fluid thermal conductivity, $T_w(a,x)$ the local wire surface temperature, and T_∞ the far-field temperature. The local heat transfer coefficient scaled as $h_x 2a/k$ is shown in Fig. 3.7 (a) as a function of the axial co-ordinate at the instant corresponding to 6-seconds along with the steady-state value with dotted lines for comparison. Note that a steady solution exists because of the nature of the boundary conditions imposed. The right and top boundaries have been specified as pressure inlet while the left boundary is a pressure outlet. This would not hold true for an enclosed container, but is appropriate for an infinite fluid medium. In order to examine the variation of the local heat transfer coefficient with the distance from the 'entrance' on the right boundary of the simulation we define $x' = 150a - x$, where $150a$ is the total axial extent of the simulation domain. This x' is consistent with the distance commonly used in the literature. A plot of the variation of the scaled heat transfer coefficient under steady-state conditions is shown with x'/a in Fig. 3.7 (b). The local heat transfer coefficient for the steady state solution exhibits a power law variation with respect to the distance from the entrance. Note that the computed data shown in Fig. 3.7 (b) begins and ends at $x'/a = 1$ and 149 respectively, i.e. one wire diameter has been excluded from either end.

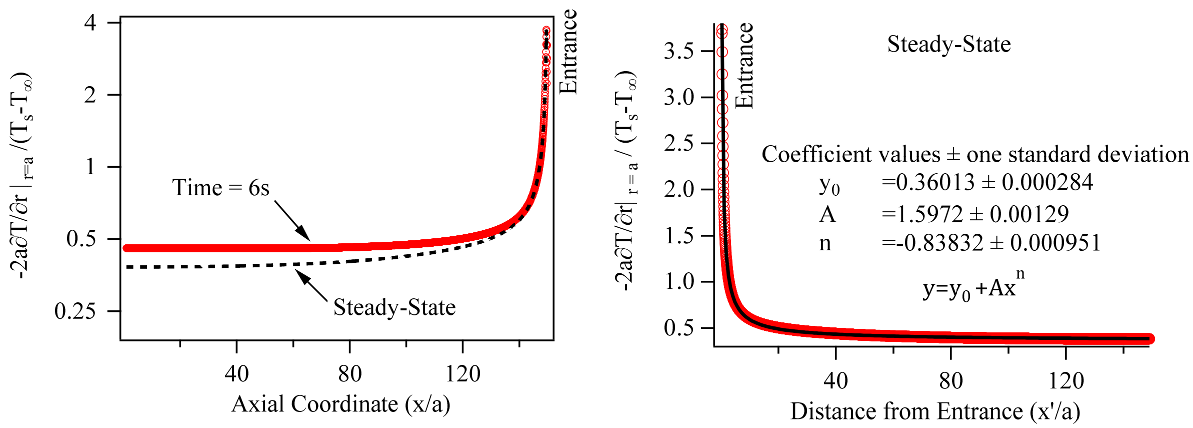

Figure 3.7: (a) Scaled local heat transfer coefficient (a) as a function of distance (b) Fit (solid line) to the steady state distribution as a function of distance, x' , from the entrance.

The variation of the scaled local heat transfer coefficient with time at a fixed location axially midway is shown in Fig. 3.8. The plot in Fig. 3.8 shows that the magnitude of the local heat transfer coefficient midway along the wire $(x/a = 75)$.

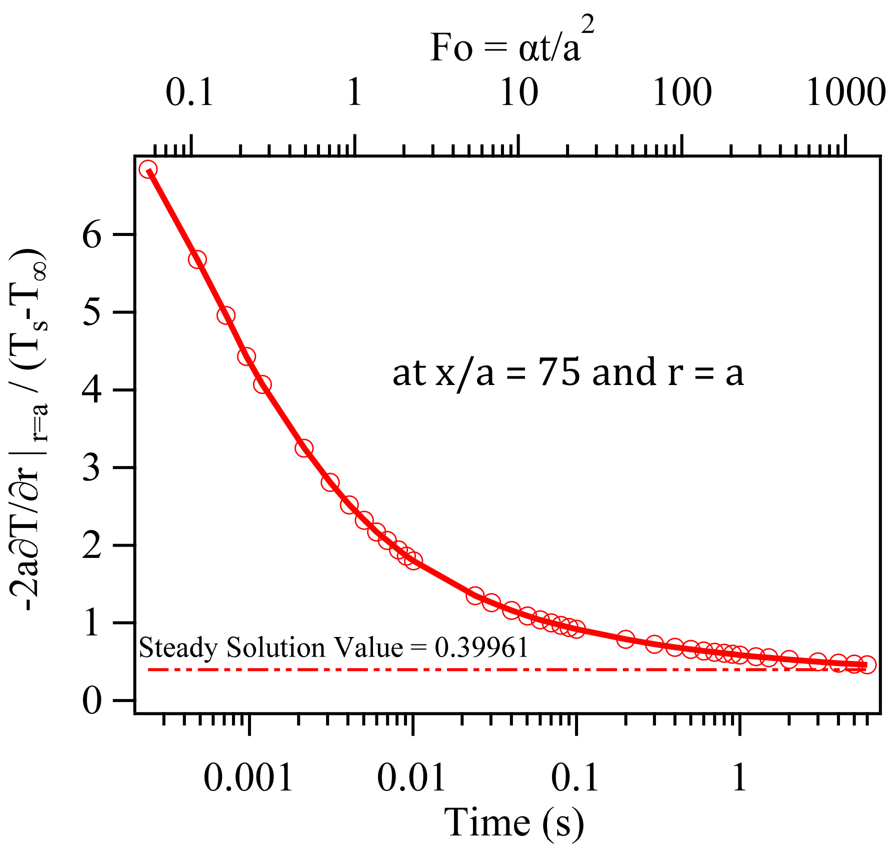

Figure 3.8: Scaled local heat transfer coefficient at $x/a = 75$ as a function of time.

Its magnitude decays monotonically with time and approaches a value of 0.3996 for the steady solution. The rate of change of the local heat transfer coefficient with time at the centerline is extremely rapid for $Fo < 1$, gradually tapers off in the range of $1 < Fo < 100$, and is negligible for $Fo > 1000$. Note that the appearance of the rapid change of slope has been somewhat suppressed due to the stretching out of the time axis on account of being plotted on a logarithmic axis. The smallest and largest values of times in the plot correspond to 0.24×10^{-3} and 6 seconds, respectively.

3.2.3 Velocity Field

The velocity magnitude field for $t = 6$ seconds is shown in Fig. 3.9 (a). The contours correspond to values of $\frac{|V|}{\sqrt{ag\beta(T_W - T_\infty)}}$. As noted previously, the wall temperature was evaluated at the axial midpoint on the surface of the wire. The peak velocity magnitude occurs radially at a distance of approximately 5 wire diameters from the surface and is shifted slightly toward the outlet side with respect to the center of the wire.

The peak velocity magnitude in Fig. 3.9 (a) is equal to 11.02 microns/second. This implies that a fluid parcel near the wire can translate roughly 0.441 wire diameters every second because of the buoyancy-induced force resulting from the density gradient. The axial velocity profile as a function of the radial coordinate is plotted for various times in Fig. 3.9 (b). The profiles were obtained at a fixed axial location in the middle of the domain. The axial velocity profiles exhibit a peak and then gradually reduce to zero within about 40 wire diameters.

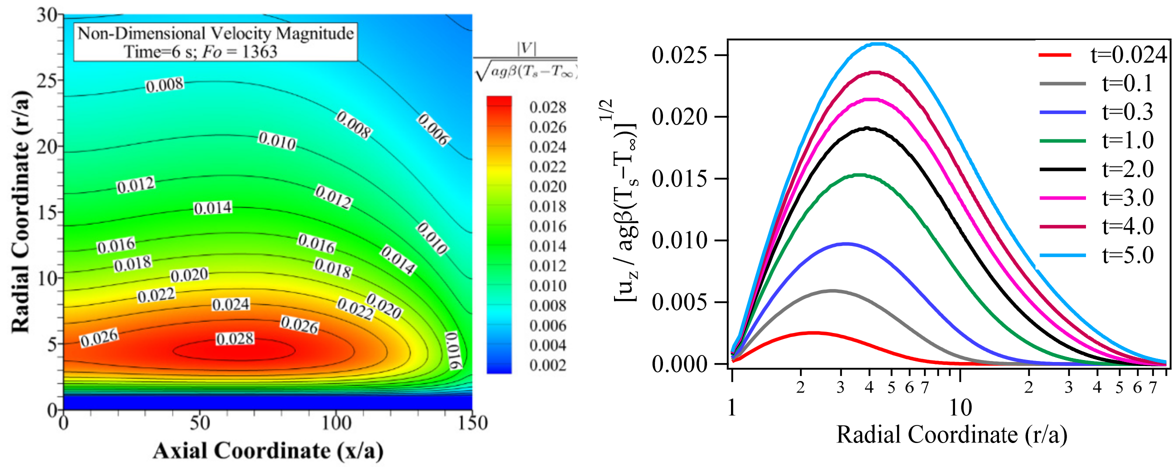

Figure 3.9: Non-dimensional radial temperature and axial velocity profiles at $x = L/2$.

3.3 Comparison of Experimental and Computed Results

While there have been several experimental efforts using the transient hot-wire method that are far less studies that computationally examine the temperature and flow-fields for this configuration. The computational study shown in the previous sections enables us to compare the experimentally deduced temperature profiles to those obtained from simulations as shown in Fig. 3.10 (a). The agreement between the experimental and computed temperature is within approximately 0.5 K within the entire time span. The difference in temperature rise (ΔT) increases for up to approximately 0.01s and then is nearly constant for the subsequent time duration. Furthermore, the shape of the experimental temperature time curves is well predicted by the simulations, including the early nonlinear temperature rise on a log scale during the early part of the transient $t < 0.01\ s$. The slopes of the experimental and computed results are also very similar during later times.

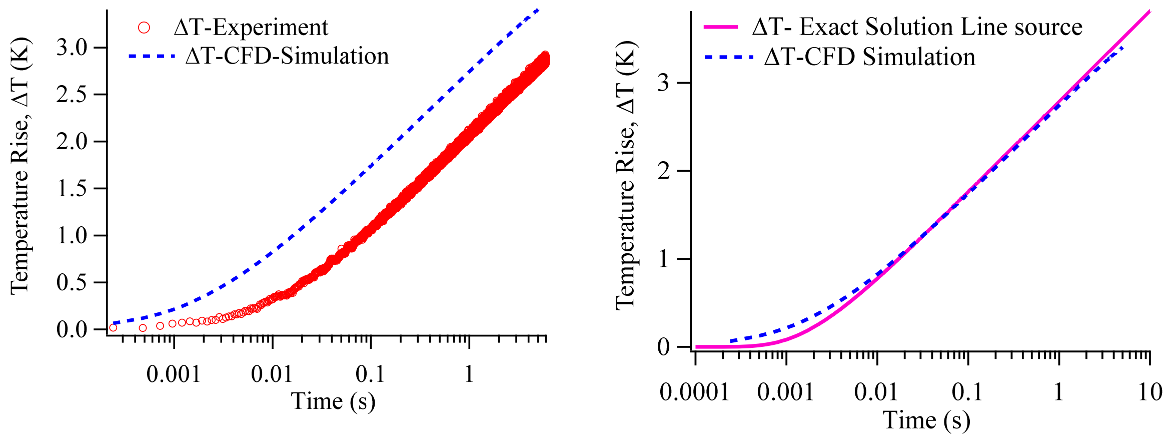

Figure 3.10: Comparative temperature-time history for (a) Experiments versus CFD results, and (b) Exact solution to heat diffusion equation for a line source in an infinite media versus CFD results.

The temperature rise from the CFD simulations is also compared to the analytical solution for the heated line source in an infinite solid medium, as shown in Fig. 3.10 (b). It can be seen that there is a very good agreement between the two, thereby implying that there is only a limited influence of the convective effects on the temperature rise for the duration of heating under consideration.

3.4 Summary

The transient hot-wire technique was used to obtain the temperature dependence of the thermal conductivity of liquid water over a temperature range of 273 to 301 K. The experimentally determined values show close agreement to the standard reference values. We find that in order to obtain the correct temperature dependence of the thermal conductivity it is essential to determine the variation of temperature coefficient of resistance of the platinum wire and not assume it to be a constant. A method to minimize user bias in determining the slope of the temperature-rise versus logarithm of time curve used to determine the thermal conductivity was presented. 2-D Axisymmetric CFD simulations were conducted to understand the nature of the temperature of velocity field in the vicinity of the wire. A comparison of the experimental and computed results showed a good agreement for the temperature rise of the wire with respect to time at a constant heating rate.

Chapter 4: Temperature Dependence of Thermal Conductivity for Ethylene Glycol, Glycerol, and Propylene Glycol

4.1. Ethylene Glycol

Ethylene glycol is an organic compound produced on an industrial scale. The molecular formula of ethylene glycol is $C_2H_6O_2$, and the melting and boiling point are $260.5\,K$ and $270\,K$ respectively [35, 36] The compound is a common heat transfer fluid and used as an antifreeze and deicing agent. It is also used as a solvent and in hydraulic brake fluids. It is therefore important to study the thermal transport properties of this liquid.

DiGuillo and Teja [35] were two early experimentalists who measured the thermal conductivity of the first-six members of the poly ethylene glycols and their binary blends. Their study also included measurements for ethylene glycol. The temperature range of their experiment was from $298.6\,K - 471.3\,K$, and the reported thermal conductivity for ethylene glycol was $0.2541\,W/(m \cdot K)$ to $0.2444\,W/(m \cdot K)$ at the high and low temperature limits. They used the transient hot-wire method to carry out their measurements. Their results exhibit a slight increase in the thermal conductivity of ethylene glycol with temperature for temperatures between $290 - 415\,K$ followed by a reduction for temperatures up to $480\,K$.

Another study by Azarfar et al. [37] also used the transient hot-wire to study the thermal conductivity of ethylene glycol. They used a copper micro-wire instead of the conventional platinum wire in their apparatus. Measurements for ethylene glycol were carried out in the temperature range of $283 - 313K$. Their reported thermal conductivity values for the thermal conductivity of ethylene glycol were 0.2433 and $0.2537\ W/m \cdot K$ for temperatures of 283 and $313\ K$, respectively. They reported that the average uncertainties were in the range of $\pm\ 0.9$ percent.

Lin et al. [38] used molecular dynamics simulations to investigate the thermal conductivity of ethylene glycol. This study computationally identified the major contributions to thermal conductivity from rotational energy transfer, intramolecular interactions, and hydrogen bonds. They conclude that intramolecular hydrogen bonds can have a major influence on the variation of thermal conductivity with temperature. A temperature range of $298 - 470\ K$ was investigated in their work. Various molecular models were used to obtain thermal conductivity as a function of temperature. The thermal conductivity was relatively high at $298\ K$ compared to Digullo's and Teja's [35] experiment, but the thermal conductivity showed a good match at $470\ K$.

Beck et al. [39] enhanced the thermal conductivity of ethylene glycol by adding aluminum oxide nanoparticles to ethylene glycol. They measured the thermal conductivity by using the hot-wire transient method, and the temperature range was 290 to 298 411 K. The volume fraction of Al_2O_3 was 1% to 4%, and the thermal conductivity exhibited and increase to 0.285 $W/(m \cdot K)$ at 409 K in 3.71% of the volume fraction of Al_2O_3.

For the current experiments presented in this thesis, ethylene glycol was purchased from Fisher Scientific, and the purity of ethylene glycol is greater than 99.96%. In this current work, the thermal conductivity of ethylene glycol was measured over a temperature range of $260 - 340\ K$ using the transient hot-wire method. The temperature range was traversed thrice to produce three data sets which were the aggregated to obtain the final results for the temperature dependence of the thermal conductivity.

4.1.1 Thermal Conductivity Results for Ethylene Glycol

The results for three different experimental runs for ethylene glycol are shown in Figs. 4(a)-(c). It can be seen that the thermal conductivity of the three sets shows an increasing trend with temperature. For the current ethylene glycol experiments, more than 300 pieces of individual data are collected for each run. It was found that for each run, convection starts at around 340 to 350 K. Therefore, the data collection was stopped in that temperature range. There is an excellent run-to-run reproducibility among the three datasets shown in Fig. 4.1.

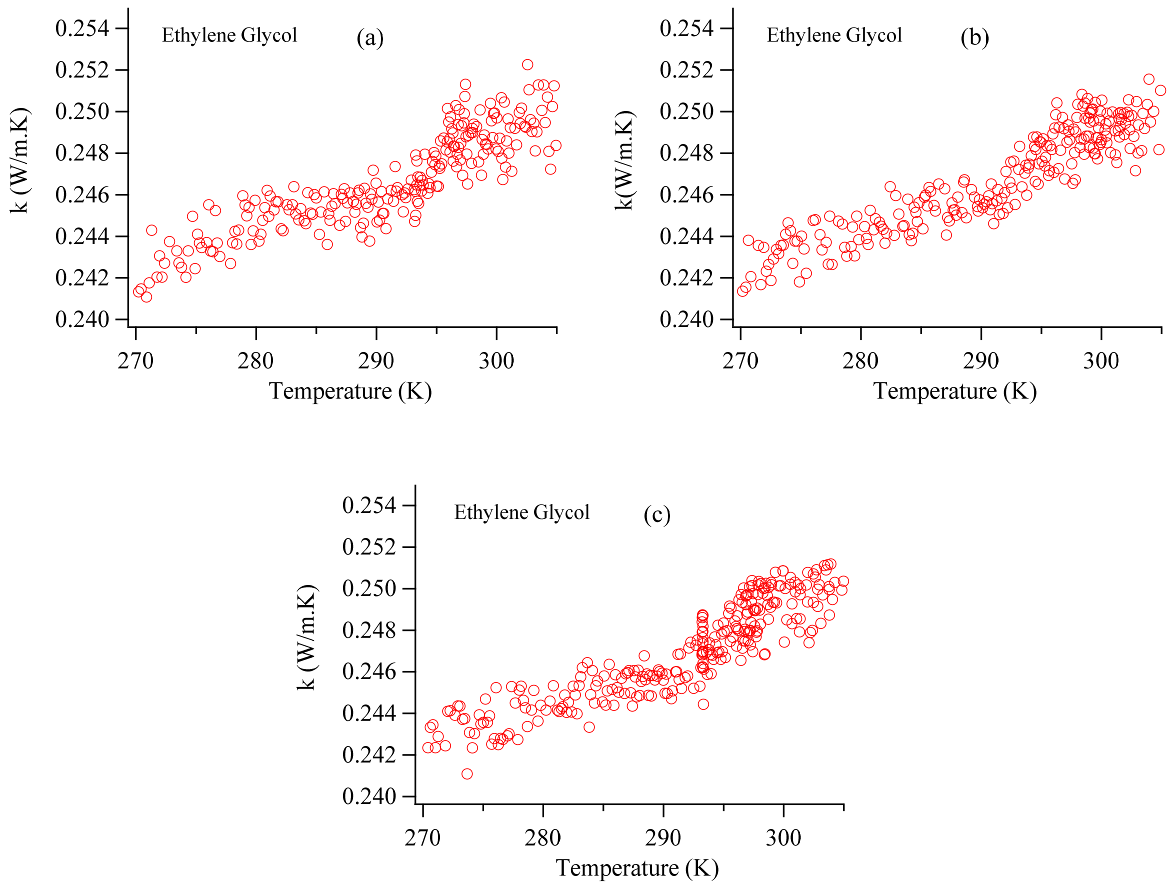

Figure 4.1: Three sets of experimental runs showing thermal conductivity variation with temperature for ethylene glycol.

The three datasets are combined to obtain a consolidated plot for the thermal conductivity as a function of temperature and is shown in Fig. 4.2. A linear fit to the data is also shown as a dashed line. It can be seen that overall the thermal conductivity shows an increasing trend with temperature for the given test range. The slope of the straight line for ethylene glycol

($b = 1.8548 \times 10^{-4}$) though is significantly lower compared to that of water ($b = 18.482 \times 10^{-3}$). The thermal conductivity variation for ethylene glycol is approximately 6.16 % over the entire temperature range.

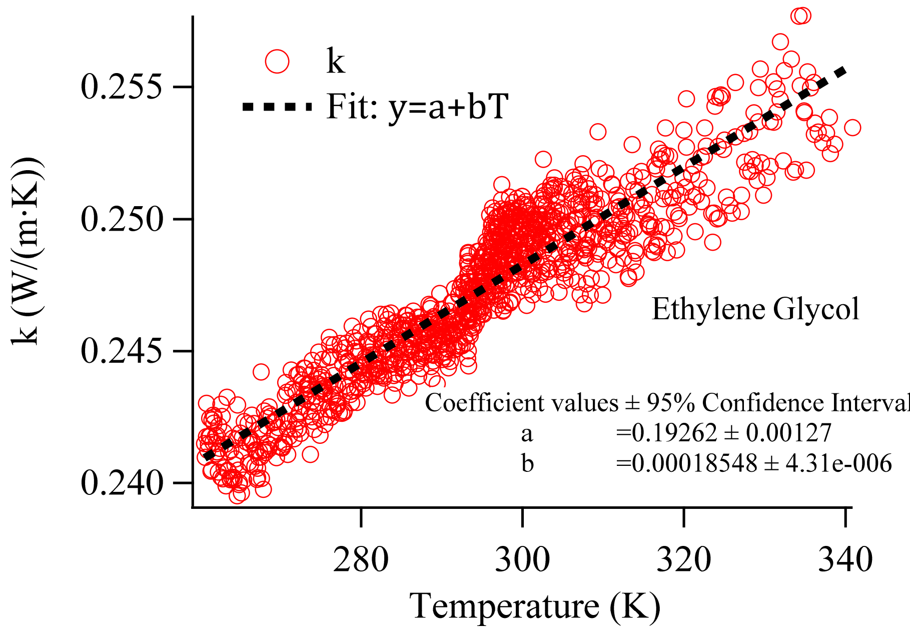

Figure 4.2: Consolidated data set for thermal conductivity as a function of temperature for current experiments for ethylene glycol.

The experimental results a 6.2 percent change in thermal conductivity when the temperature varies over the range of $260 - 340\ K$.

For clarity, Fig. 4.3 separately plots the residuals, confidence, and prediction bands (95%) for the linear fit to the current experimental data for ethylene glycol. There are very few data points that are outliers when assessed by the criterion of inclusion within the prediction band.

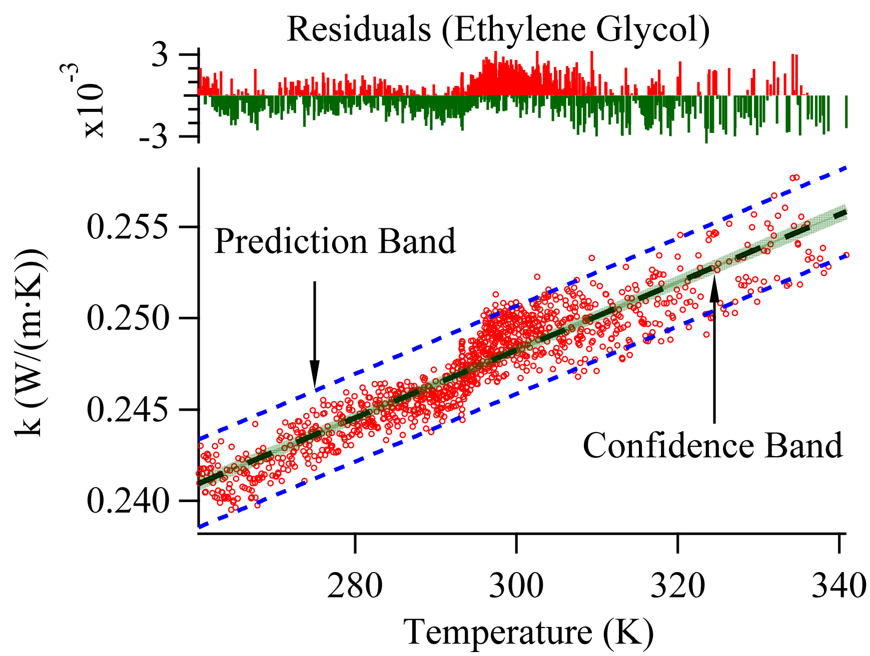

Figure 4.3: Residuals, confidence, and prediction bands (95%) for the linear fit to the current experimental data for ethylene glycol.

In order to validate the current results we compare it with data reported in some recently published work. Figure 4.4 shows the comparison between the current work, the study Azarfar et al. [37], Digullo et al. [35], and Pastoriza-Gallego et al. [40]. The current results are in good comparison with all three previously reported work. Interestingly, the current experimental results fall between the results of DiGuilio et al. [35], and Pastoriza-Gallego et al. [40] over the entire temperature range, with the results from Pastoriza-Gallego et al. [40] being consistently lower than the current study. The results for the other two studies are slightly on the higher side as compared to the current data. Furthermore, though the results of Pastoriza-Gallego et al. [40] exhibit as slope similar to the current data for temperatures below 323 K. Another noteworthy point is that all the datasets, including that of the current work, show an increase in thermal conductivity of ethylene glycol with increasing temperature. Note that that the comparison in Fig. 4.4 has been restricted to the first of the three runs in the current study. This is to enable clarity in the Fig. 4.4, as the combination of all three sets would suppress the limited number of data points from the other studies.

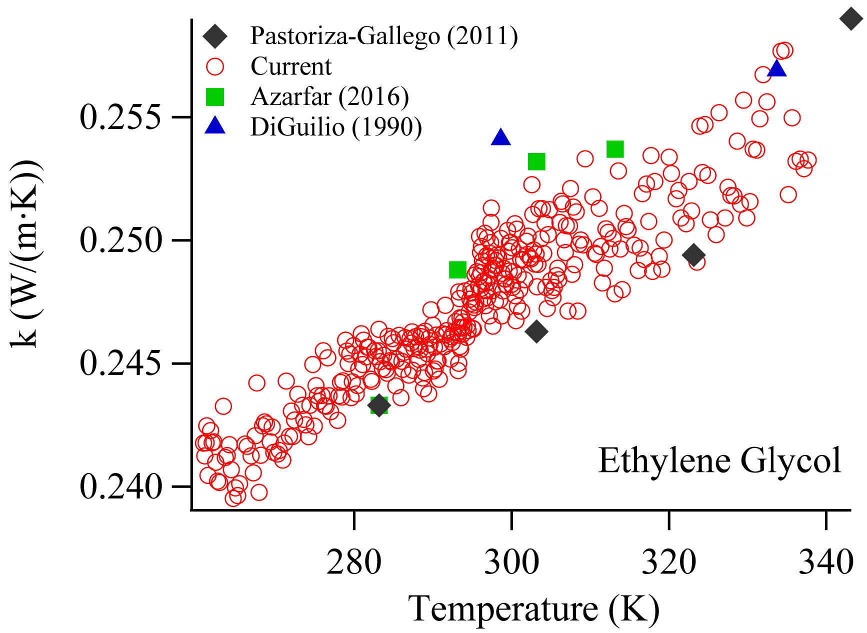

Figure 4.4: Comparison of current data with other recent studies for ethylene glycol.

4. 2 Glycerol

The word glycerol derives from the Greek term for sweet "glykys", because of its sweet taste. Glycerol was discovered in 1779 by the Swedish chemist Carl W Scheele. The molecular formula of glycerol is $C_3H_5(OH)_3$. It has a melting point close to room temperature ($291.35\ K$), and the boiling point is $563.15\ K$ [41, 42]. It is also commonly referred to as glycerin or glycerine. Glycerol-water solution is used to prevent freezing at low temperatures, and it was used as antifreeze before the discovery of ethylene glycol. At low temperatures, glycerol has a tendency to supercool rather than crystallize [43]. Given its interesting heat transfer characteristics it was decided to study the response of its thermal conductivity to temperature variation at temperatures near and above room temperatures.

Among the studies related to the measurement of transport properties of glycerol are those of Sun et al. [44] who used a laser based thermal pulse technique to make simultaneous measurements of thermal conductivity and diffusivity. There experimental efforts yielded a value of $0.29\ W/(m \cdot K)$ corresponding to a temperature value of $296.45\ K$. The principle of their measurements was based on photothermal deflection of a laser probe beam that occurs due to a temperature gradient resulting from a prior square heating pulse applied to a thin heating wire. This work provided values for thermal conductivity at a single temperature. Determination of the thermophysical/transport properties in their work was done by fitting computed results for solutions to the heat conduction problem to the measured time-dependent beam deflection.

Another experimental study that reported the thermal conductivity of glycerol is that by LeBrun and Markides [45] who used deionized water and glycerol as validation targest for a Galinstan-filled capillary probe for thermal conductivity measurement of molten salts. Their apparatus was a modified transient-hot wire and was designed to function in harsh environments and work with ionic liquids under high temperature conditions. The sensing element in their device comprised of a U-shaped quartz-capillary filled with liquid Galinstan. The temperature range of their measurements for the thermal conductivity of glycerol was between $301.7 - 431.2\ K$, and the thermal conductivity at those two temperatures were $0.2903\ W/(m \cdot K)$ and $0.3028\ W/(m \cdot K)$, respectively. Their reported estimate of error for the measurements was less than 2%.

There have also been attempts to enhance the thermal conductivity of heat transfer liquids by dispersing nanoparticles in them in order to create so-called nanofluid. A study by Sharifpur et al. [46] looked at enhancing the thermal conductivity of glycerol by mixing glycerol with nanoparticles of aluminum oxide. They measured the thermal conductivity with nanoparticles of three different sizes corresponding to $31\ nm$, $55\ nm$ and $134\ nm$ in diameter. They pointed out that the thermal conductivity of the glycerol-based nanofluids with aluminum oxide Al_2O_3 increased by 19.5% at a 4% volume fraction for the $31\ nm$ particles. The device used in their measurements was from a commercial vendor (KD2 Pro, Decagon Devices, Pullman, WA) and the temperature range reported in their study was from $293.15 - 318.15\ K$. The underlying principle of KD2 Pro was the transient hot-wire method. The reported uncertainty in measurements of the thermal conductivity was between $5.1\% - 8.5\%$.

Another effort to increase the thermal conductivity of glycerol was reported by S. Akilu et al. [47] who dispersed silicon carbide nanoparticles in a mixture of glycerol and ethylene glycol The ratio of the glycerol to ethylene glycol was in the proportion of $60{:}40$ by weight. The temperature range of their experiment was between $288.15 - 348.15\ K$, and the size of the SiC nanoparticles of ranged between $45 - 65\ nm$. The maximum concentration of nanoparticles in the mixture was 1% of weight. They noted that the thermal conductivity of the mixture with the nanoparticles of (SiC) increased 24.5% at $304\ K$ compared to the base liquid mixture.

The current experiments examine the thermal conductivity of neat glycerol in the temperature range of $290 - 350\ K$. Glycerol for this study was obtained from Macron Fine Chemicals™, and had a purity of 99.99%. The temperature dependence was obtained by concatenating three independent sets of data that were collected during different days over a one-month period. Note that the test for glycerol begin very close to the room temperature since it has a melting point of $291.35\ K$.

4.2.1 Thermal Conductivity Results for Glycerol

The plots in Fig. 4.5 (a-c) show the results of the three sets of experiments conducted to obtain the thermal conductivity of glycerol. There is a relatively larger scatter in the data compared to ethylene glycol over the same temperature range. One must not over-interpret the result since the variation at a given temperature is still less than $0.003\ W/m \cdot K$. The plots show a very good run-to-run reproducibility with very similar thermal conductivity values both the lower and higher temperature ends.

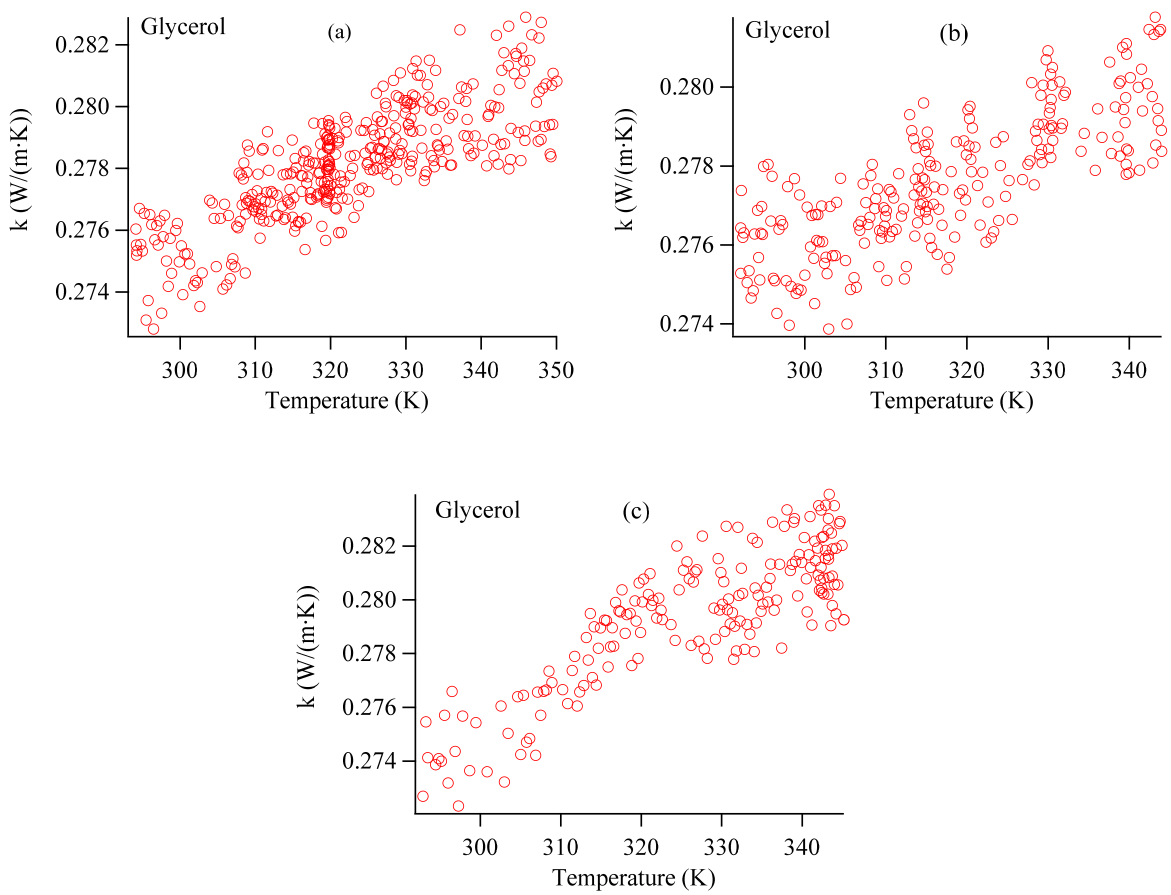

Figure 4.5: Three sets of experimental runs showing thermal conductivity variation with temperature for glycerol.

The data points obtained from the three distinct runs are combined into a single plot. A linear regression is performed on the consolidated data set. The slope of the line fit to thermal conductivity versus the temperature for glycerol ($b = 1.1321 \times 10^{-4}$) is of the same order of magnitude, but slightly lesser that of ethylene glycol ($b = 1.8548 \times 10^{-4}$). The thermal conductivity variation for glycerol is approximately 3.34 % over the entire temperature range while a 6.16 % was observed for ethylene glycol for the same temperature range.

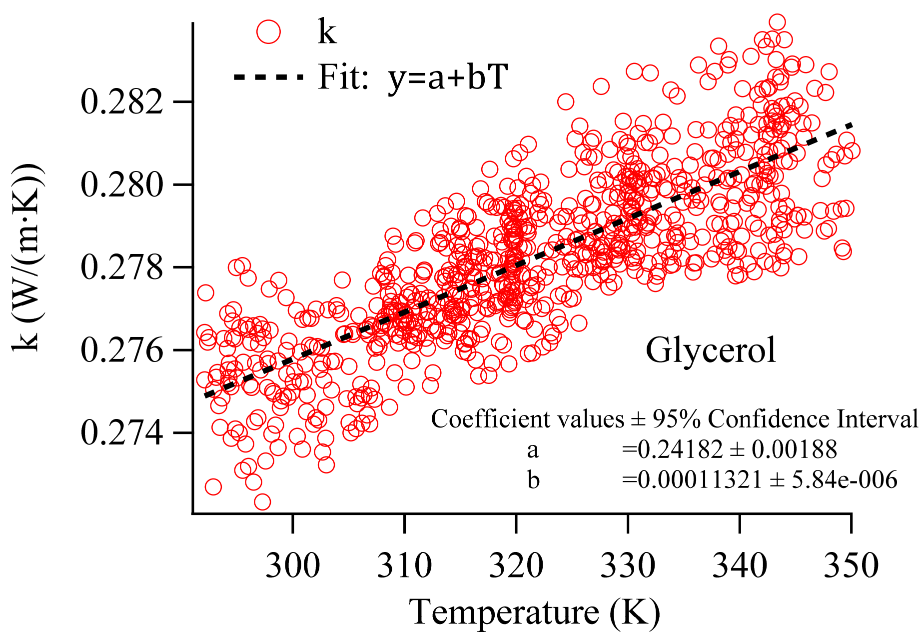

Figure 4.6: Consolidated data set for thermal conductivity as a function of temperature for current experimental sets for glycerol.

A most remarkable point is that the current apparatus can distinguish very minute differences in thermal conductivity with relative ease. This can be clearly seen if one compares the values for thermal conductivities for glycerol with ethylene glycol as predicted by the straight line fit for the two liquids at, say $300\ K$. At that temperature the difference in the predicted thermal conductivities differ by only 0.02752 units.

For clarity, Fig. 4.7 separately shows the residuals, confidence, and prediction bands (95%) for the linear fit to the current experimental data for glycerol. Most of the outliers are seen to occur in the high temperature range with data points located outside the upper line for the prediction band.

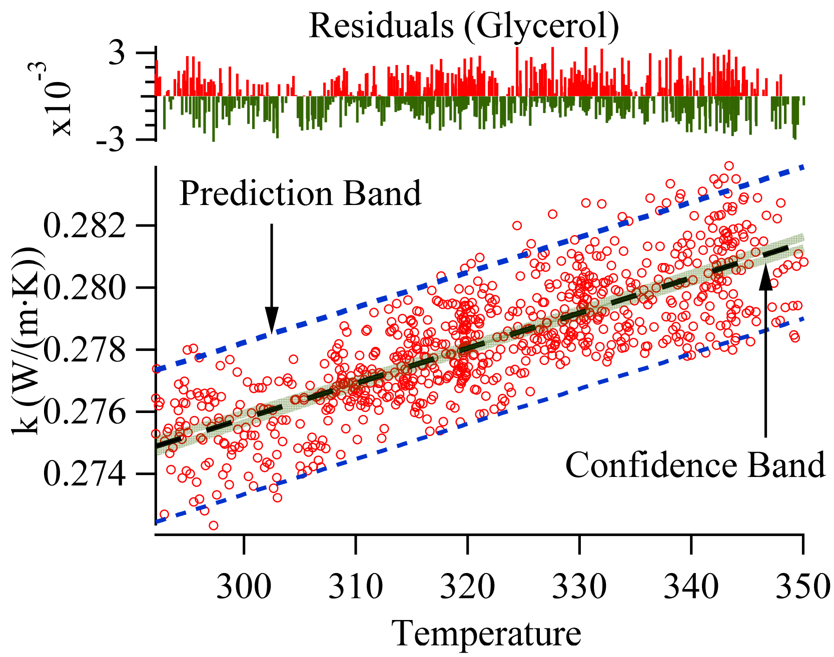

Figure 4.7: Residuals, confidence, and prediction bands (95%) for the linear fit to the current experimental data for glycerol.

The current experimental data is next compared to some previously reported results in the literature. The comparative plot in Fig. 4.8 shows that the study of Sharifpur [46] shows a good agreement in the low temperature region but deviates towards higher values for higher temperatures. Another set of data from the study of Gelder [48] is higher by approximately 4% over the entire temperature range. Finally, the results reported by LeBrun and Markides [45] are the highest among all the reported results. These differences, except for the results by LeBrun and Markides [45] are less than 10%. Therefore, we can say that the current experiments are in fair agreement with most of the previous studies. Note however, that all the three datasets predict an increasing thermal conductivity for glycerol with increasing temperature, similar to the current results.

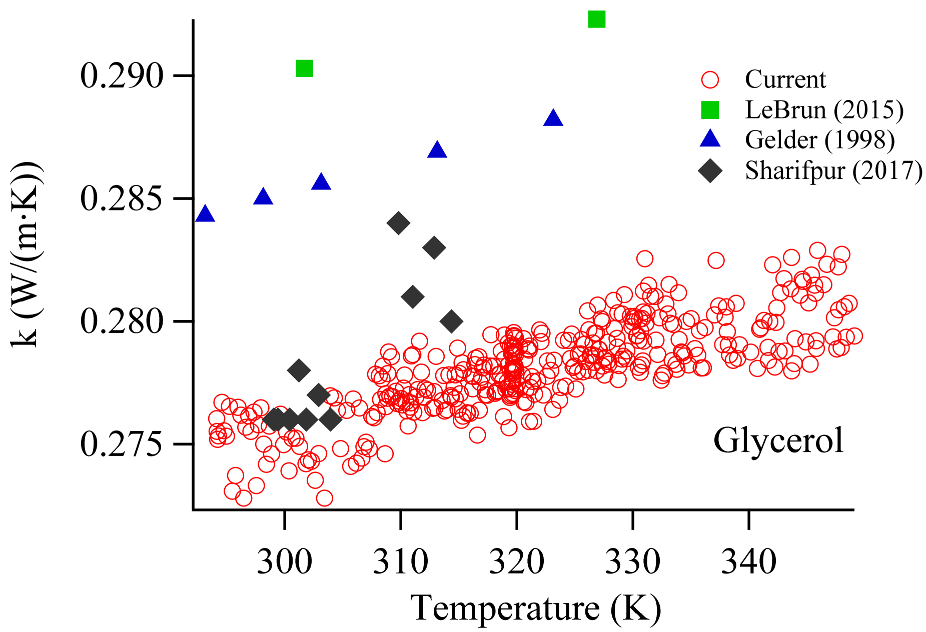

Figure 4.8: Comparison of current data with other recent studies for glycerol.

4.3 Propylene Glycol

Propylene glycol is a synthetic liquid which is hygroscopic in nature. It is also known as such as 1,2-dihydroxypropane, and 1,2-propanediol. The molecular formula of propylene glycol is $C_3H_8O_2$. Propylene glycol is used in producing polyester compounds, de-icing solutions, antifreeze and in heat transfer the same way ethylene glycol is used. For safety reasons, it is preferable to use propylene glycol instead of ethylene glycol because of the high toxicity of ethylene glycol [49]. The melting point of propylene glycol is $213.15\ K$ and the boiling point is $460.15\ K$ [50]

Sun and Teja [51] studied the thermal conductivities, densities, and viscosities of propylene glycol, dipropylene glycol, and tripropylene glycol. The technique used in their experiment was the transient hot-wire method. The temperature range for their experiment was $290\ K - 460\ K$. The reported uncertainty of their results was ± 2%.

Deng et al. [52] examined the thermal conductivities of 1, 2-Ethanediol and 1, 2-Propanediol also using the transient hot-wire method, and the temperature range for the experiments was $253.15 - 373.15\ K$, at atmospheric pressure condition. The uncertainty in the results for thermal conductivity was better than ± 2%. Interestingly, their results showed that the thermal conductivity decreased with increasing temperature.

Another study by Palabiyik et al [53] was related to the enhancement of the thermal conductivity of propylene glycol by the addition of Al_2O_3 and TiO_2 nanoparticles. The temperature range for this study was $293.15 - 353.15\ K$. The size of nanoparticles of Al_2O_3 and TiO_2 nanoparticles were 13 nm and 21 nm, respectively. They compared their result for thermal conductivity of pure propylene glycol with Sun's and Teja's work [51], and found that the difference between their and Sun's and Teja's results was less than ± 5%. They reported that the thermal conductivities of propylene glycol based Al_2O_3 and TiO_2 nanofluids showed an increase of 11%, and 9%, respectively.

Suganthi et al. [54] obtained the thermal conductivity of propylene glycol based ZnO nanofluids as a function of temperature and nanoparticles concentration. The temperature range for their study was $283.15 - 333.15\ K$. The volume fraction of nanoparticles was less than 2%. The size of nanoparticles was between 35 and 40 nm. They report that the highest enhancement of the thermal conductivity occurred at the lowest temperature.

We examine the thermal conductivity of pure propylene glycol in this study in the temperature range of $235 - 360\ K$. Propylene glycol was purchased from Tokyo Chemical Industry Co., Ltd, and its purity was greater than 99.0 %.

4.3.1 Thermal Conductivity of Propylene Glycol

In a procedure similar to the other three liquids, we obtain three independent data sets over a wide range of temperature, which are shown in Fig. 4.9. The three are very similar to each other.

The only difference for these three sets is that the readings were collected while the temperature range was traversed from the high to the low temperature region. The data for the three other fluids presented previously were collected with the temperature range being traversed from the low to the high region. Regardless of the direction of traversal, the propylene glycol thermal conductivity still shows an increase with increasing temperature. The experiments had to be limited to a value of $360K$ because of the onset of convection for the current operating conditions. Typically, about 180 thermal conductivity data points were collected over the entire temperature range for each of the three runs.

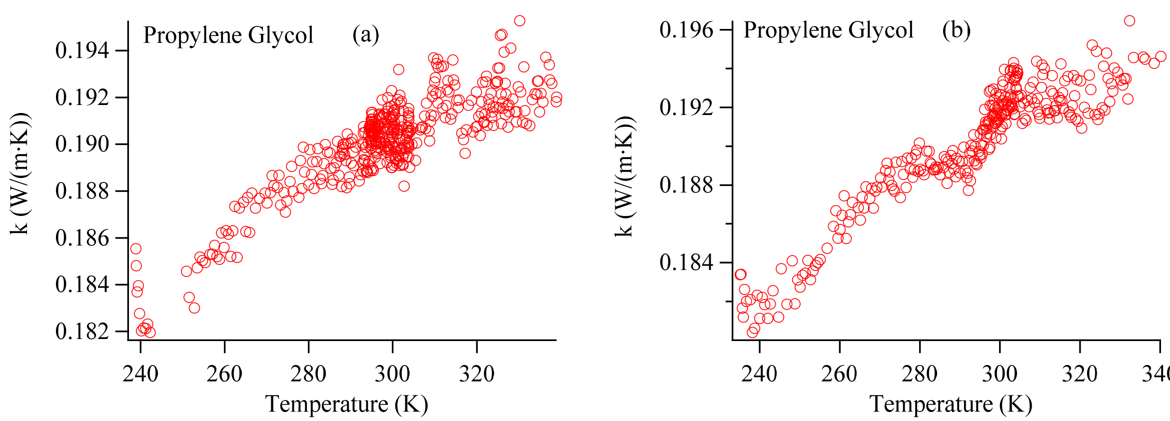

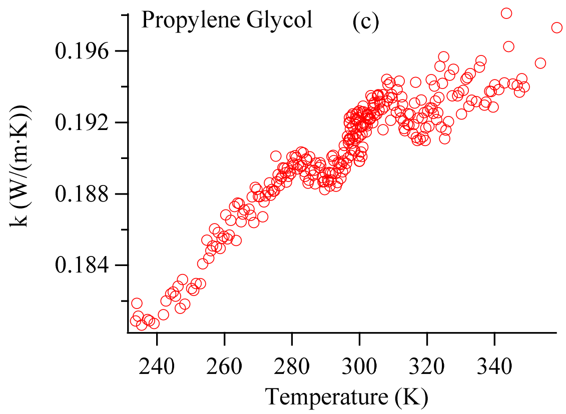

Figure 4.9: Three sets of experimental runs showing thermal conductivity variation with temperature for propylene glycol.

The three sets of data shown in Fig. 4.9 are combined to produce a consolidated data set. A linear regression is done on the combined data set to assess the influence of temperature by examining the slope of the fitted thermal conductivity values with respect to temperature.

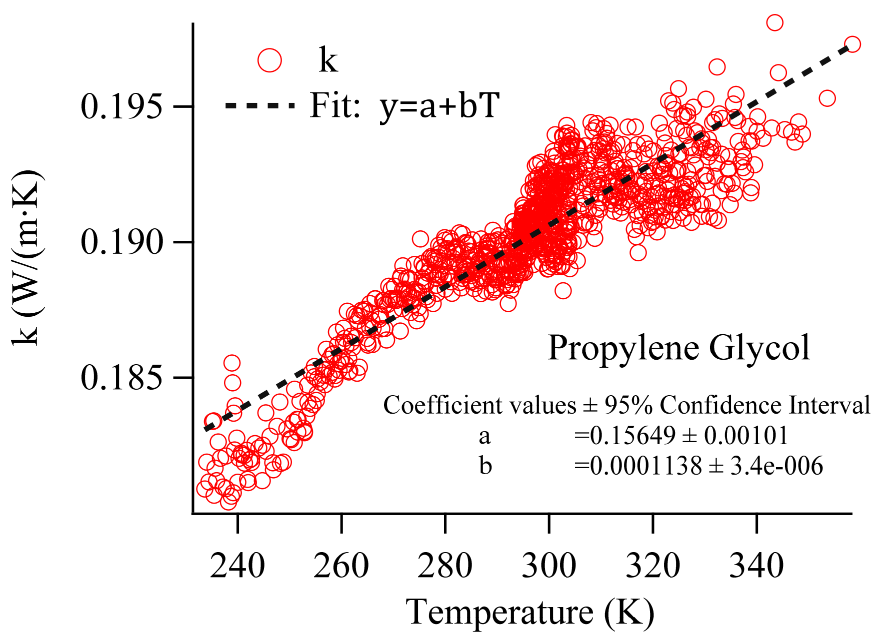

Figure 4.10: Consolidated data set for thermal conductivity as a function of temperature for current experimental sets for propylene glycol.

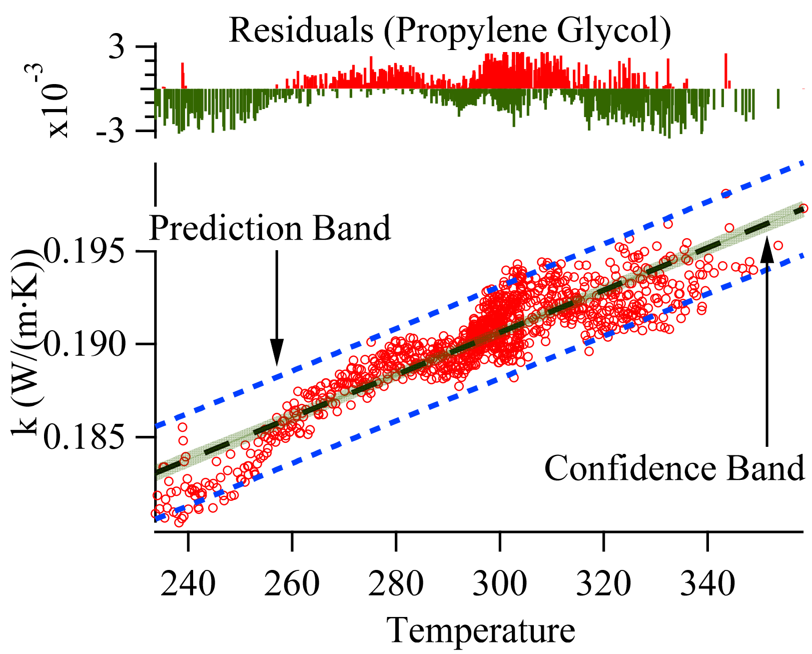

Figure 4.11: Residuals, confidence, and prediction bands (95%) for the linear fit to the current experimental data for propylene glycol.

The slope of the fit for propylene glycol lies midway between those of ethylene glycol and glycerol. It shows a 4.89 % variation in thermal conductivity between the temperatures of $260 - 340\ K$ as determined from the coefficients of the linear fit. The linear fit for the entire propylene glycol data, and the residuals, confidence, and prediction bands (95%) are shown in Fig. 4.10 and 4.11, respectively.

A comparison of the current experimental data set with previous studies in the literature for propylene glycol is shown in Fig. 4.12. The experiment results of Cabaleiro et al.[55] are about 8% higher than the current study, but show an increase with temperature similar to this work. On the other hand, the experimental of Sun et al.[51], and the experiment of Suganthi et al.[54] show that the thermal conductivity decreases when the temperature increases. Note however that both their results are in good agreement with the current study in the high temperature region. This inconsistency related to the trend of variation of a materials thermal conductivity, especially for liquids can be commonly found in the literature. This illustrates the importance of developing further systematic experimental and computational approaches to examine transport property trends with temperatures especially for fluids commonly using in engineering heat transfer applications.

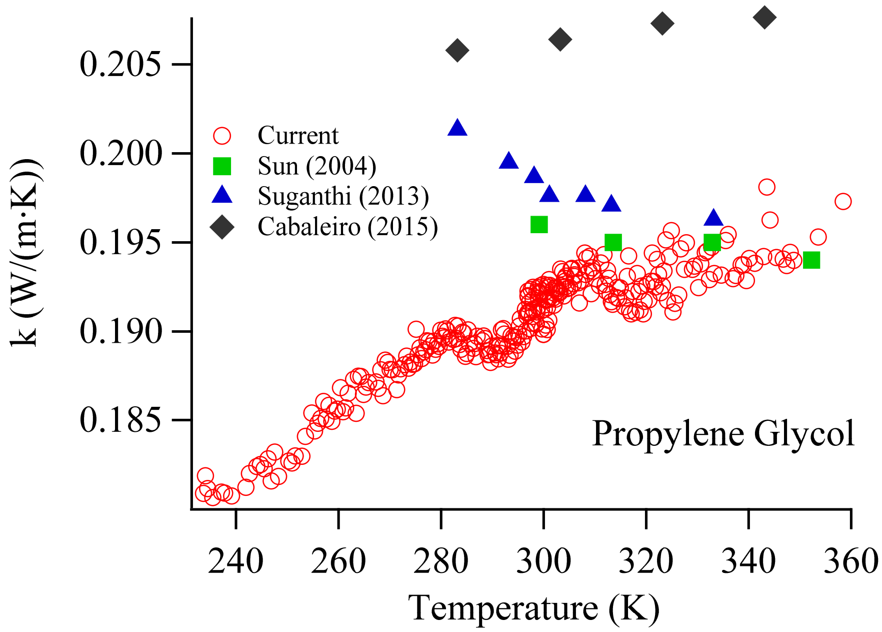

Figure 4.12: Comparison of current data with other recent studies for propylene glycol.

4.4 Comparative Thermal Conductivities for the Four Liquids

A summary plot of the thermal conductivity of all of the four heat transfer liquids is shown in Fig. 4.13. The thermal conductivities for the four liquids can be ranked in the following order:

$$\text{Water} > \text{Glycerol} > \text{Ethylene Glycol} > \text{Propylene Glycol}$$

It can be seen that the temperature range of the results for water is significantly smaller than the other liquids. This is because it is extremely difficult to measure thermal conductivities for low viscosity liquids in general. Water also shows the largest variation in thermal conductivity even over this limited range. Another important conclusion that can be drawn is that the apparatus and techniques developed in this work are capable of consistently resolving small differences between liquids such as glycerol and ethylene glycol. This minute difference is of the order of the experimental uncertainty and scatter that are found in data reported in the literature (cf. comparison plots with literature data for the fluids)

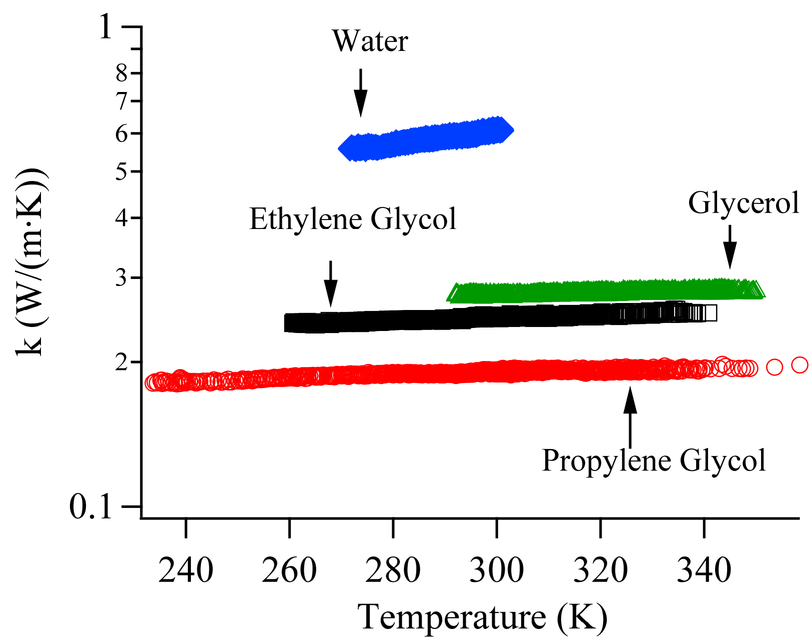

Figure 4.13: Comparative thermal conductivities of all four liquids obtained in this work.

Having described the capabilities of the apparatus developed and the results obtained, it is also important to provide a measure of the variability in the current data set. We chose a small temperature interval $297 < T < 299\ K$, centered on $298\ K$ to provide the extent of scatter. The bounds of the boxes indicate the limits of 25th and 75th percentile with the line as the median. The whiskers from the top and bottom of each extend to values that are 1.5 times the interquartile range, and the outliers are shown as empty circles.

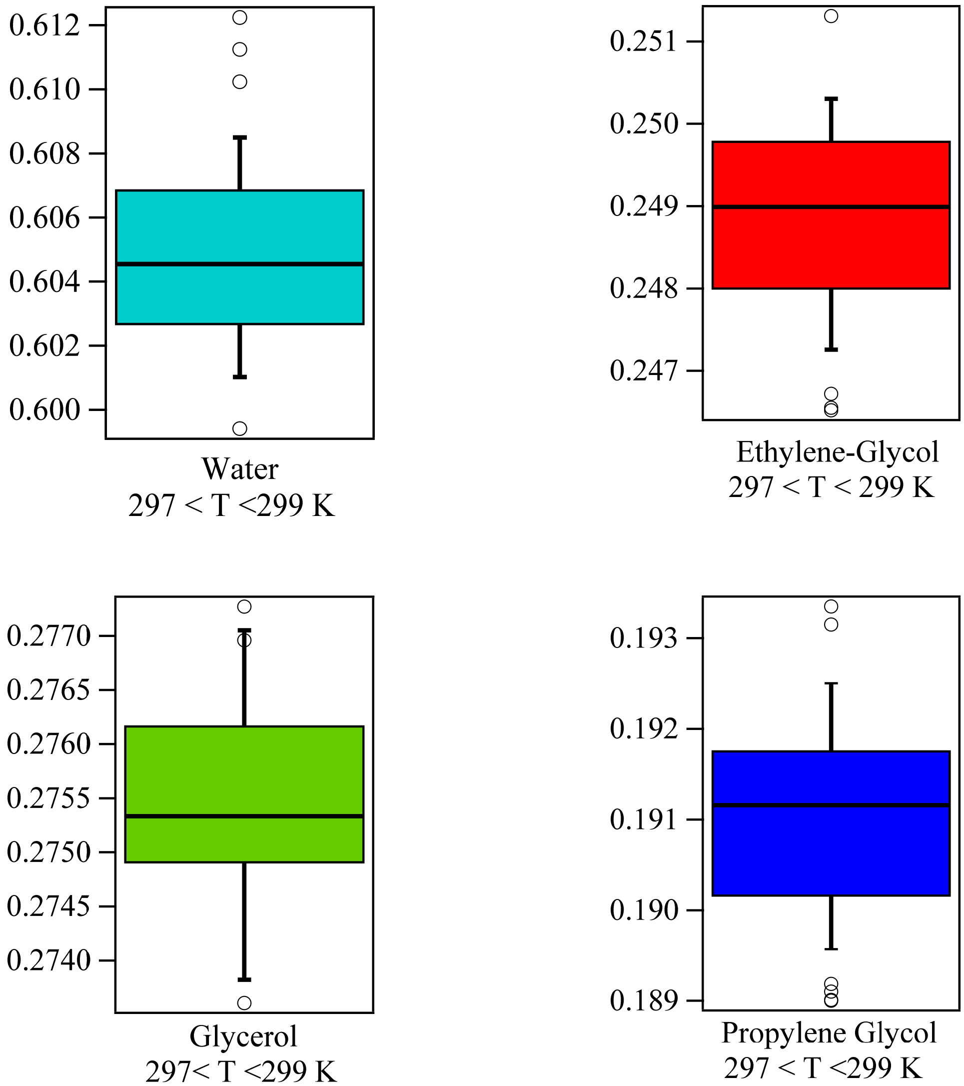

Figure 4.14: Plot showing the variability in the thermal conductivity values for the four liquids in the neighborhood of 298 ± 1K.

Chapter 5: Conclusions and Future Work

5.1 Summary of this Study

A transient hot-wire apparatus was used to obtain the thermal conductivities of four common heat transfer liquids. A transient hot-wire apparatus was designed and constructed to enable these measurements. The cell used a 25 micron radius platinum wire that was 95.33 mm long. In addition to the cell, the setup required the integration of heating and cooling baths, high-speed data acquisition system, and the processing software. It was found that in order to obtain reliable estimates of the variation of the thermal conductivities with temperature it is important to account for the variation of temperature coefficient of resistance of the platinum heating/temperature sensing wire.

This study used a constant current of 250 mA for all the fluids studied, and the test time was limited to six seconds. A data reduction procedure for the unambiguous identification of the slope and the portion of the ΔT vs $ln(t)$ was outlined. It was found that for the lowest viscosity fluid, water, effects of natural convection led to a non-linear relationship between the temperature rise and the logarithm of time after a time of approximately six seconds for the given current and wire length. Based on the experience for measuring the four different liquids it can be concluded that the measurement of thermal conductivity of low viscosity liquids is an extremely challenging task, especially as the temperature is raised. An earlier onset of convection occurs as the temperature is raised.

Liquid water was used for validating the results from this test cell, and the results showed a very agreement with the recommended values over the entire temperature range. Numerical studies were carried out to understand the effect of the transient heating of the wire on the temperature and velocity field in the surrounding medium. It was found that the computationally observed temperature rise of the wire agreed quite well with the theoretical results for a line source in an infinite medium, as well as the experimental data. This implies that there is only a limited influence of the convective effects on the temperature rise for the duration of heating under consideration. The effect of wire heating on the velocity field over a heating duration of six seconds (similar to the experiments) was found to be negligible beyond 40 wire diameters for the computations.

The temperature dependence of the thermal conductivities of water, ethylene glycol, glycerol, and propylene glycol were measured. All four liquids exhibited an increase in their respective thermal conductivities with increasing temperature. As previously noted, it was difficult to measure thermal conductivity of water above $300\ K$ on account of its low viscosity. However, good experimental data for water was obtained from near its freezing point up to room temperature. The high temperature limit was approximately $340K$ for this study.

5.2 Future Work

There are several possibilities of improvement and additional work that could enhance this research. It may be worthwhile to obtain improved measurements of the local slope for the temperature coefficient of resistance as a function of temperature. Furthermore, these experiments could be extended to measure the thermal diffusivity of the liquids by suitable modifications to the apparatus. There is need for further research on explaining the differences observed in the temperature rise profiles between the experimental and computed results. Two specific suggestions for future work include (a) using the current apparatus to examine the effect of nanoparticle addition to the base fluid, and (b) characterization of thermal conductivity of phase change materials for both solid and liquid phases.

References Cited

[1] Anonymous, Scala Graduum Caloris. Calorum Descriptiones & Figna, Philosophical Transactions (1683-1775) 22 (1700) 824-829.

[2] R. M. Sayre, The "Scala Granduum Caloris" and Sir Isaac Newton, Proceedings of the Oklahoma Academy of Science 43 (1963) 198-202.

[3] H. L. Callendar, The caloric theory of heat and Carnot's principle, Proc. Phys. Soc. Lond. 23 (1911) 153-189.

[4] S. C. Brown, The caloric theory of heat, Am. J. Phys. 18 (6) (1950) 367-373.

[5] M. Wilson, Count Rumford, Scientific American 203 (4) (1960) 158-171.

[6] D. S. L. Cardwell, From Watt to Clausius: The rise of thermodynamics in the early industrial age, Cornell University Press, 1971

[7] J. P. Joule, On the Mechanical Equivalent of Heat, Philosophical Transactions of the Royal Society of London 140 (1850) 61-82.

[8] J. B. J. Fourier, Théorie analytique de la chaleur, Breslau: Guillaume Koebner, 1883

[9] F. P. Incropera, D. P. D. Witt, Introduction to Heat Transfer, John Wiley & Sons, 1990

[10] R. Haberman, Elementary applied partial differential equations, Prentice Hall Englewood Cliffs, NJ, 1983

[11] T. Narasimhan, Fourier's heat conduction equation: History, influence, and connections, Reviews of Geophysics 37 (1) (1999) 151-172.

[12] R. Powell, C. Y. Ho, P. E. Liley, Thermal conductivity of selected materials; National Standards Reference Data Series, 1966.

[13] E. W. Lemmon, M. L. Huber, M. O. McLinden, NIST reference fluid thermodynamic and transport properties—REFPROP, NIST standard reference database 23 (2002) v7.

[14] M. L. Huber, A. H. Harvey, Thermal Conductivity of Gases: CRC Handbook of Chemistry and Physics, 2011

[15] J. Jaeger, Conduction of heat in an infinite region bounded internally by a circular cylinder of a perfect conductor, Australian Journal of Physics 9 (2) (1956) 167-179.

[16] H. S. Carslaw, J. C. Jaeger, Conduction of Heat in Solids, Oxford University Press, 1959

[17] J. Blackwell, A transient-flow method for determination of thermal constants of insulating materials in bulk part I—Theory, Journal of Applied Physics 25 (2) (1954) 137-144.

[18] J. J. Healy, J. J. deGroot, J. Kestin, The theory of the transient hot-wire method for measuring thermal conductivity, Physica 82C (1976) 392-408.

[19] H. M. Roder, A Transient Hot Wire Thermal Conductivity Apparatus for Fluids, Journal of Research of the National Bureau of Standards 86 (5) (1981) 457-493.

[20] J. F. T. Pittman, Fluid thermal conductivity determination by the transient, line source method. Imperial College of Science and Technology, University of London, 1968.

[21] Y. Nagasaka, A. Nagashima, Simultaneous measurement of the thermal conductivity and the thermal diffusivity of liquids by the transient hot-wire method, Review of Scientific Instruments 52 (2) (1981) 229-232.

[22] J. G. Bleazard, T. F. Sun, R. D. Johnson, R. M. DiGuillio, A. S. Teja, The transport properties of seven alkanediols, Fluid Phase Equilibria 117 (1) (1996) 386-393.

[23] C. Codreanu, N. Codreanu, V. Obreja, Experimental set-up for the measurement of the thermal conductivity of liquids, Romanian Journal of Information Science and Technology 10 (3) (2007) 215-231.

[24] X. Zhang, H. Gu, M. Fujii, Effective thermal conductivity and thermal diffusivity of nanofluids containing spherical and cylindrical nanoparticles, Experimental Thermal and Fluid Science 31 (6) (2007) 593-599.

[25] M. Kostic, K. C. Simham, Computerized, transient hot-wire thermal conductivity (HWTC) apparatus for nanofluids, Proceedings of the 6th WSEAS International Conference on Heat and Mass Transfer, 2009; 71-78.

[26] C. Nieto de Castro, S. Li, A. Nagashima, R. Trengove, W. Wakeham, Standard reference data for the thermal conductivity of liquids, Journal of physical and chemical reference data 15 (3) (1986) 1073-1086.

[27] J. Woolf, W. Sibbitt, Thermal conductivity of liquids, Industrial & Engineering Chemistry 46 (9) (1954) 1947-1952.

[28] A. Lawson, R. Lowell, A. Jain, Thermal conductivity of water at high pressures, The Journal of Chemical Physics 30 (3) (1959) 643-647.

[29] R. V. Theiss, G. Thodos, Viscosity and Thermal Conductivity of Water: Gaseous and liquid States, Journal of Chemical and Engineering Data 8 (3) (1963) 390-395.

[30] J. Sengers, J. Watson, R. Basu, B. Kamgar-Parsi, R. Hendricks, Representative equations for the thermal conductivity of water substance, Journal of physical and chemical reference data 13 (3) (1984) 893-933.

[31] M. L. V. Ramires, C. A. N. d. Castro, Y. Nagasaka, A. Nagashima, M. J. Assael, W. A. Wakeham, Standard Reference Data for the Thermal Conductivity of Water, Journal of Physical and Chemical Reference Data 24 (3) (1995) 1377-1381.

[32] R. S. Figliola, Theory and design for mechanical measurements, Hoboken : John Wiley & Sons, Hoboken, 2015

[33] E. W. Lemmon, M. L. Huber, M. O. McLinden NIST Standard Reference Database 23: Reference Fluid Thermodynamic and Transport Properties-REFPROP, Version 9.1, National Institute of Standards and Technology, Standard Reference Data Program, Gaithersburg, 2013.

[34] in: *Ansys Fluent Theory Guide, Release 18.1*, 2017.

[35] R. DiGuilio, A. S. Teja, Thermal conductivity of poly(ethylene glycols) and their binary mixtures, Journal of Chemical & Engineering Data 35 (2) (1990) 117-121.

[36] O. Faroon, U. S. A. f. T. Substances, D. Registry, Toxicological Profile for Ethylene Glycol, U.S. Department of Health & Human Services, Public Health Service, Agency for Toxic Substances and Disease Registry, 2010

[37] S. Azarfar, S. Movahedirad, A. A. Sarbanha, R. Norouzbeigi, B. Beigzadeh, Low cost and new design of transient hot-wire technique for the thermal conductivity measurement of fluids, Appl. Therm. Eng. 105 (2016) 142-150.

[38] Y. S. Lin, P. Y. Hsiao, C. C. Chieng, Constructing a force interaction model for thermal conductivity computation using molecular dynamics simulation: Ethylene glycol as an example, J. Chem. Phys. 134 (15) (2011) 12.

[39] M. P. Beck, T. F. Sun, A. S. Teja, The thermal conductivity of alumina nanoparticles dispersed in ethylene glycol, Fluid Phase Equilibria 260 (2) (2007) 275-278.

[40] M. J. Pastoriza-Gallego, L. Lugo, J. L. Legido, M. M. Pineiro, Thermal conductivity and viscosity measurements of ethylene glycol-based Al2O3 nanofluids, Nanoscale Research Letters 6 (2011) 11.

[41] M. Pagliaro, M. Rossi, in: The Future of Glycerol, The Royal Society of Chemistry: 2010; pp 1-28.

[42] T. T. Duong, H. Tanaka, N. Tsuzuki, H. Kawai, H. Kikura, Measurement of Joule-heating flow convection induced by internal heat generation using ultrasound velocity profiler in glycerin fluid, Flow Meas. Instrum. 52 (2016) 261-268.

[43] C. A. G. Quispe, C. J. R. Coronado, J. A. Carvalho, Glycerol: Production, consumption, prices, characterization and new trends in combustion, Renewable & Sustainable Energy Reviews 27 (2013) 475-493.

[44] J. Sun, J. P. Longtin, T. F. Irvine, Laser-based thermal pulse measurement of liquid thermophysical properties, International Journal of Heat and Mass Transfer 44 (3) (2001) 645-657.

[45] N. Le Brun, C. N. Markides, A Galinstan-Filled Capillary Probe for Thermal Conductivity Measurements and Its Application to Molten Eutectic -- (HTS) up to 700 K, International Journal of Thermophysics 36 (10-11) (2015) 3222-3238.

[46] M. Sharifpur, N. Tshimanga, J. P. Meyer, O. Manca, Experimental investigation and model development for thermal conductivity of alpha-Al2O3-glycerol nanofluids, Int. Commun. Heat Mass Transf. 85 (2017) 12-22.

[47] S. Akilu, K. V. Sharma, T. B. Aklilu, M. S. M. Azman, P. T. Bhaskoro, in: Proceeding of 4th International Conference on Process Engineering and Advanced Materials, M. A. Bustam; Z. Man; L. K. Keong; A. A. Hassankiadeh; Y. Y. Fong; M. Ayoub; M. Moniruzzaman; P. Mandal, (Eds.) Elsevier Science Bv: Amsterdam, 2016; Vol. 148, pp 774-778.

[48] M. F. v. Gelder, A Thermistor Based Method for Measurement of Thermal Conductivity and Thermal Diffusivity of Moist Food Materials at High Temperatures. Virginia Polytechnic Institute and State University, 1998.

[49] C. Talon, Q. W. Zou, M. A. Ramos, R. Villar, S. Vieira, Low-temperature specific heat and thermal conductivity of glycerol, Phys. Rev. B 65 (1) (2002) 4.

[50] G. Committee on Spacecraft Exposure, T. Committee on, T. Board on Environmental Studies and, S. Division on Earth and Life, C. National Research, Propylene Glycol, 2008

[51] T. Sun, A. S. Teja, Density, Viscosity and Thermal Conductivity of Aqueous Solutions of Propylene Glycol, Dipropylene Glycol, and Tripropylene Glycol between 290 K and 460 K, Journal of Chemical & Engineering Data 49 (5) (2004) 1311-1317.

[52] C. Deng, K. Zhang, T. Yang, Thermal Conductivity of 1,2-Ethanediol and 1,2-Propanediol Binary Aqueous Solutions at Temperature from (253 to 373) K, (2017).

[53] I. Palabiyik, Z. Musina, S. Witharana, Y. L. Ding, Dispersion stability and thermal conductivity of propylene glycol-based nanofluids, Journal of Nanoparticle Research 13 (10) (2011) 5049-5055.

[54] K. S. Suganthi, M. Parthasarathy, K. S. Rajan, Liquid-layering induced, temperature-dependent thermal conductivity enhancement in ZnO-propylene glycol nanofluids, Chemical Physics Letters 561 (2013) 120-124.

[55] D. Cabaleiro, J. Nimo, M. J. Pastoriza-Gallego, M. M. Pineiro, J. L. Legido, L. Lugo, Thermal conductivity of dry anatase and rutile nano-powders and ethylene and propylene glycol-based TiO2 nanofluids, J. Chem. Thermodyn. 83 (2015) 67-76.

Appendix A: Tabulated Thermal Conductivity Results for Water

Thermal Conductivity Values for Water in W/m.K (Run-1)													
T (K)	k		T (K)	k		T (K)	k		T (K)	k		T (K)	k
275.14	0.5676		285.37	0.5809		290.79	0.5908		296.08	0.6013		299.39	0.6034
275.29	0.5667		285.45	0.5832		290.87	0.5982		296.26	0.5979		299.42	0.6046
275.69	0.5645		285.53	0.5843		290.96	0.5921		296.30	0.6014		299.71	0.6117
275.91	0.5635		285.65	0.5819		291.13	0.5933		296.36	0.6069		299.84	0.6097
276.16	0.5641		285.82	0.5802		291.28	0.5890		296.48	0.5981		299.96	0.6054
276.97	0.5625		285.89	0.5822		291.33	0.5901		296.54	0.6002		299.96	0.6067
277.86	0.5625		286.00	0.5856		291.50	0.5931		296.58	0.5998		300.07	0.6099
278.02	0.5647		286.10	0.5847		291.61	0.5911		296.69	0.5977		300.09	0.6078
278.16	0.5624		286.26	0.5900		291.67	0.5914		296.79	0.6001		300.14	0.6155
278.35	0.5636		286.49	0.5830		292.03	0.5910		296.82	0.6027		300.19	0.6062
278.52	0.5667		286.63	0.5877		292.27	0.5959		296.98	0.6009		300.27	0.6143
278.65	0.5647		286.91	0.5849		292.31	0.5947		297.03	0.6059		300.28	0.6092
278.95	0.5683		287.00	0.5842		293.20	0.5922		297.15	0.6053		300.33	0.6112
279.41	0.5669		287.05	0.5824		293.32	0.5976		297.23	0.6102		300.40	0.6068
280.11	0.5701		287.26	0.5843		293.47	0.5987		297.33	0.6009		300.47	0.6117
280.42	0.5740		287.36	0.5825		293.50	0.5954		297.40	0.6079		300.49	0.6110
280.53	0.5769		287.44	0.5896		293.67	0.5954		297.66	0.6035		300.52	0.6069
280.65	0.5707		287.62	0.5847		293.72	0.6006		297.73	0.5994		300.57	0.6115
280.77	0.5737		287.71	0.5854		293.76	0.5944		297.85	0.6036		300.64	0.6049
281.02	0.5716		287.75	0.5861		293.82	0.5958		297.86	0.6013		300.69	0.6056
281.13	0.5721		287.95	0.5865		293.88	0.5956		297.92	0.6014		300.72	0.6082
281.25	0.5735		287.98	0.5892		294.05	0.5970		298.09	0.6016		300.80	0.6082
281.69	0.5745		288.07	0.5914		294.22	0.6019		298.15	0.6053		300.84	0.6108
281.94	0.5768		288.20	0.5868		294.22	0.6019		298.18	0.6027		300.86	0.6138
282.05	0.5738		288.28	0.5885		294.46	0.5935		298.33	0.6059		300.90	0.6110
282.65	0.5784		288.36	0.5898		294.52	0.5947		298.38	0.6045		300.93	0.6125
282.76	0.5751		288.45	0.5862		294.58	0.5966		298.44	0.6086		301.00	0.6097
283.17	0.5772		288.58	0.5863		294.84	0.5960		298.45	0.6010		301.06	0.6074
283.34	0.5804		288.99	0.5882		294.87	0.5980		298.54	0.6038			
283.46	0.5814		289.26	0.5880		294.94	0.5963		298.62	0.6025			
283.54	0.5779		289.42	0.5880		295.22	0.6000		298.64	0.6075			
283.62	0.5805		289.60	0.5899		295.26	0.5995		298.69	0.6037			
283.92	0.5808		289.74	0.5882		295.63	0.5984		298.78	0.6037			
284.25	0.5779		289.94	0.5914		295.73	0.6035		298.83	0.6048			
284.32	0.5817		290.09	0.5865		295.80	0.5994		298.94	0.6074			
284.89	0.5839		290.18	0.5892		295.82	0.5965		298.96	0.6062			
285.08	0.5801		290.37	0.5937		295.89	0.5978		299.16	0.6115			
285.16	0.5809		290.53	0.5919		295.93	0.5984		299.28	0.6074			
285.27	0.5854		290.73	0.5944		296.03	0.5968		299.34	0.6064			

Thermal Conductivity Values for Water in W/m.K (Run-2)									
T (K)	k	T (K)	k	T (K)	k	T (K)	k	T (K)	k
271.72	0.5577	275.19	0.5623	279.11	0.5651	282.60	0.5754	285.76	0.5824
271.66	0.5576	275.26	0.5595	279.20	0.5637	282.65	0.5760	285.80	0.5808
271.61	0.5558	275.33	0.5660	279.28	0.5669	282.72	0.5745	285.86	0.5860
271.60	0.5592	275.45	0.5632	279.36	0.5670	282.82	0.5779	285.92	0.5800
271.60	0.5584	275.54	0.5641	279.42	0.5642	282.87	0.5708	286.03	0.5794
271.62	0.5568	275.64	0.5625	279.50	0.5650	282.94	0.5738	286.06	0.5814
271.76	0.5568	275.73	0.5600	279.58	0.5704	283.00	0.5742	286.13	0.5814
271.93	0.5633	275.83	0.5599	279.67	0.5653	283.15	0.5772	286.21	0.5796
271.98	0.5634	275.90	0.5631	279.75	0.5719	283.24	0.5765	286.26	0.5804
272.07	0.5609	275.98	0.5592	279.82	0.5677	283.28	0.5758	286.42	0.5880
272.16	0.5597	276.06	0.5581	279.88	0.5686	283.33	0.5750	286.43	0.5823
272.33	0.5602	276.14	0.5593	279.97	0.5666	283.39	0.5777	286.49	0.5808
272.43	0.5608	276.22	0.5612	280.04	0.5662	283.46	0.5760	286.56	0.5814
272.51	0.5554	276.29	0.5598	280.15	0.5702	283.49	0.5784	286.60	0.5842
272.71	0.5579	276.36	0.5597	280.21	0.5711	283.58	0.5746	286.64	0.5809
272.81	0.5541	276.42	0.5621	280.37	0.5656	283.71	0.5730	286.69	0.5843
272.91	0.5600	276.50	0.5622	280.43	0.5726	283.80	0.5759	286.77	0.5865
273.02	0.5577	276.57	0.5635	280.48	0.5688	283.99	0.5755	286.85	0.5833
273.11	0.5609	276.63	0.5652	280.55	0.5723	284.06	0.5788	286.96	0.5786
273.20	0.5605	276.69	0.5623	280.71	0.5729	284.12	0.5815	287.01	0.5833
273.28	0.5623	276.78	0.5604	280.88	0.5729	284.17	0.5798	287.08	0.5854
273.35	0.5583	276.85	0.5599	280.91	0.5741	284.21	0.5794	287.18	0.5844
273.42	0.5574	276.91	0.5609	281.06	0.5687	284.26	0.5822	287.29	0.5820
273.54	0.5602	277.12	0.5614	281.13	0.5714	284.33	0.5786	287.34	0.5814
273.66	0.5624	277.23	0.5605	281.29	0.5694	284.59	0.5802	287.37	0.5818
273.74	0.5565	277.62	0.5610	281.34	0.5694	284.67	0.5784	287.42	0.5837
273.80	0.5628	277.68	0.5617	281.42	0.5719	284.75	0.5783	287.47	0.5869
273.92	0.5608	277.78	0.5594	281.50	0.5753	284.89	0.5813	287.51	0.5895
274.02	0.5585	277.89	0.5644	281.55	0.5741	284.95	0.5807	287.57	0.5888
274.11	0.5621	277.98	0.5623	281.71	0.5761	285.02	0.5802	287.63	0.5831
274.31	0.5630	278.16	0.5654	281.75	0.5720	285.08	0.5802	287.73	0.5840
274.38	0.5609	278.24	0.5642	281.84	0.5720	285.18	0.5791	287.82	0.5813
274.52	0.5606	278.33	0.5660	281.91	0.5732	285.26	0.5811	288.02	0.5879
274.58	0.5619	278.50	0.5648	282.14	0.5771	285.38	0.5823	288.06	0.5826
274.65	0.5647	278.59	0.5635	282.19	0.5707	285.47	0.5841	288.11	0.5862
274.74	0.5609	278.66	0.5662	282.34	0.5698	285.55	0.5815	288.31	0.5865
274.83	0.5627	278.80	0.5658	282.40	0.5725	285.60	0.5797	288.37	0.5823
274.91	0.5605	278.89	0.5659	282.45	0.5735	285.67	0.5816	288.43	0.5868
275.11	0.5627	279.02	0.5666	282.55	0.5761	285.69	0.5819	288.49	0.5876

Thermal Conductivity Values for Water in W/m.K (Run-2)													
T (K)	k		T (K)	k		T (K)	k		T (K)	k		T (K)	k
288.52	0.5837		290.93	0.5930		292.96	0.5911		294.65	0.5959		296.76	0.6009
288.60	0.5911		291.06	0.5911		292.96	0.5961		294.73	0.5941		296.85	0.6029
288.67	0.5874		291.09	0.5907		293.00	0.5944		294.76	0.5930		297.13	0.6012
288.74	0.5877		291.14	0.5926		293.13	0.5974		294.79	0.5982		297.39	0.6036
288.78	0.5869		291.18	0.5906		293.16	0.5947		294.86	0.5935		297.50	0.6027
288.81	0.5880		291.24	0.5907		293.25	0.5966		294.88	0.5918		297.80	0.6028
288.85	0.5860		291.27	0.5881		293.27	0.5876		294.92	0.5943		298.12	0.6051
288.90	0.5857		291.40	0.5884		293.34	0.5915		294.99	0.5945		298.45	0.6122
289.01	0.5893		291.43	0.5885		293.46	0.5956		295.02	0.5982		298.55	0.6029
289.06	0.5876		291.47	0.5961		293.49	0.5925		295.14	0.6015		298.63	0.6053
289.11	0.5863		291.51	0.5935		293.55	0.5967		295.15	0.5963		298.82	0.6075
289.16	0.5857		291.56	0.5910		293.55	0.5971		295.19	0.5972		298.84	0.6072
289.18	0.5864		291.65	0.5892		293.58	0.5958		295.23	0.5953		299.13	0.6044
289.22	0.5894		291.68	0.5921		293.64	0.5935		295.26	0.6026		299.44	0.6038
289.29	0.5861		291.71	0.5902		293.65	0.5929		295.32	0.5983		299.49	0.6089
289.32	0.5871		291.77	0.5909		293.70	0.5941		295.36	0.5935		299.59	0.6074
289.43	0.5914		291.85	0.5938		293.71	0.5955		295.40	0.5960		299.62	0.6115
289.47	0.5866		291.87	0.5940		293.71	0.5972		295.45	0.5996		299.75	0.6096
289.51	0.5872		291.92	0.5946		293.84	0.5906		295.47	0.5967		300.05	0.6083
289.56	0.5940		291.99	0.5928		293.92	0.5964		295.47	0.5928		300.13	0.6076
289.61	0.5881		292.05	0.5905		293.94	0.5930		294.68	0.5983		300.20	0.6129
289.65	0.5886		292.08	0.5896		293.99	0.5930		294.35	0.5939		300.25	0.6089
289.68	0.5885		292.15	0.5937		294.02	0.5981		294.27	0.5918			
289.78	0.5897		292.16	0.5908		294.07	0.5935		294.19	0.5980			
289.84	0.5861		292.22	0.5858		294.11	0.5977		294.33	0.5931			
289.88	0.5889		292.25	0.5957		294.16	0.5918		294.32	0.5894			
289.95	0.5891		292.29	0.5909		294.18	0.5942		294.35	0.5920			
290.00	0.5946		292.37	0.5917		294.21	0.5988		294.52	0.5941			
290.07	0.5907		292.45	0.5902		294.24	0.5963		294.64	0.5925			
290.12	0.5902		292.48	0.5910		294.26	0.5906		294.67	0.5962			
290.16	0.5925		292.50	0.5911		294.30	0.5956		294.70	0.5917			
290.20	0.5874		292.59	0.5937		294.38	0.5955		294.77	0.5915			
290.28	0.5899		292.58	0.5932		294.43	0.5909		294.93	0.5929			
290.63	0.5922		292.63	0.5930		294.46	0.5924		295.01	0.5958			
290.67	0.5880		292.70	0.5916		294.47	0.5958		295.20	0.5935			
290.74	0.5875		292.75	0.5925		294.51	0.5986		296.08	0.5924			
290.79	0.5864		292.85	0.5962		294.54	0.5933		296.15	0.5955			
290.81	0.5937		292.88	0.5918		294.55	0.5990		296.34	0.5978			
290.85	0.5896		292.91	0.5924		294.64	0.5957		296.50	0.5973			

Thermal Conductivity Values for Water in W/m.K (Run-3)							
T (K)	k	T (K)	k	T (K)	k	T (K)	k
273.28	0.5662	282.33	0.5768	290.42	0.5925	296.39	0.5965
273.15	0.5646	282.53	0.5750	290.53	0.5884	296.50	0.5988
273.12	0.5631	282.93	0.5740	290.63	0.5881	296.60	0.5993
273.12	0.5650	283.15	0.5791	290.82	0.5924	296.76	0.6034
273.31	0.5570	283.31	0.5797	290.93	0.5940	296.79	0.5994
273.51	0.5560	283.51	0.5760	291.06	0.5935	297.13	0.6001
273.74	0.5605	283.67	0.5754	291.25	0.5926	297.37	0.6027
273.98	0.5568	283.89	0.5826	291.32	0.5902	297.49	0.6092
274.16	0.5622	284.06	0.5799	291.76	0.5975	297.59	0.6031
274.41	0.5612	284.20	0.5787	291.89	0.5964	297.71	0.6013
274.62	0.5539	284.43	0.5827	292.06	0.5950	297.80	0.6045
275.03	0.5637	284.59	0.5766	292.18	0.5958	297.93	0.6056
275.30	0.5592	284.76	0.5794	292.25	0.5926	298.12	0.6069
275.68	0.5611	284.94	0.5789	292.39	0.5965	298.30	0.6010
275.83	0.5661	285.11	0.5786	292.70	0.5939	298.40	0.6054
276.42	0.5613	285.30	0.5787	292.80	0.5923	298.48	0.6036
276.64	0.5579	285.65	0.5811	292.96	0.5967	298.55	0.6071
276.74	0.5582	285.81	0.5822	293.25	0.5940	298.61	0.6056
276.90	0.5574	285.96	0.5843	293.32	0.5950	298.82	0.6112
277.04	0.5577	286.17	0.5833	293.39	0.5967	298.91	0.6063
277.26	0.5599	286.55	0.5820	293.56	0.5931	298.96	0.6068
277.89	0.5651	286.68	0.5815	293.74	0.5949	299.08	0.6131
278.19	0.5619	286.79	0.5847	293.84	0.5978	299.19	0.6147
278.40	0.5653	287.30	0.5829	293.96	0.5983	299.24	0.6030
278.59	0.5652	287.48	0.5858	294.19	0.5941	299.35	0.6120
279.08	0.5665	287.64	0.5801	294.36	0.5974	299.53	0.6075
279.31	0.5668	287.80	0.5850	294.72	0.5941	299.58	0.6039
279.53	0.5685	288.01	0.5914	294.85	0.5958	299.67	0.6099
279.72	0.5663	288.12	0.5871	295.06	0.5959	299.79	0.6066
280.11	0.5712	288.46	0.5880	295.15	0.5932	299.94	0.6099
280.34	0.5715	288.60	0.5835	295.37	0.5953	300.01	0.6114
280.55	0.5710	288.77	0.5842	295.50	0.5949	300.20	0.6152
280.76	0.5740	288.92	0.5867	295.71	0.5990		
280.91	0.5709	289.34	0.5882	295.81	0.5935		
281.17	0.5715	289.65	0.5917	295.90	0.5947		
281.34	0.5691	289.80	0.5891	296.00	0.5983		
281.55	0.5737	289.97	0.5879	296.08	0.5948		
281.93	0.5731	290.11	0.5915	296.20	0.5982		
282.12	0.5772	290.28	0.5896	296.30	0.5958		

Appendix B: Tabulated Thermal Conductivity Results for Ethylene Glycol

Thermal Conductivity Values for Ethylene Glycol in W/m.K (Run-1)									
T (K)	k	T (K)	k	T (K)	k	T (K)	k	T (K)	k
293.18	0.2447	322.17	0.2507	308.77	0.2500	302.43	0.2493	297.91	0.2492
293.23	0.2462	321.53	0.2509	308.56	0.2499	302.33	0.2493	297.86	0.2475
293.26	0.2479	321.22	0.2520	308.39	0.2471	302.07	0.2502	297.65	0.2490
293.35	0.2465	320.92	0.2517	308.18	0.2512	301.97	0.2494	297.58	0.2489
293.41	0.2457	320.31	0.2527	308.01	0.2490	301.87	0.2500	297.51	0.2465
293.65	0.2468	319.99	0.2534	307.82	0.2514	301.65	0.2484	297.44	0.2480
293.80	0.2467	319.38	0.2500	307.66	0.2486	301.51	0.2492	297.41	0.2488
337.66	0.2533	319.09	0.2488	307.48	0.2521	301.26	0.2471	297.36	0.2513
337.16	0.2529	318.77	0.2494	307.33	0.2506	301.13	0.2492	297.30	0.2507
336.63	0.2533	318.20	0.2524	307.13	0.2471	301.01	0.2480	297.27	0.2499
336.12	0.2532	317.92	0.2487	306.95	0.2506	300.95	0.2497	297.16	0.2495
335.65	0.2550	317.68	0.2535	306.81	0.2495	300.83	0.2486	297.08	0.2469
335.16	0.2519	317.39	0.2508	306.63	0.2500	300.74	0.2473	297.01	0.2493
334.71	0.2577	317.13	0.2523	306.46	0.2515	300.64	0.2505	296.97	0.2485
334.23	0.2577	316.85	0.2492	306.27	0.2516	300.52	0.2467	296.87	0.2477
332.42	0.2556	316.59	0.2519	306.12	0.2507	300.43	0.2478	296.82	0.2501
331.96	0.2567	316.31	0.2497	305.97	0.2484	300.40	0.2507	296.80	0.2483
331.52	0.2549	316.08	0.2488	305.82	0.2489	300.25	0.2487	296.72	0.2494
331.11	0.2537	315.54	0.2498	305.67	0.2486	300.12	0.2481	296.67	0.2480
330.69	0.2537	314.78	0.2504	305.38	0.2481	300.02	0.2497	296.60	0.2474
330.29	0.2516	314.52	0.2506	305.22	0.2477	299.94	0.2482	296.47	0.2503
329.86	0.2509	314.28	0.2511	305.09	0.2480	299.82	0.2499	296.40	0.2483
329.46	0.2557	314.03	0.2480	304.93	0.2484	299.73	0.2499	296.38	0.2483
329.04	0.2515	313.81	0.2497	304.77	0.2512	299.67	0.2488	296.36	0.2476
328.66	0.2540	313.57	0.2528	304.64	0.2502	299.57	0.2496	296.27	0.2490
328.24	0.2518	313.11	0.2478	304.49	0.2472	299.48	0.2504	296.16	0.2492
327.86	0.2518	312.89	0.2501	304.34	0.2481	299.28	0.2482	296.12	0.2498
327.50	0.2522	312.45	0.2497	304.22	0.2507	299.19	0.2484	296.07	0.2481
327.11	0.2509	312.24	0.2503	304.04	0.2495	299.06	0.2484	296.01	0.2487
326.34	0.2552	311.99	0.2505	303.90	0.2513	298.97	0.2489	295.91	0.2495
325.96	0.2502	311.76	0.2489	303.75	0.2501	298.89	0.2480	295.88	0.2502
325.26	0.2508	311.54	0.2483	303.46	0.2513	298.78	0.2487	260.82	0.2485
324.90	0.2526	311.31	0.2498	303.34	0.2490	298.73	0.2469	260.97	0.2418
324.56	0.2547	311.11	0.2513	303.21	0.2481	298.61	0.2501	261.15	0.2412
324.22	0.2528	310.74	0.2494	303.08	0.2494	298.50	0.2476	261.23	0.2418
323.90	0.2546	310.56	0.2495	302.93	0.2490	298.32	0.2493	261.38	0.2425
323.54	0.2491	310.32	0.2518	302.81	0.2496	298.09	0.2494	261.73	0.2405
322.85	0.2512	309.32	0.2533	302.69	0.2511	298.00	0.2490	261.92	0.2423
322.53	0.2524	309.12	0.2498	302.56	0.2523	297.98	0.2492	262.14	0.2418

Thermal Conductivity Values for Ethylene Glycol in W/m.K (Run-1)													
T (K)	k		T (K)	k		T (K)	k		T (K)	k		T (K)	k
262.36	0.2410		274.16	0.2420		282.74	0.2453		289.29	0.2454		294.79	0.2480
262.59	0.2402		274.35	0.2433		283.01	0.2455		289.43	0.2438		294.87	0.2475
262.85	0.2402		274.72	0.2450		283.13	0.2464		289.51	0.2460		294.93	0.2479
263.35	0.2433		274.92	0.2425		283.29	0.2451		289.62	0.2458		295.01	0.2464
263.57	0.2412		275.13	0.2441		283.55	0.2448		289.72	0.2472		295.14	0.2464
263.84	0.2413		275.28	0.2437		283.71	0.2453		289.96	0.2466		295.23	0.2474
264.09	0.2417		275.47	0.2435		284.00	0.2448		290.05	0.2447		295.27	0.2473
264.34	0.2407		275.88	0.2437		284.14	0.2446		290.16	0.2457		295.34	0.2486
264.61	0.2395		276.05	0.2455		284.29	0.2461		290.26	0.2448		295.43	0.2475
264.87	0.2399		276.22	0.2433		284.54	0.2451		290.42	0.2462		295.59	0.2487
265.16	0.2396		276.41	0.2433		284.68	0.2451		290.52	0.2451		295.78	0.2482
265.41	0.2401		276.61	0.2452		284.82	0.2460		290.61	0.2451			
266.12	0.2417		276.76	0.2437		284.99	0.2459		290.80	0.2444			
266.40	0.2416		276.97	0.2430		285.26	0.2441		290.93	0.2458			
266.88	0.2413		277.87	0.2427		285.38	0.2452		291.22	0.2462			
267.15	0.2406		278.05	0.2437		285.66	0.2461		291.42	0.2457			
267.40	0.2421		278.24	0.2442		285.91	0.2436		291.56	0.2474			
267.60	0.2442		278.38	0.2436		286.03	0.2451		291.65	0.2462			
267.87	0.2398		278.54	0.2443		286.14	0.2448		291.75	0.2463			
268.10	0.2413		278.88	0.2460		286.30	0.2455		292.15	0.2460			
268.33	0.2425		279.07	0.2455		286.43	0.2461		292.23	0.2452			
268.58	0.2426		279.22	0.2450		286.56	0.2456		292.34	0.2461			
268.82	0.2425		279.41	0.2454		286.94	0.2445		292.43	0.2459			
269.31	0.2418		279.57	0.2436		287.08	0.2460		292.62	0.2463			
269.54	0.2424		279.75	0.2443		287.20	0.2458		292.91	0.2467			
269.74	0.2414		279.91	0.2457		287.32	0.2463		293.15	0.2463			
270.22	0.2413		280.24	0.2438		287.43	0.2447		293.26	0.2450			
270.44	0.2415		280.39	0.2441		287.58	0.2456		293.36	0.2476			
270.88	0.2411		280.54	0.2448		287.79	0.2461		293.43	0.2469			
271.10	0.2418		280.71	0.2454		288.09	0.2457		293.50	0.2456			
271.32	0.2443		280.90	0.2462		288.20	0.2452		293.61	0.2465			
271.76	0.2420		281.05	0.2450		288.33	0.2455		293.76	0.2462			
271.97	0.2431		281.17	0.2459		288.46	0.2461		293.89	0.2465			
272.18	0.2420		281.48	0.2453		288.55	0.2462		294.02	0.2480			
272.38	0.2427		281.65	0.2457		288.67	0.2444		294.26	0.2461			
272.80	0.2438		281.82	0.2457		288.80	0.2440		294.35	0.2465			
273.40	0.2433		282.08	0.2444		288.92	0.2446		294.45	0.2463			
273.58	0.2427		282.23	0.2443		289.01	0.2463		294.58	0.2471			
273.80	0.2425		282.57	0.2455		289.13	0.2456		294.66	0.2476			

Thermal Conductivity Values for Ethylene Glycol in W/m.K													(Run-2)
T (K)	k		T (K)	k		T (K)	k		T (K)	k		T (K)	k
350.50	0.2486		321.23	0.2488		309.73	0.2477		301.99	0.2494		264.48	0.2417
349.33	0.2491		320.93	0.2487		309.50	0.2519		301.88	0.2499		264.76	0.2405
348.25	0.2493		320.62	0.2505		309.32	0.2487		301.58	0.2500		264.99	0.2419
347.17	0.2492		320.32	0.2546		309.16	0.2501		301.46	0.2497		265.28	0.2417
346.16	0.2488		320.06	0.2486		309.01	0.2483		301.40	0.2491		266.03	0.2408
345.17	0.2528		319.82	0.2482		308.80	0.2499		301.28	0.2476		266.31	0.2407
344.23	0.2503		319.56	0.2509		308.52	0.2478		301.15	0.2479		266.57	0.2415
343.32	0.2485		319.30	0.2478		308.38	0.2507		300.76	0.2480		266.82	0.2406
342.44	0.2491		319.01	0.2511		308.19	0.2507		300.63	0.2496		267.07	0.2401
341.65	0.2520		318.77	0.2477		308.01	0.2494		300.45	0.2485		267.30	0.2410
340.89	0.2535		317.71	0.2524		307.92	0.2493		300.36	0.2494		267.54	0.2410
340.12	0.2523		317.46	0.2476		307.81	0.2490		300.28	0.2491		267.77	0.2419
339.37	0.2506		317.21	0.2497		307.62	0.2489		299.95	0.2485		268.01	0.2427
338.69	0.2528		316.94	0.2523		307.26	0.2509		299.85	0.2484		268.29	0.2422
338.01	0.2539		316.64	0.2489		306.93	0.2494		299.75	0.2492		268.52	0.2413
337.34	0.2521		316.39	0.2520		306.76	0.2500		299.67	0.2477		268.76	0.2414
336.07	0.2552		315.99	0.2490		306.53	0.2487		299.57	0.2487		269.26	0.2423
335.47	0.2515		315.75	0.2499		306.21	0.2492		299.48	0.2504		270.15	0.2414
334.92	0.2540		315.51	0.2498		305.97	0.2499		299.41	0.2480		270.44	0.2416
334.36	0.2504		315.33	0.2502		305.78	0.2487		299.32	0.2482		270.63	0.2438
333.82	0.2519		315.11	0.2507		305.59	0.2497		299.27	0.2501		270.84	0.2421
333.30	0.2561		314.88	0.2516		305.48	0.2488		299.16	0.2501		271.46	0.2436
330.41	0.2501		314.10	0.2507		305.29	0.2489		298.95	0.2497		271.67	0.2417
329.98	0.2495		313.94	0.2488		305.09	0.2497		298.84	0.2506		271.91	0.2435
329.59	0.2521		313.77	0.2511		304.91	0.2510		298.73	0.2488		272.12	0.2423
329.16	0.2537		313.27	0.2495		304.78	0.2482		298.64	0.2497		272.33	0.2427
327.93	0.2525		313.09	0.2514		304.35	0.2500		298.56	0.2479		272.52	0.2419
327.15	0.2491		312.90	0.2494		304.07	0.2495		261.50	0.2424		272.72	0.2429
325.37	0.2496		312.66	0.2502		303.94	0.2516		261.67	0.2426		272.96	0.2434
325.02	0.2530		312.48	0.2493		303.81	0.2503		261.77	0.2425		273.15	0.2432
324.68	0.2484		312.20	0.2498		303.58	0.2492		261.98	0.2411		273.35	0.2436
324.32	0.2500		311.79	0.2489		303.44	0.2499		262.15	0.2412		273.54	0.2436
324.01	0.2483		311.62	0.2504		303.35	0.2481		262.35	0.2422		273.74	0.2441
323.71	0.2502		311.24	0.2496		303.04	0.2480		262.59	0.2430		273.94	0.2447
323.41	0.2502		311.05	0.2513		302.82	0.2472		263.00	0.2406		274.15	0.2443
323.05	0.2483		310.66	0.2484		302.69	0.2488		263.25	0.2399		274.33	0.2427
322.74	0.2528		310.47	0.2491		302.52	0.2498		263.52	0.2404		274.51	0.2438
322.12	0.2523		310.13	0.2496		302.37	0.2482		263.80	0.2401		274.69	0.2438
321.81	0.2484		309.94	0.2471		302.26	0.2498		264.24	0.2401		274.89	0.2418

Thermal Conductivity Values for Ethylene Glycol in W/m.K (Run-2)									
T (K)	k	T (K)	k	T (K)	k	T (K)	k	T (K)	k
275.06	0.2440	284.18	0.2438	290.92	0.2456	295.67	0.2472	299.70	0.2487
275.27	0.2434	284.31	0.2442	291.04	0.2446	295.74	0.2484	299.86	0.2496
275.46	0.2422	284.43	0.2454	291.29	0.2457	295.87	0.2482	299.91	0.2500
276.02	0.2448	284.57	0.2452	291.38	0.2463	295.96	0.2489	300.01	0.2487
276.19	0.2448	284.68	0.2447	291.50	0.2451	296.04	0.2471	300.03	0.2505
276.59	0.2441	284.83	0.2456	291.71	0.2458	296.11	0.2492	300.39	0.2488
276.76	0.2434	285.15	0.2444	291.82	0.2451	296.19	0.2498	300.46	0.2499
277.11	0.2437	285.28	0.2459	291.95	0.2461	296.28	0.2504	300.91	0.2500
277.28	0.2427	285.38	0.2460	292.06	0.2471	296.42	0.2473	301.15	0.2491
277.41	0.2450	285.52	0.2455	292.19	0.2454	296.48	0.2493	301.42	0.2499
277.60	0.2427	285.66	0.2463	292.38	0.2466	296.60	0.2481	301.50	0.2488
278.13	0.2447	285.79	0.2462	292.45	0.2476	296.75	0.2497	301.55	0.2493
278.46	0.2446	286.06	0.2455	292.53	0.2463	296.87	0.2492	301.67	0.2496
278.65	0.2435	286.19	0.2452	292.71	0.2476	296.94	0.2468	301.90	0.2489
278.82	0.2431	286.46	0.2465	292.82	0.2455	297.13	0.2485	302.13	0.2500
279.19	0.2435	286.97	0.2463	293.13	0.2472	297.22	0.2494	302.26	0.2506
279.31	0.2444	287.11	0.2441	293.19	0.2483	297.28	0.2490	302.35	0.2491
279.48	0.2431	287.21	0.2449	293.39	0.2464	297.35	0.2486	302.92	0.2505
279.64	0.2450	287.35	0.2447	293.62	0.2470	297.52	0.2475	303.07	0.2494
279.82	0.2438	287.57	0.2456	293.71	0.2474	297.61	0.2465		
280.30	0.2445	287.67	0.2453	293.78	0.2460	297.69	0.2492		
280.46	0.2439	287.79	0.2453	293.90	0.2473	297.77	0.2480		
280.60	0.2436	287.92	0.2450	294.00	0.2475	297.82	0.2467		
280.77	0.2453	288.05	0.2459	294.17	0.2479	297.85	0.2490		
281.06	0.2443	288.39	0.2451	294.35	0.2488	297.96	0.2497		
281.20	0.2448	288.53	0.2466	294.43	0.2483	298.02	0.2503		
281.53	0.2447	288.61	0.2467	294.49	0.2466	298.22	0.2483		
281.67	0.2445	288.76	0.2449	294.55	0.2482	298.31	0.2487		
281.84	0.2443	289.19	0.2463	294.62	0.2488	298.38	0.2508		
282.00	0.2437	289.44	0.2459	294.73	0.2465	298.46	0.2503		
282.14	0.2442	289.69	0.2454	294.79	0.2475	298.54	0.2487		
282.42	0.2464	289.75	0.2452	294.87	0.2486	298.61	0.2504		
282.77	0.2440	289.84	0.2458	294.96	0.2485	298.91	0.2488		
282.89	0.2460	290.13	0.2454	295.06	0.2476	298.99	0.2483		
283.15	0.2451	290.24	0.2456	295.14	0.2487	299.04	0.2499		
283.48	0.2445	290.43	0.2457	295.28	0.2474	299.04	0.2495		
283.58	0.2445	290.62	0.2460	295.36	0.2478	299.07	0.2499		
283.89	0.2458	290.75	0.2453	295.45	0.2484	299.34	0.2495		
284.02	0.2441	290.83	0.2465	295.59	0.2469	299.47	0.2480		

Thermal Conductivity Values for Ethylene Glycol in W/m.K (Run-3)													
T (K)	k		T (K)	k		T (K)	k		T (K)	k		T (K)	k
293.31	0.2444		325.66	0.2505		309.77	0.2508		302.95	0.2502		297.70	0.2477
293.28	0.2487		324.73	0.2547		309.43	0.2492		302.83	0.2491		297.54	0.2489
293.27	0.2476		324.42	0.2546		308.81	0.2506		302.73	0.2509		297.44	0.2498
293.28	0.2470		324.12	0.2500		308.35	0.2509		302.62	0.2506		297.36	0.2504
293.29	0.2464		323.81	0.2543		307.90	0.2475		302.47	0.2493		297.26	0.2484
293.29	0.2470		322.55	0.2535		307.72	0.2486		302.37	0.2480		297.21	0.2480
293.29	0.2482		321.87	0.2515		307.53	0.2489		302.23	0.2479		297.15	0.2501
293.29	0.2475		321.38	0.2495		307.22	0.2504		302.10	0.2474		297.07	0.2479
293.29	0.2462		321.09	0.2509		307.07	0.2512		301.99	0.2508		297.02	0.2497
293.27	0.2479		320.19	0.2512		306.78	0.2476		301.87	0.2502		296.91	0.2497
293.26	0.2474		319.88	0.2516		306.61	0.2505		301.36	0.2485		296.85	0.2492
293.23	0.2479		319.33	0.2501		306.48	0.2500		301.30	0.2479		296.79	0.2481
293.22	0.2484		318.81	0.2503		305.99	0.2478		301.20	0.2502		296.67	0.2500
293.23	0.2469		318.60	0.2508		309.46	0.2488		301.07	0.2486		296.58	0.2471
293.24	0.2487		318.28	0.2508		309.12	0.2506		300.93	0.2503		296.46	0.2497
293.24	0.2479		317.98	0.2519		308.94	0.2509		300.69	0.2493		296.26	0.2495
293.25	0.2462		317.78	0.2497		308.76	0.2493		300.54	0.2502		296.13	0.2487
293.24	0.2468		317.52	0.2511		308.56	0.2500		300.25	0.2485		296.02	0.2482
293.24	0.2470		317.29	0.2525		308.17	0.2489		300.12	0.2500		260.59	0.2415
293.24	0.2487		316.83	0.2527		307.81	0.2485		300.04	0.2474		260.68	0.2410
293.23	0.2486		316.56	0.2490		307.64	0.2468		299.95	0.2509		260.82	0.2430
338.10	0.2525		316.30	0.2487		307.46	0.2501		299.73	0.2501		261.08	0.2415
336.23	0.2536		316.03	0.2509		307.15	0.2517		299.60	0.2501		261.25	0.2418
335.32	0.2556		315.83	0.2497		306.96	0.2513		299.30	0.2508		261.45	0.2405
334.86	0.2541		315.63	0.2497		306.09	0.2510		299.21	0.2494		261.62	0.2415
334.40	0.2551		314.71	0.2518		305.95	0.2492		299.09	0.2493		262.06	0.2415
333.54	0.2518		314.04	0.2487		305.75	0.2498		298.94	0.2503		262.28	0.2404
332.30	0.2522		313.86	0.2516		305.42	0.2512		298.72	0.2485		262.50	0.2413
331.89	0.2545		313.63	0.2484		305.30	0.2496		298.64	0.2497		262.76	0.2425
331.50	0.2541		313.15	0.2478		304.97	0.2504		298.51	0.2503		262.98	0.2419
331.10	0.2552		312.70	0.2505		304.83	0.2499		298.44	0.2469		263.22	0.2415
330.69	0.2520		312.49	0.2485		304.24	0.2503		298.39	0.2468		263.45	0.2405
329.21	0.2550		312.30	0.2492		304.05	0.2495		298.34	0.2500		263.73	0.2402
328.82	0.2520		312.03	0.2500		303.92	0.2512		298.26	0.2498		263.96	0.2402
328.46	0.2523		311.89	0.2507		303.80	0.2487		298.07	0.2483		264.19	0.2402
328.13	0.2533		311.67	0.2509		303.66	0.2512		298.00	0.2490		264.44	0.2409
327.44	0.2532		311.12	0.2499		303.38	0.2511		297.93	0.2504		264.68	0.2430
327.09	0.2503		310.33	0.2492		303.24	0.2497		297.86	0.2497		264.92	0.2400
326.36	0.2531		310.15	0.2496		303.09	0.2483		297.80	0.2480		265.22	0.2412

Thermal Conductivity Values for Ethylene Glycol in W/m.K (Run-3)									
T (K)	k	T (K)	k	T (K)	k	T (K)	k	T (K)	k
265.50	0.2423	275.37	0.2436	283.67	0.2464	289.47	0.2458	294.60	0.2470
265.75	0.2416	275.54	0.2439	283.83	0.2433	289.58	0.2461	294.76	0.2466
265.99	0.2423	275.71	0.2425	283.95	0.2449	289.68	0.2460	294.83	0.2478
266.22	0.2415	275.93	0.2428	284.09	0.2461	289.88	0.2459	294.89	0.2470
266.45	0.2426	276.08	0.2452	284.25	0.2445	289.99	0.2456	294.99	0.2484
266.69	0.2423	276.26	0.2425	284.38	0.2453	290.12	0.2450	295.04	0.2479
266.95	0.2412	276.45	0.2428	284.52	0.2456	290.23	0.2459	295.14	0.2467
267.17	0.2402	276.64	0.2427	284.93	0.2446	290.32	0.2450	295.29	0.2480
267.39	0.2412	277.03	0.2429	285.07	0.2458	290.65	0.2447	295.42	0.2488
267.62	0.2402	277.16	0.2430	285.20	0.2444	290.75	0.2451	295.49	0.2492
267.88	0.2412	277.37	0.2453	285.33	0.2451	291.00	0.2460	295.56	0.2475
268.12	0.2412	277.68	0.2445	285.48	0.2464	291.09	0.2460	295.62	0.2491
268.38	0.2415	277.88	0.2427	285.74	0.2452	291.21	0.2468	295.76	0.2477
268.59	0.2429	278.01	0.2451	285.88	0.2444	291.30	0.2456	295.94	0.2485
269.02	0.2423	278.17	0.2453	286.00	0.2459	291.40	0.2469	296.08	0.2472
269.27	0.2423	278.36	0.2446	286.14	0.2452	291.51	0.2452	296.12	0.2481
269.49	0.2410	278.51	0.2443	286.28	0.2450	291.79	0.2457	296.22	0.2480
269.71	0.2421	278.68	0.2434	286.52	0.2457	292.00	0.2458	296.44	0.2466
270.42	0.2423	279.03	0.2442	286.76	0.2450	292.10	0.2472	296.54	0.2493
270.60	0.2433	279.22	0.2451	286.87	0.2459	292.26	0.2474	296.63	0.2475
270.82	0.2434	279.56	0.2436	287.02	0.2460	292.51	0.2452	296.71	0.2479
271.03	0.2423	279.78	0.2444	287.14	0.2461	292.70	0.2473	296.78	0.2475
271.26	0.2429	280.24	0.2442	287.27	0.2450	292.81	0.2475	296.84	0.2497
271.86	0.2424	280.57	0.2446	287.41	0.2444	293.03	0.2453	296.92	0.2488
272.05	0.2441	280.83	0.2453	287.55	0.2461	293.11	0.2462	296.99	0.2489
272.26	0.2441	281.18	0.2442	287.66	0.2457	293.20	0.2468	297.05	0.2475
272.66	0.2439	281.33	0.2441	287.77	0.2448	293.35	0.2461	297.15	0.2480
272.90	0.2444	281.51	0.2442	287.89	0.2461	293.59	0.2469	297.22	0.2473
273.08	0.2443	281.64	0.2443	288.02	0.2449	293.65	0.2459	297.30	0.2494
273.29	0.2437	281.78	0.2449	288.16	0.2455	293.76	0.2471	297.36	0.2501
273.47	0.2438	281.94	0.2441	288.28	0.2458	293.84	0.2474	297.42	0.2470
273.68	0.2411	282.09	0.2445	288.40	0.2468	293.89	0.2468	297.50	0.2490
273.87	0.2431	282.36	0.2441	288.50	0.2456	293.96	0.2459	297.58	0.2482
274.11	0.2423	282.50	0.2453	288.63	0.2459	294.08	0.2468	297.64	0.2490
274.28	0.2430	282.66	0.2449	288.74	0.2449	294.17	0.2466	297.73	0.2479
274.67	0.2439	282.81	0.2440	288.87	0.2458	294.26	0.2477	297.81	0.2491
274.82	0.2435	282.97	0.2453	288.99	0.2448	294.36	0.2473	297.87	0.2502
275.02	0.2436	283.12	0.2458	289.13	0.2458	294.45	0.2469	298.09	0.2503
275.20	0.2447	283.26	0.2462	289.27	0.2456	294.53	0.2482	298.43	0.2500

Thermal Conductivity Values for Ethylene Glycol in W/m.K (Run-3)	
T (K)	k
298.69	0.2492
298.74	0.2501
298.90	0.2491
298.97	0.2502
299.40	0.2493
299.93	0.2509
300.56	0.2505
300.69	0.2483
300.96	0.2498
301.36	0.2497
301.40	0.2500
301.98	0.2494
302.46	0.2507
302.83	0.2500
303.51	0.2509
303.76	0.2501
303.77	0.2500

Appendix C: Tabulated Thermal Conductivity Results for Glycerol

Thermal Conductivity Values for Glycerol in W/m.K (Run-1)									
T (K)	k	T (K)	k	T (K)	k	T (K)	k	T (K)	k
294.19	0.2755	304.28	0.2769	310.77	0.2770	316.09	0.2778	319.57	0.2790
294.14	0.2760	304.54	0.2764	310.81	0.2765	316.19	0.2773	319.54	0.2787
294.23	0.2752	304.82	0.2748	310.86	0.2767	316.29	0.2778	319.64	0.2770
294.29	0.2753	305.36	0.2764	310.91	0.2786	316.39	0.2782	319.74	0.2779
294.60	0.2767	305.68	0.2741	311.03	0.2786	316.46	0.2785	319.67	0.2787
294.78	0.2755	305.90	0.2768	311.11	0.2763	316.61	0.2754	319.62	0.2771
294.98	0.2753	306.18	0.2742	311.30	0.2769	316.73	0.2786	319.63	0.2789
295.25	0.2765	306.44	0.2765	311.47	0.2772	316.78	0.2764	319.62	0.2790
295.50	0.2731	306.66	0.2744	311.62	0.2792	316.83	0.2775	319.66	0.2774
295.76	0.2737	306.84	0.2749	311.78	0.2779	316.96	0.2777	319.61	0.2776
295.98	0.2765	307.01	0.2751	311.88	0.2763	317.07	0.2781	319.63	0.2787
296.23	0.2762	307.29	0.2748	312.01	0.2769	317.17	0.2782	319.60	0.2781
296.47	0.2728	307.50	0.2761	312.10	0.2773	317.30	0.2772	319.71	0.2776
296.66	0.2757	307.70	0.2761	312.30	0.2772	317.32	0.2770	319.71	0.2780
296.90	0.2762	307.84	0.2778	312.75	0.2765	317.48	0.2770	319.75	0.2783
297.10	0.2755	307.97	0.2763	312.89	0.2771	317.69	0.2782	319.73	0.2794
297.35	0.2763	308.15	0.2778	312.96	0.2765	317.77	0.2795	319.79	0.2781
297.57	0.2733	308.27	0.2768	313.05	0.2786	318.01	0.2782	319.76	0.2782
297.74	0.2758	308.39	0.2777	313.56	0.2768	318.12	0.2771	319.74	0.2781
297.95	0.2765	308.47	0.2782	313.69	0.2778	318.23	0.2771	319.79	0.2795
298.20	0.2750	308.66	0.2746	313.78	0.2763	318.34	0.2772	319.77	0.2794
298.44	0.2742	308.72	0.2765	313.98	0.2764	318.44	0.2778	319.85	0.2789
298.68	0.2757	308.73	0.2771	314.15	0.2778	318.57	0.2779	319.83	0.2788
298.87	0.2746	308.84	0.2769	314.30	0.2770	318.67	0.2788	319.88	0.2789
299.43	0.2760	308.88	0.2779	314.36	0.2769	318.77	0.2776	319.91	0.2786
299.65	0.2762	308.96	0.2788	314.59	0.2773	318.85	0.2761	319.87	0.2780
299.90	0.2750	309.06	0.2770	314.69	0.2778	318.93	0.2794	319.89	0.2781
300.16	0.2755	309.20	0.2786	314.69	0.2768	318.92	0.2785	319.85	0.2793
300.38	0.2739	309.30	0.2769	314.90	0.2789	319.06	0.2772	319.88	0.2773
300.64	0.2752	309.57	0.2772	314.94	0.2764	319.18	0.2775	320.04	0.2772
300.97	0.2752	309.70	0.2767	315.04	0.2779	319.22	0.2773	320.25	0.2774
301.29	0.2749	309.83	0.2768	315.12	0.2771	319.24	0.2782	320.48	0.2790
301.84	0.2742	310.04	0.2769	315.24	0.2760	319.26	0.2791	320.58	0.2778
302.05	0.2744	310.11	0.2766	315.29	0.2783	319.33	0.2757	320.67	0.2793
302.31	0.2743	310.23	0.2773	315.37	0.2761	319.36	0.2773	320.78	0.2785
302.64	0.2735	310.34	0.2778	315.41	0.2780	319.41	0.2769	320.79	0.2767
302.93	0.2746	310.44	0.2767	315.72	0.2763	319.45	0.2780	320.97	0.2772
303.43	0.2728	310.53	0.2764	315.75	0.2763	319.44	0.2770	321.06	0.2789
303.93	0.2770	310.64	0.2757	315.99	0.2763	319.44	0.2790	321.12	0.2788

Thermal Conductivity Values for Glycerol in W/m.K (Run-1)									
T (K)	k	T (K)	k	T (K)	k	T (K)	k	T (K)	k
321.17	0.2773	322.27	0.2770	330.52	0.2792	335.58	0.2786	344.39	0.2811
321.28	0.2778	322.63	0.2784	330.58	0.2801	335.73	0.2796	344.60	0.2817
321.39	0.2776	322.93	0.2780	330.63	0.2779	335.89	0.2781	344.68	0.2816
321.54	0.2770	323.21	0.2784	330.66	0.2796	336.07	0.2781	344.91	0.2792
321.81	0.2776	323.78	0.2773	330.74	0.2782	336.22	0.2797	345.15	0.2808
321.97	0.2797	324.03	0.2792	330.80	0.2801	337.04	0.2803	345.38	0.2819
322.08	0.2792	324.73	0.2795	330.85	0.2784	337.17	0.2825	345.27	0.2783
322.17	0.2795	324.97	0.2782	330.88	0.2804	337.40	0.2806	345.72	0.2811
322.60	0.2778	325.23	0.2780	330.91	0.2812	337.73	0.2791	345.65	0.2815
323.11	0.2764	325.58	0.2793	330.92	0.2792	337.95	0.2802	345.78	0.2792
323.68	0.2768	325.84	0.2791	331.03	0.2826	338.05	0.2806	345.80	0.2789
324.21	0.2774	325.96	0.2784	331.13	0.2799	338.13	0.2796	345.91	0.2829
324.44	0.2792	326.09	0.2804	331.22	0.2803	338.22	0.2790	346.44	0.2815
324.61	0.2785	326.20	0.2797	331.35	0.2815	338.34	0.2786	346.72	0.2823
324.86	0.2781	326.56	0.2791	331.54	0.2810	338.65	0.2784	347.23	0.2794
325.09	0.2773	326.72	0.2795	331.92	0.2810	338.90	0.2807	347.36	0.2801
325.29	0.2787	326.85	0.2795	331.98	0.2792	339.03	0.2785	347.58	0.2789
325.51	0.2787	326.97	0.2807	332.14	0.2787	339.18	0.2791	347.69	0.2822
325.70	0.2779	327.11	0.2789	332.31	0.2801	340.16	0.2788	347.72	0.2805
326.17	0.2780	327.37	0.2800	332.44	0.2776	340.73	0.2781	347.95	0.2789
326.32	0.2786	327.50	0.2785	332.56	0.2778	340.92	0.2797	348.00	0.2827
326.45	0.2786	327.83	0.2791	332.72	0.2779	341.01	0.2797	348.22	0.2806
326.61	0.2783	328.40	0.2797	332.84	0.2807	341.29	0.2800	348.38	0.2794
326.79	0.2786	328.70	0.2804	333.02	0.2803	341.64	0.2789	348.63	0.2807
326.87	0.2780	328.73	0.2776	333.12	0.2815	341.69	0.2784	349.09	0.2794
327.06	0.2789	329.05	0.2785	333.23	0.2799	341.80	0.2800		
327.27	0.2801	329.07	0.2803	333.37	0.2784	342.04	0.2823		
327.40	0.2782	329.19	0.2786	333.51	0.2799	342.24	0.2781		
327.56	0.2778	329.27	0.2811	333.71	0.2783	342.33	0.2800		
327.64	0.2785	329.45	0.2785	333.79	0.2780	342.39	0.2805		
327.82	0.2784	329.48	0.2788	333.94	0.2812	342.60	0.2788		
327.91	0.2783	329.78	0.2802	333.99	0.2793	342.73	0.2812		
328.35	0.2808	329.92	0.2798	334.18	0.2788	343.02	0.2817		
328.64	0.2793	330.01	0.2800	334.28	0.2787	343.10	0.2788		
328.81	0.2782	330.14	0.2802	334.43	0.2786	343.60	0.2813		
328.66	0.2790	330.17	0.2801	334.62	0.2800	343.69	0.2780		
320.61	0.2767	330.31	0.2794	334.81	0.2782	343.67	0.2826		
321.09	0.2759	330.39	0.2794	335.02	0.2801	343.90	0.2783		
321.44	0.2759	330.47	0.2781	335.35	0.2789	343.97	0.2793		

Thermal Conductivity Values for Glycerol in W/m.K (Run-2)													
T (K)	k		T (K)	k		T (K)	k		T (K)	k		T (K)	k
292.10	0.2764		301.10	0.2757		309.73	0.2769		315.13	0.2766		323.55	0.2786
292.11	0.2753		301.22	0.2745		309.83	0.2765		315.22	0.2786		323.90	0.2766
292.19	0.2774		301.34	0.2768		309.95	0.2767		315.40	0.2781		324.12	0.2780
292.36	0.2762		301.48	0.2761		310.06	0.2769		315.42	0.2762		324.47	0.2787
292.48	0.2763		301.62	0.2768		310.12	0.2751		315.53	0.2780		324.76	0.2772
292.90	0.2750		301.78	0.2761		310.39	0.2774		315.64	0.2759		325.18	0.2776
293.12	0.2753		302.08	0.2770		310.45	0.2762		315.87	0.2770		325.58	0.2766
293.37	0.2747		302.20	0.2761		310.63	0.2773		315.98	0.2775		326.85	0.2777
293.64	0.2748		302.43	0.2755		310.78	0.2763		316.14	0.2780		327.52	0.2780
293.83	0.2763		302.62	0.2757		310.97	0.2772		316.35	0.2758		327.78	0.2781
294.17	0.2769		302.75	0.2753		311.27	0.2764		316.52	0.2769		327.98	0.2801
294.32	0.2757		302.94	0.2739		311.57	0.2778		316.93	0.2765		328.28	0.2775
294.45	0.2751		303.14	0.2770		311.94	0.2767		317.02	0.2774		328.45	0.2789
294.58	0.2763		303.41	0.2757		312.16	0.2769		317.54	0.2754		328.63	0.2786
294.68	0.2770		303.77	0.2757		312.30	0.2751		317.81	0.2757		328.78	0.2791
294.80	0.2763		303.92	0.2771		312.53	0.2755		318.05	0.2779		328.96	0.2783
294.92	0.2780		304.42	0.2777		312.94	0.2793		318.48	0.2762		329.11	0.2798
295.48	0.2780		305.01	0.2756		313.19	0.2789		318.70	0.2786		329.18	0.2784
295.81	0.2766		305.20	0.2740		313.41	0.2787		319.09	0.2773		329.26	0.2781
295.98	0.2777		305.64	0.2749		313.49	0.2773		319.21	0.2768		329.40	0.2801
296.13	0.2752		306.08	0.2752		313.58	0.2762		319.47	0.2774		329.42	0.2791
296.30	0.2751		306.36	0.2749		313.62	0.2777		319.60	0.2786		329.77	0.2807
296.55	0.2743		306.63	0.2765		313.73	0.2785		319.81	0.2771		329.98	0.2809
296.81	0.2764		306.79	0.2764		313.90	0.2766		319.91	0.2783		330.05	0.2784
297.04	0.2766		306.94	0.2766		313.99	0.2779		320.11	0.2794		330.14	0.2793
297.28	0.2765		307.20	0.2775		314.06	0.2775		320.29	0.2792		330.13	0.2789
297.71	0.2751		307.35	0.2760		314.14	0.2769		320.24	0.2785		330.26	0.2795
297.88	0.2775		307.53	0.2771		314.24	0.2770		320.39	0.2795		330.30	0.2803
298.09	0.2740		307.80	0.2765		314.40	0.2774		320.49	0.2782		330.32	0.2782
298.29	0.2750		308.01	0.2767		314.51	0.2777		320.57	0.2779		330.39	0.2797
298.72	0.2777		308.14	0.2778		314.56	0.2771		320.67	0.2790		330.41	0.2790
298.94	0.2748		308.32	0.2780		314.65	0.2796		321.00	0.2785		330.49	0.2801
299.16	0.2749		308.63	0.2769		314.71	0.2785		321.31	0.2775		330.54	0.2805
299.38	0.2773		308.77	0.2772		314.79	0.2777		321.61	0.2765		330.55	0.2786
299.56	0.2749		308.98	0.2774		314.89	0.2768		321.93	0.2778		330.59	0.2790
300.01	0.2752		309.11	0.2755		314.91	0.2784		322.35	0.2761		331.45	0.2801
300.29	0.2770		309.23	0.2764		315.01	0.2773		322.59	0.2771		331.61	0.2790
300.69	0.2760		309.43	0.2762		315.07	0.2770		323.00	0.2762		331.76	0.2791
300.88	0.2767		309.57	0.2763		315.11	0.2789		323.30	0.2763		331.96	0.2798

Thermal Conductivity Values for Glycerol in W/m.K (Run-3)													
T (K)	k		T (K)	k		T (K)	k		T (K)	k		T (K)	k
292.88	0.2727		313.19	0.2786		324.22	0.2785		334.03	0.2781		341.91	0.2819
293.25	0.2755		313.41	0.2778		324.42	0.2820		334.15	0.2804		341.99	0.2809
293.47	0.2741		313.66	0.2795		324.72	0.2804		334.30	0.2791		342.03	0.2835
294.47	0.2739		313.92	0.2771		325.25	0.2811		334.39	0.2821		342.13	0.2804
294.85	0.2741		314.16	0.2790		325.67	0.2814		334.54	0.2802		342.24	0.2807
295.18	0.2740		314.42	0.2768		325.97	0.2808		334.90	0.2796		342.36	0.2833
295.56	0.2757		314.67	0.2782		326.21	0.2783		335.09	0.2798		342.35	0.2812
296.00	0.2732		314.93	0.2790		326.48	0.2807		335.32	0.2778		342.41	0.2804
296.49	0.2766		315.45	0.2792		326.68	0.2810		335.55	0.2805		342.44	0.2823
296.89	0.2744		315.68	0.2792		326.92	0.2811		335.74	0.2799		342.44	0.2803
297.29	0.2723		315.90	0.2775		327.15	0.2785		336.01	0.2808		342.66	0.2824
297.79	0.2757		316.17	0.2782		327.61	0.2824		336.08	0.2813		342.70	0.2802
298.29	0.2719		316.41	0.2790		327.82	0.2782		336.32	0.2829		342.69	0.2808
298.69	0.2736		316.59	0.2783		328.22	0.2778		336.51	0.2796		342.89	0.2818
299.13	0.2722		316.81	0.2799		329.05	0.2797		336.84	0.2800		342.87	0.2815
299.45	0.2754		317.23	0.2796		329.21	0.2785		337.18	0.2813		342.91	0.2835
300.84	0.2736		317.40	0.2795		329.55	0.2815		337.44	0.2782		342.97	0.2774
302.57	0.2760		317.61	0.2804		329.73	0.2796		337.77	0.2827		343.19	0.2802
302.99	0.2732		318.01	0.2788		329.90	0.2810		338.12	0.2833		343.23	0.2826
303.46	0.2750		318.21	0.2794		330.09	0.2798		338.52	0.2811		343.24	0.2817
304.65	0.2764		318.62	0.2795		330.25	0.2807		338.56	0.2780		343.27	0.2815
305.02	0.2742		318.81	0.2776		330.38	0.2788		338.77	0.2813		343.25	0.2830
305.36	0.2764		319.21	0.2800		330.57	0.2827		338.94	0.2829		343.21	0.2784
305.76	0.2747		319.38	0.2792		330.71	0.2796		339.05	0.2830		343.34	0.2808
306.15	0.2748		319.59	0.2778		330.84	0.2800		339.18	0.2814		343.40	0.2837
306.88	0.2742		319.72	0.2806		331.04	0.2791		339.44	0.2801		343.36	0.2839
307.13	0.2766		319.92	0.2788		331.33	0.2795		339.64	0.2817		343.57	0.2790
307.51	0.2757		320.15	0.2799		331.49	0.2778		339.94	0.2814		343.63	0.2825
307.89	0.2766		320.31	0.2808		331.61	0.2790		340.07	0.2778		343.73	0.2809
308.19	0.2766		320.90	0.2802		331.83	0.2781		340.26	0.2823		343.74	0.2798
308.54	0.2773		321.09	0.2810		332.00	0.2827		340.51	0.2808		343.75	0.2819
308.89	0.2769		321.27	0.2798		332.14	0.2802		340.62	0.2796		344.00	0.2806
310.24	0.2767		321.46	0.2800		332.29	0.2792		340.83	0.2817		344.00	0.2835
310.85	0.2761		321.91	0.2793		332.46	0.2812		340.98	0.2831		344.20	0.2795
311.41	0.2774		322.18	0.2801		332.60	0.2802		341.04	0.2812		344.23	0.2819
311.73	0.2779		322.45	0.2796		332.85	0.2782		341.22	0.2791		344.45	0.2806
312.04	0.2760		322.61	0.2793		333.13	0.2791		341.50	0.2784		344.63	0.2828
312.36	0.2766		323.14	0.2820		333.50	0.2787		341.58	0.2822		344.72	0.2829
312.87	0.2768		323.71	0.2791		333.83	0.2823		341.65	0.2814		344.95	0.2820

Thermal Conductivity Values for Glycerol in W/m.K (Run-3)													
T (K)	k		T (K)	k		T (K)	k		T (K)	k		T (K)	k
345.13	0.2779												
345.18	0.2793												
345.36	0.2783												
345.70	0.2768												
345.87	0.2795												

Appendix D: Tabulated Thermal Conductivity Results for Propylene Glycol

Thermal Conductivity Values for Propylene Glycol in W/m.K (Run-1)									
T (K)	k	T (K)	k	T (K)	k	T (K)	k	T (K)	k
238.88	0.1855	270.06	0.1875	287.35	0.1895	296.48	0.1899	293.73	0.1905
239.00	0.1848	270.91	0.1879	287.66	0.1895	296.64	0.1912	293.87	0.1888
239.19	0.1837	271.31	0.1887	287.84	0.1882	296.94	0.1904	294.09	0.1889
239.49	0.1840	271.72	0.1882	288.54	0.1896	297.21	0.1901	294.25	0.1891
239.78	0.1828	272.52	0.1882	288.79	0.1900	297.44	0.1919	294.39	0.1904
240.20	0.1820	272.91	0.1887	289.02	0.1882	297.60	0.1912	294.51	0.1906
240.75	0.1821	273.31	0.1874	289.71	0.1883	297.87	0.1913	294.64	0.1908
241.23	0.1821	274.11	0.1879	290.13	0.1892	298.02	0.1913	294.72	0.1902
241.72	0.1823	274.47	0.1871	288.09	0.1898	298.43	0.1911	294.79	0.1908
242.27	0.1820	274.81	0.1876	288.02	0.1899	298.55	0.1906	294.85	0.1909
250.92	0.1846	275.54	0.1884	288.07	0.1896	298.66	0.1914	294.86	0.1889
251.59	0.1835	275.93	0.1891	288.20	0.1900	298.78	0.1920	294.95	0.1906
252.82	0.1830	276.30	0.1880	288.28	0.1900	298.90	0.1916	294.99	0.1908
253.47	0.1847	277.68	0.1877	288.83	0.1893	299.17	0.1912	295.00	0.1910
254.15	0.1852	278.02	0.1893	289.19	0.1904	299.29	0.1907	295.07	0.1905
254.73	0.1850	278.37	0.1881	289.43	0.1900	299.39	0.1911	295.07	0.1911
255.35	0.1849	278.72	0.1899	289.66	0.1886	299.52	0.1911	295.03	0.1913
256.52	0.1853	279.03	0.1888	290.09	0.1901	299.63	0.1916	295.02	0.1908
257.09	0.1853	280.01	0.1883	290.29	0.1902	299.74	0.1923	294.96	0.1914
257.63	0.1857	280.31	0.1898	290.53	0.1897	300.00	0.1912	294.90	0.1913
258.19	0.1852	280.67	0.1887	290.72	0.1891	300.10	0.1912	294.88	0.1900
258.75	0.1851	280.91	0.1893	291.18	0.1899	300.22	0.1906	294.89	0.1907
259.27	0.1862	281.26	0.1881	291.99	0.1884	300.31	0.1915	294.85	0.1903
259.85	0.1856	281.89	0.1893	292.40	0.1887	300.41	0.1914	294.91	0.1905
260.37	0.1863	282.16	0.1898	292.93	0.1889	300.51	0.1917	294.97	0.1911
260.87	0.1862	282.77	0.1885	293.14	0.1893	300.95	0.1905	295.06	0.1910
261.42	0.1852	283.05	0.1883	293.28	0.1893	301.02	0.1907	295.10	0.1904
261.92	0.1863	283.34	0.1887	293.49	0.1899	301.10	0.1905	295.19	0.1901
262.44	0.1873	283.62	0.1892	294.01	0.1888	301.23	0.1919	295.21	0.1905
262.98	0.1852	283.92	0.1900	294.17	0.1901	301.42	0.1932	295.27	0.1905
263.51	0.1873	284.46	0.1897	294.33	0.1893	301.72	0.1921	295.50	0.1905
264.49	0.1875	285.01	0.1896	294.87	0.1898	302.05	0.1918	295.60	0.1903
265.02	0.1863	285.28	0.1890	295.02	0.1901	292.97	0.1905	295.66	0.1907
265.46	0.1877	285.56	0.1883	295.19	0.1890	292.90	0.1900	295.73	0.1905
265.95	0.1862	285.81	0.1885	295.34	0.1889	292.85	0.1892	295.80	0.1908
266.47	0.1879	286.04	0.1890	295.69	0.1908	292.89	0.1901	295.85	0.1907
267.35	0.1873	286.58	0.1892	295.88	0.1897	293.05	0.1907	295.89	0.1901
268.28	0.1877	286.86	0.1901	296.00	0.1902	293.16	0.1895	295.96	0.1907
269.62	0.1879	287.14	0.1887	296.32	0.1908	293.36	0.1905	296.08	0.1897

Thermal Conductivity Values for Propylene Glycol in W/m.K (Run-1)													
T (K)	k		T (K)	k		T (K)	k		T (K)	k		T (K)	k
296.14	0.1906		300.18	0.1907		303.73	0.1912		309.13	0.1912		321.39	0.1926
296.21	0.1896		300.21	0.1901		303.74	0.1913		309.40	0.1920		321.69	0.1909
296.25	0.1901		300.33	0.1906		303.76	0.1900		309.56	0.1923		321.93	0.1913
296.30	0.1906		300.40	0.1909		303.71	0.1907		309.71	0.1937		322.16	0.1927
296.36	0.1903		300.43	0.1908		294.41	0.1907		309.80	0.1912		322.42	0.1908
296.46	0.1908		300.47	0.1913		294.89	0.1910		309.92	0.1927		322.94	0.1917
296.52	0.1908		300.66	0.1897		295.34	0.1903		310.15	0.1928		323.49	0.1911
296.60	0.1905		300.79	0.1894		295.84	0.1894		310.26	0.1922		323.69	0.1914
296.64	0.1908		300.93	0.1892		296.39	0.1899		310.41	0.1934		323.90	0.1908
296.69	0.1911		301.12	0.1906		296.95	0.1892		310.65	0.1936		324.40	0.1926
296.75	0.1913		301.28	0.1893		297.44	0.1907		310.76	0.1918		324.57	0.1916
296.79	0.1903		301.40	0.1895		298.98	0.1898		310.81	0.1933		324.75	0.1927
296.83	0.1908		301.62	0.1902		299.83	0.1890		311.33	0.1922		324.97	0.1932
297.01	0.1901		301.87	0.1897		300.25	0.1891		311.51	0.1933		325.41	0.1915
297.19	0.1898		301.96	0.1898		300.58	0.1894		311.85	0.1915		325.58	0.1946
297.45	0.1903		301.99	0.1897		300.95	0.1899		312.04	0.1933		325.77	0.1921
297.59	0.1912		302.06	0.1910		301.31	0.1895		312.52	0.1911		325.98	0.1947
297.98	0.1900		302.37	0.1892		301.65	0.1891		312.73	0.1917		326.16	0.1918
298.09	0.1909		301.72	0.1918		302.05	0.1898		312.92	0.1923		326.30	0.1915
298.32	0.1899		302.14	0.1907		302.44	0.1891		313.10	0.1927		326.48	0.1939
298.58	0.1897		302.42	0.1895		302.70	0.1882		313.33	0.1922		326.71	0.1926
298.64	0.1892		302.54	0.1914		303.05	0.1902		313.77	0.1911		326.91	0.1921
298.76	0.1899		302.67	0.1896		303.31	0.1904		314.06	0.1913		327.44	0.1907
298.95	0.1897		302.78	0.1900		303.76	0.1899		314.27	0.1936		327.68	0.1914
299.04	0.1902		302.91	0.1899		304.01	0.1890		314.45	0.1927		328.57	0.1919
299.12	0.1899		303.23	0.1898		304.21	0.1906		314.74	0.1925		329.40	0.1909
299.18	0.1901		303.32	0.1907		304.58	0.1900		315.23	0.1919		330.45	0.1922
299.30	0.1898		303.40	0.1895		304.78	0.1907		315.52	0.1916		330.87	0.1909
299.36	0.1906		303.46	0.1905		305.39	0.1893		315.79	0.1919		317.52	0.1906
299.48	0.1894		303.51	0.1906		305.68	0.1901		316.40	0.1905		319.78	0.1907
299.55	0.1895		303.59	0.1901		306.52	0.1906		316.80	0.1902		320.45	0.1912
299.63	0.1909		303.76	0.1910		306.79	0.1907		317.19	0.1896		321.12	0.1918
299.70	0.1890		303.80	0.1899		307.03	0.1907		318.00	0.1917		321.66	0.1910
299.76	0.1903		303.83	0.1905		307.57	0.1912		318.72	0.1919		322.28	0.1929
299.81	0.1905		303.82	0.1905		307.84	0.1907		319.10	0.1905		322.81	0.1919
299.89	0.1900		303.77	0.1915		308.04	0.1917		319.84	0.1922		323.35	0.1922
299.99	0.1913		303.80	0.1895		308.63	0.1906		320.12	0.1908		323.86	0.1916
300.01	0.1903		303.81	0.1912		308.77	0.1901		320.80	0.1904		324.89	0.1927
300.13	0.1899		303.78	0.1907		308.99	0.1910		321.07	0.1913		325.38	0.1933

Thermal Conductivity Values for Propylene Glycol in W/m.K (Run-1)													
T (K)	k		T (K)	k		T (K)	k		T (K)	k		T (K)	k
325.86	0.1909		336.88	0.1904		322.33	0.1934		309.44	0.1923		302.16	0.1931
326.80	0.1913		337.23	0.1934		322.03	0.1933		309.28	0.1926		302.03	0.1911
327.22	0.1917		337.36	0.1927		321.40	0.1938		309.08	0.1939		301.94	0.1928
327.64	0.1917		337.83	0.1926		320.83	0.1939		308.91	0.1939		301.73	0.1921
328.06	0.1941		338.32	0.1903		320.54	0.1921		308.72	0.1931		301.36	0.1931
329.15	0.1914		338.54	0.1911		319.86	0.1933		308.54	0.1930		301.23	0.1939
329.51	0.1914		338.86	0.1918		319.56	0.1911		308.35	0.1933		300.89	0.1932
329.84	0.1925		338.97	0.1920		319.00	0.1933		308.18	0.1944		300.80	0.1927
330.20	0.1953		337.91	0.1935		318.71	0.1922		307.99	0.1928		300.71	0.1931
331.17	0.1933		337.41	0.1923		318.41	0.1922		307.84	0.1918			
331.42	0.1914		336.87	0.1933		318.14	0.1925		307.66	0.1921			
331.74	0.1909		336.32	0.1962		317.85	0.1910		307.49	0.1917			
332.60	0.1908		335.83	0.1945		317.55	0.1929		307.34	0.1932			
333.19	0.1919		335.39	0.1920		317.23	0.1918		306.84	0.1918			
333.83	0.1922		334.89	0.1943		316.93	0.1914		306.49	0.1942			
334.28	0.1921		334.41	0.1944		316.68	0.1920		306.34	0.1932			
334.44	0.1927		333.99	0.1923		316.41	0.1927		306.17	0.1920			
334.62	0.1927		333.52	0.1935		316.17	0.1916		305.99	0.1936			
334.92	0.1914		333.06	0.1954		315.94	0.1940		305.84	0.1912			
335.26	0.1922		332.58	0.1928		315.68	0.1933		305.69	0.1939			
335.72	0.1918		332.15	0.1956		314.93	0.1919		305.56	0.1932			
336.41	0.1937		331.22	0.1930		314.71	0.1929		305.41	0.1921			
337.23	0.1934		330.79	0.1949		314.44	0.1937		305.22	0.1928			
337.36	0.1927		330.48	0.1916		314.14	0.1933		304.93	0.1931			
337.83	0.1926		330.07	0.1934		313.42	0.1913		304.79	0.1913			
338.86	0.1918		329.24	0.1935		313.02	0.1924		304.66	0.1933			
338.97	0.1920		328.88	0.1941		312.81	0.1929		304.50	0.1917			
333.65	0.1904		328.52	0.1916		312.54	0.1938		304.24	0.1937			
333.83	0.1922		328.11	0.1928		312.33	0.1949		304.09	0.1937			
334.12	0.1926		327.71	0.1937		312.08	0.1945		303.97	0.1930			
334.28	0.1921		326.98	0.1959		311.88	0.1919		303.78	0.1929			
334.44	0.1927		326.56	0.1919		311.43	0.1916		303.63	0.1924			
334.62	0.1927		326.15	0.1927		311.02	0.1921		303.24	0.1930			
334.92	0.1914		325.82	0.1926		310.81	0.1940		302.94	0.1942			
335.26	0.1922		325.11	0.1913		310.65	0.1940		302.86	0.1921			
335.72	0.1918		324.76	0.1909		310.43	0.1927		302.69	0.1943			
336.22	0.1907		324.40	0.1924		310.05	0.1931		302.56	0.1929			
336.41	0.1937		324.10	0.1951		309.84	0.1929		302.43	0.1928			
336.66	0.1908		323.42	0.1933		309.61	0.1928		302.29	0.1936			

Thermal Conductivity Values for Propylene Glycol in W/m.K (Run-2)									
T (K)	k	T (K)	k	T (K)	k	T (K)	k	T (K)	k
235.12	0.1834	262.16	0.1861	281.71	0.1897	294.26	0.1890	300.84	0.1922
235.34	0.1834	262.64	0.1865	282.31	0.1897	294.79	0.1897	301.15	0.1940
235.62	0.1817	263.14	0.1871	282.59	0.1892	294.90	0.1895	301.24	0.1921
235.91	0.1812	264.63	0.1868	282.87	0.1891	295.07	0.1906	301.33	0.1925
236.22	0.1826	265.13	0.1862	283.43	0.1888	295.25	0.1894	301.36	0.1916
236.66	0.1820	265.60	0.1874	283.72	0.1888	295.40	0.1901	301.48	0.1916
237.68	0.1821	266.08	0.1868	283.98	0.1889	295.52	0.1896	301.64	0.1923
238.20	0.1804	266.54	0.1879	284.23	0.1888	295.71	0.1908	301.84	0.1919
238.77	0.1806	267.49	0.1873	284.53	0.1889	295.87	0.1900	302.04	0.1921
239.37	0.1823	267.95	0.1878	285.06	0.1885	295.99	0.1908	302.11	0.1921
240.00	0.1811	268.37	0.1868	285.86	0.1889	296.15	0.1919	302.30	0.1920
240.64	0.1822	268.85	0.1877	286.09	0.1895	296.29	0.1911	302.51	0.1930
241.25	0.1818	269.28	0.1879	286.57	0.1893	296.40	0.1913	302.56	0.1935
242.00	0.1811	270.19	0.1884	286.80	0.1881	296.56	0.1909	302.60	0.1925
242.64	0.1819	270.56	0.1879	287.05	0.1892	296.67	0.1905	302.70	0.1939
243.33	0.1826	271.43	0.1887	287.30	0.1886	296.80	0.1907	302.76	0.1926
244.72	0.1812	271.80	0.1891	287.76	0.1895	296.99	0.1913	302.86	0.1920
245.39	0.1837	272.20	0.1883	288.00	0.1891	297.15	0.1911	303.29	0.1919
246.76	0.1819	272.55	0.1887	288.25	0.1898	297.28	0.1898	303.34	0.1939
248.12	0.1841	272.95	0.1880	288.49	0.1888	297.40	0.1913	303.41	0.1943
248.80	0.1819	273.30	0.1878	288.95	0.1884	297.49	0.1899	303.46	0.1940
249.47	0.1831	273.70	0.1877	289.12	0.1894	297.62	0.1906	303.50	0.1935
250.11	0.1827	274.05	0.1892	289.81	0.1892	298.26	0.1910	303.57	0.1916
250.74	0.1833	275.15	0.1873	290.03	0.1886	298.50	0.1915	303.68	0.1934
251.40	0.1835	275.49	0.1892	290.60	0.1892	298.60	0.1916	303.78	0.1935
252.02	0.1841	275.88	0.1886	291.00	0.1900	298.75	0.1912	303.89	0.1936
252.69	0.1831	276.57	0.1879	291.40	0.1888	298.84	0.1920	303.99	0.1930
253.29	0.1836	276.91	0.1894	291.77	0.1884	298.94	0.1904	304.11	0.1936
253.91	0.1839	277.59	0.1888	291.95	0.1886	299.08	0.1912	304.24	0.1936
254.52	0.1840	277.93	0.1894	292.13	0.1877	299.18	0.1915	304.23	0.1938
255.11	0.1842	278.25	0.1884	292.27	0.1893	299.30	0.1913	304.29	0.1939
256.81	0.1847	278.58	0.1888	292.47	0.1897	299.62	0.1921	304.37	0.1926
258.43	0.1859	278.90	0.1896	292.63	0.1882	299.82	0.1914	304.44	0.1938
259.01	0.1867	279.21	0.1898	292.79	0.1900	300.14	0.1909	340.21	0.1946
259.52	0.1853	279.59	0.1887	292.98	0.1898	300.26	0.1917	338.50	0.1943
260.05	0.1857	279.87	0.1902	293.47	0.1906	300.36	0.1904	336.29	0.1945
260.58	0.1864	280.16	0.1888	293.65	0.1893	300.58	0.1910	335.82	0.1946
261.07	0.1875	280.84	0.1887	293.81	0.1900	300.67	0.1931	333.37	0.1946
261.61	0.1852	281.09	0.1885	293.98	0.1891	300.79	0.1933	332.40	0.1965

Thermal Conductivity Values for Propylene Glycol in W/m.K (Run-2)													
T (K)	k		T (K)	k		T (K)	k		T (K)	k		T (K)	k
331.96	0.1924		315.45	0.1923		303.64	0.1917						
331.50	0.1935		315.21	0.1942		303.34	0.1924						
331.06	0.1935		314.96	0.1924		303.03	0.1921						
330.67	0.1931		314.72	0.1925		302.78	0.1922						
330.23	0.1934		314.28	0.1915		302.59	0.1939						
329.45	0.1938		314.01	0.1921		301.78	0.1918						
328.57	0.1940		313.79	0.1918		301.51	0.1912						
328.17	0.1928		313.54	0.1918		300.89	0.1917						
327.81	0.1932		313.28	0.1927		300.57	0.1923						
327.41	0.1923		313.07	0.1936		300.36	0.1916						
327.02	0.1935		312.78	0.1928		300.17	0.1927						
326.63	0.1948		312.56	0.1917		299.82	0.1925						
326.23	0.1919		312.35	0.1914		299.55	0.1913						
325.90	0.1941		312.11	0.1917		299.35	0.1919						
325.53	0.1920		311.76	0.1919		299.18	0.1914						
324.82	0.1917		311.57	0.1922		299.01	0.1927						
324.45	0.1914		311.11	0.1940		298.84	0.1917						
324.12	0.1949		310.70	0.1937		298.63	0.1924						
323.76	0.1916		310.53	0.1942		298.52	0.1921						
323.05	0.1952		310.35	0.1930		298.38	0.1929						
322.71	0.1929		309.95	0.1914		298.14	0.1915						
322.35	0.1937		309.72	0.1916		298.01	0.1921						
322.01	0.1917		309.50	0.1918		297.70	0.1929						
321.06	0.1920		309.38	0.1925		297.52	0.1921						
320.44	0.1909		309.17	0.1944		297.37	0.1928						
320.14	0.1934		308.63	0.1922									
319.51	0.1913		308.30	0.1933									
319.20	0.1934		307.93	0.1924									
318.91	0.1914		307.59	0.1930									
318.66	0.1926		307.30	0.1920									
318.37	0.1936		306.89	0.1924									
318.09	0.1921		306.51	0.1913									
317.82	0.1915		306.23	0.1914									
317.53	0.1916		305.93	0.1922									
317.27	0.1918		305.59	0.1912									
317.01	0.1936		305.30	0.1926									
316.17	0.1934		305.02	0.1920									
315.88	0.1920		304.72	0.1926									
315.67	0.1927		304.15	0.1929									

Thermal Conductivity Values for Propylene Glycol in W/m.K (Run-3)									
T (K)	k	T (K)	k	T (K)	k	T (K)	k	T (K)	k
233.64	0.1809	264.89	0.1864	281.50	0.1894	293.62	0.1898	300.75	0.1913
234.02	0.1819	265.38	0.1869	281.82	0.1896	293.96	0.1895	300.86	0.1918
234.43	0.1812	265.86	0.1871	282.46	0.1895	294.12	0.1897	300.97	0.1906
235.44	0.1807	267.28	0.1872	282.72	0.1903	294.46	0.1889	301.06	0.1929
237.14	0.1810	267.75	0.1868	283.04	0.1896	294.66	0.1896	301.16	0.1926
237.78	0.1809	268.20	0.1878	283.30	0.1903	294.95	0.1892	301.30	0.1919
239.12	0.1807	268.65	0.1864	283.60	0.1893	295.14	0.1898	301.84	0.1919
241.91	0.1812	269.12	0.1884	283.87	0.1890	295.28	0.1903	301.97	0.1915
242.64	0.1820	269.58	0.1882	284.15	0.1900	295.44	0.1907	302.53	0.1923
244.06	0.1824	270.02	0.1879	284.42	0.1899	295.76	0.1894	302.98	0.1922
244.76	0.1825	270.46	0.1878	284.71	0.1886	296.09	0.1897	303.32	0.1926
245.47	0.1823	271.32	0.1867	284.98	0.1888	296.44	0.1912	358.47	0.1973
246.20	0.1828	271.71	0.1875	285.24	0.1901	296.56	0.1900	353.59	0.1953
246.85	0.1816	272.11	0.1879	285.56	0.1893	296.68	0.1909	348.81	0.1940
247.55	0.1832	272.92	0.1881	286.28	0.1890	296.82	0.1910	348.09	0.1944
248.26	0.1818	273.30	0.1886	286.57	0.1893	297.01	0.1911	347.42	0.1937
250.27	0.1827	273.63	0.1879	286.80	0.1886	297.16	0.1910	346.72	0.1941
250.89	0.1826	274.03	0.1883	287.06	0.1897	297.29	0.1916	345.42	0.1941
251.55	0.1830	274.43	0.1881	288.04	0.1895	297.41	0.1902	344.17	0.1962
252.86	0.1830	274.81	0.1882	288.28	0.1897	297.66	0.1905	343.54	0.1981
253.52	0.1841	275.17	0.1901	288.51	0.1896	297.81	0.1908	342.93	0.1942
254.75	0.1854	275.52	0.1887	288.99	0.1889	297.94	0.1913	341.21	0.1938
255.32	0.1844	275.88	0.1891	289.19	0.1887	298.07	0.1912	340.10	0.1941
255.95	0.1848	276.23	0.1885	289.50	0.1887	298.50	0.1904	339.57	0.1929
256.49	0.1851	276.63	0.1888	289.67	0.1882	298.58	0.1904	339.03	0.1937
257.06	0.1860	277.00	0.1890	289.86	0.1892	298.71	0.1911	338.52	0.1937
257.60	0.1851	277.29	0.1895	290.54	0.1888	298.86	0.1914	337.48	0.1931
258.14	0.1858	277.63	0.1894	290.78	0.1887	298.95	0.1925	336.97	0.1930
258.69	0.1849	278.00	0.1892	290.96	0.1892	299.09	0.1922	336.00	0.1954
259.22	0.1855	278.31	0.1887	291.17	0.1884	299.20	0.1921	335.53	0.1951
259.77	0.1856	278.64	0.1894	291.39	0.1892	299.43	0.1926	334.61	0.1932
260.35	0.1868	278.95	0.1890	291.61	0.1888	299.56	0.1912	333.25	0.1932
260.84	0.1855	279.30	0.1893	291.80	0.1901	299.67	0.1901	332.80	0.1947
261.38	0.1857	279.60	0.1891	292.01	0.1892	299.92	0.1898	332.34	0.1929
261.86	0.1865	279.95	0.1901	292.17	0.1902	300.01	0.1898	331.92	0.1945
262.93	0.1873	280.27	0.1897	292.35	0.1899	300.14	0.1912	331.52	0.1944
263.41	0.1854	280.57	0.1896	292.89	0.1891	300.25	0.1918	330.68	0.1938
263.89	0.1875	280.90	0.1901	293.07	0.1884	300.45	0.1903	330.23	0.1925
264.39	0.1875	281.20	0.1900	293.45	0.1886	300.68	0.1901	329.42	0.1937

Thermal Conductivity Values for Propylene Glycol in W/m.K (Run-3)													
T (K)	k		T (K)	k		T (K)	k		T (K)	k		T (K)	k
329.03	0.1935		314.19	0.1919		303.20	0.1922						
327.83	0.1950		313.44	0.1915		303.05	0.1922						
327.47	0.1935		313.19	0.1917		302.92	0.1922						
326.71	0.1946		312.96	0.1921		302.58	0.1924						
326.34	0.1920		312.73	0.1930		302.42	0.1925						
325.62	0.1916		312.46	0.1934		302.29	0.1918						
325.26	0.1911		312.24	0.1923		302.08	0.1924						
324.90	0.1957		312.00	0.1926		300.92	0.1925						
324.55	0.1942		311.76	0.1943		300.79	0.1918						
324.20	0.1917		311.13	0.1938		300.70	0.1926						
323.84	0.1951		310.88	0.1926		300.51	0.1917						
323.50	0.1934		310.08	0.1930		299.92	0.1926						
323.20	0.1925		309.64	0.1934		299.67	0.1923						
322.82	0.1922		309.45	0.1936		298.97	0.1919						
322.44	0.1932		309.26	0.1921		298.69	0.1922						
322.12	0.1940		309.03	0.1942		297.96	0.1925						
321.84	0.1925		308.82	0.1934		297.95	0.1918						
321.46	0.1928		308.40	0.1941		297.59	0.1924						
321.20	0.1944		308.21	0.1932		296.98	0.1923						
320.91	0.1928		308.03	0.1944		296.98	0.1920						
320.55	0.1918		307.35	0.1929		296.92	0.1920						
320.18	0.1926		306.96	0.1916									
319.65	0.1917		306.88	0.1935									
319.42	0.1910		306.71	0.1927									
319.14	0.1925		306.06	0.1932									
318.84	0.1912		305.96	0.1931									
318.54	0.1922		305.78	0.1927									
318.26	0.1933		305.54	0.1935									
317.97	0.1911		305.43	0.1935									
317.36	0.1922		305.28	0.1935									
317.10	0.1910		305.09	0.1925									
316.78	0.1912		304.58	0.1924									
316.59	0.1942		304.38	0.1931									
316.31	0.1931		304.32	0.1925									
316.04	0.1919		304.17	0.1928									
315.75	0.1914		304.08	0.1930									
314.93	0.1924		303.92	0.1920									
314.65	0.1918		303.69	0.1934									
314.39	0.1925		303.31	0.1935									